

*Surveillance for avian influenza viruses in the environment*

Inauguraldissertation

zur

Erlangung des akademischen Grades eines

Doktors der Naturwissenschaften (Dr. rer. nat.)

der

Mathematisch-Naturwissenschaftlichen Fakultät

der

Universität Greifswald

vorgelegt von

Ann Kathrin Ahrens

Greifswald, August 2022

Dekan\*in: Prof. Dr. Gerald Kerth

1. Gutachter\*in: Prof. Dr. Dr. h.c. mult. Thomas C. Mettenleiter

2. Gutachter\*in: Prof. Dr. Stephan Ludwig

Tag der Promotion: 20.02.2023

## Table of content

List of abbreviations and symbols.....	I
List of Tables.....	IV
List of Figures .....	IV
1 Introduction .....	1
1.1 The avian influenza virus (AIV) .....	1
1.1.1 Historical background of avian influenza (AI) .....	1
1.1.2 Taxonomy.....	1
1.1.2.1 Virus morphology and genome organisation .....	2
1.1.3 Replication .....	3
1.1.4 Genetic flexibility of influenza A viruses .....	5
1.1.4.1 Replications errors.....	5
1.1.4.2 Reassortment .....	6
1.1.5 Avian influenza disease.....	6
1.1.5.1 Clinical signs, infection and transmission routes .....	6
1.1.6 Low pathogenicity avian influenza virus (LPAIV).....	8
1.1.7 High pathogenicity avian influenza virus (HPAIV).....	8
1.2 Diagnosis of AI infections.....	9
1.2.1 Virus isolation .....	9
1.2.1.1 Embryonated chicken eggs.....	9
1.2.1.2 Cell culture .....	10
1.2.2 Serology .....	10
1.2.3 Molecular detection of IAV genome fragments.....	10
1.2.3.1 Polymerase-chain-reaction, PCR .....	10
1.2.3.2 Influenza detection in environmental samples .....	11
1.2.4 Prevention of AIV infection by biosecurity .....	12
1.2.5 Prevention of AIV infections by vaccination.....	12
1.3 Epidemiology of avian influenza .....	12

1.3.1	Importance of the reservoir hosts .....	12
1.4	Impact of environmental factors on the epidemiology of avian influenza.....	13
1.4.1	Viral tenacity and dispersion in surface water .....	13
1.4.2	Temperature .....	14
1.4.3	Salinity .....	14
1.4.4	pH-value .....	14
1.5	Air born transmission of avian influenza virus .....	16
1.5.1.1	Presence and tenacity of AIV in sediments and soils.....	17
1.6	Avian influenza as a zoonotic infection .....	17
1.6.1	Recent HPAI epidemics in Europe.....	19
2	Study objectives .....	21
2.1.1	Questions and approach .....	21
3	Publications .....	22
3.1	Improved Subtyping of Avian Influenza Viruses Using an RT-qPCR-Based Low Density Array: ‘Riems Influenza a Typing Array’, Version 2 (RITA-2).....	22
3.2	Investigating environmental matrices for use in avian influenza virus surveillance – surface water, sediments and avian fecal samples .....	47
3.3	Exploring surface water as a transmission medium of avian influenza viruses – systematic infection studies in mallards.....	64
3.4	Own contributions to publications .....	80
	Investigating environmental matrices for use in avian influenza virus surveillance – surface water, sediments and avian fecal samples .....	81
4	Summarizing discussion.....	84
5	Summary .....	88
6	Zusammenfassung .....	90
7	References .....	92
8	Appendix .....	107
8.1	Eigenständigkeitserklärung .....	107

8.2	Curriculum vitae.....	108
8.3	Publications .....	109
8.4	Oral and poster presentations .....	110
8.5	Acknowledgement.....	111

## List of abbreviations and symbols

AA	Amino acid
AAF	Amnio-allantoic fluid
AIV	Avian influenza virus
B.C.	Before Christ
cDNA	Complementary DNA
CRM1	Cellular chromosome region maintenance 1
cRNA	Complementary RNA
DNA	Deoxyribonucleic acid
ECE	Embryonated chicken eggs
Etc.	<i>et cetera</i>
ELISA	Enzyme-linked immunosorbent assay
H (= HA)	Haemagglutinin
HA	Haemagglutination assay
HI	Haemagglutination inhibition assay
HP	High pathogenicity
ICTV	International Committee on Taxonomy of Viruses
i.e.	<i>id est</i> , that is
IVPI	Intravenous pathogenicity index
L	Liter
LP	Low pathogenicity
mRNA	Messenger Ribonucleic acid
M	Matrix protein, consists out of two (1 and 2) subunits
M1	Matrix protein 1
M2	Matrix protein 2
M2e	Matrix protein 2 ectodomain
MDCK	Madin Darby canine kidney (Cell line)
mL	Milliliter
N (= NA)	Neuraminidase
Nm	Nanometer
NP	Nucleoprotein
PB	Polymerase basic protein
PB1-F1	Polymerase basic protein, alternate frame-1

PB1-F2	Polymerase basic protein, alternate frame-2
PCR	Polymerase chain reaction
PEG	Polyethylene glycol
pH	Potentia hydrogenii (pH-value)
ppm	Parts per million
RdRp	RNA dependent RNA-Polymerase
RITA	Riems Influenza a Typing Array
RNA	Ribonucleic acid
RT-qPCR	Reverse transcribed semi-quantitative PCR
SIA	Sialic acid (used as receptor molecule for influenza viruses)
U.S.A.	United States of America
UV	Ultraviolet
UV-A	Ultraviolet A
UV-B	Ultraviolet B
UV-C	Ultraviolet C
vRNA	Virus RNA
WHO	World health organization
A, $\alpha$	alpha
$^{\circ}\text{C}$	Degree Celsius
-ss	Single stranded RNA with negative polarization
%	Percentage
<	Smaller
>	Greater
$\leq$	Less than or equal to
$\geq$	Greater than or equal to

**Table 1: Amino acids in their one- and three letter code abbreviation**

The table gives an overview of the different amino acids as well as their abbreviations in one or three letters, according to [1].

Name of the amino acid	Three letter code	One letter code
Alanine	ala	A
Arginine	arg	R
Asparagine	asn	N
Aspartic acid	asp	D
Asparagine or aspartic acid	asx	B
Cysteine	cys	C
Glutamic acid	glu	E
Glutamine	gln	Q
Glutamine or glutamic acid	glx	Z
Glycine	gly	G
Histidine	his	H
Isoleucine	ile	I
Leucine	leu	L
Lysine	lys	K
Methionine	met	M
Phenylalanine	phe	F
Proline	pro	P
Serine	ser	S
Threonine	thr	T
Tryptophan	trp	W
Tyrosine	tyr	Y
Valine	val	V



## List of Tables

Table 1: Amino acids in their one- and three letter code abbreviation .....	III
Table 2: Impact of abiotic factors on IA .....	15
Table 3: Overview of some recent avian influenza epidemics of clade 2.3.4.4b in Europe ....	20

## List of Figures

Figure 1: Schematic description of the features of designation of new influenza virus isolates 2	
Figure 2: Influenza-specific cellular receptors in different host species.....	4
Figure 3: Main clinical signs of avian influenza infections of different pathogenicity .....	7
Figure 4: Virus detection methods .....	9
Figure 5: Tenacity of AIV in surface water with respect to different environmental factors ..	16
Figure 6: Schematic overview of the putative role of water and sediments for AIV epidemiology .....	87

# 1 Introduction

## 1.1 The avian influenza virus (AIV)

### 1.1.1 Historical background of avian influenza (AI)

Diseases likely attributable to influenza viruses are known for quite a long time. Already in 412 B.C., HYPOCRATES described symptoms as seen today with human influenza virus infections. [2] However, it was not until 1878 that AI was described in poultry by PERRONCITO in Italy; PERRONCITO distinguished this disease from other diseases attributed to bacterial infections [cited after 3,4]. Because the initial naming of the disease as “fowl plaque” lead to confusion with the clinically distinguishable bacterial infection causing “fowl cholera”, RIVOLTA and DELPRATO renamed the disease in 1880 into *Typhus exudatiuus gallinarum* [5]. Already in 1901 CENTANNI and SAVUNZZI provided experimental evidence, that the disease was transmissible through a filterable infectious agent [5]. Later on, in 1955, SCHÄFER described that the causative virus showed sero-immunologic similarities with human influenza viruses [6] and in 1967 PEREIRA, TUMOVA and WEBSTER claimed that the human H2N2 might arose from an avian origin [7]. Shorebirds as well as wild waterfowls are the natural host of low pathogenicity AI (LPAI) [8]. It is considered, that influenza A viruses circulated in ducks well before their domestication [9]. An infection with high pathogenicity AIV (HPAIV) still ranges among the most feared infectious diseases of wild birds and poultry [10]. Until today, several major and minor AI epidemics have been described [11]. Some were associated with viruses crossing species barriers including spill over events to human hosts. These include epidemics with HPAIV H5N1 since 1997 [12], LP and HPAIV H7N9 since 2013 [13] or HPAIV H5N8 since 2017 [14].

### 1.1.2 Taxonomy

According to the International Committee on Taxonomy of Viruses (ICTV) the *Orthomyxoviridae* family consists of seven genera so far of which four are assigned to influenza viruses (**Alpha**, **Beta**, **C-Gamma** and **Delta**) [15]. Additionally, the genera of Isavirus, Quaranjavirus and Thogotovirus also belong to the *Orthomyxoviridae* family [15]. The sub-classification of the influenza viruses within their genera is based on the viral nucleo- (NP) and matrix-1 (M1) proteins, particularly on the antigenic differences [16,17]. The designation of new isolates within those genera follows the scheme outlined in Figure 1.

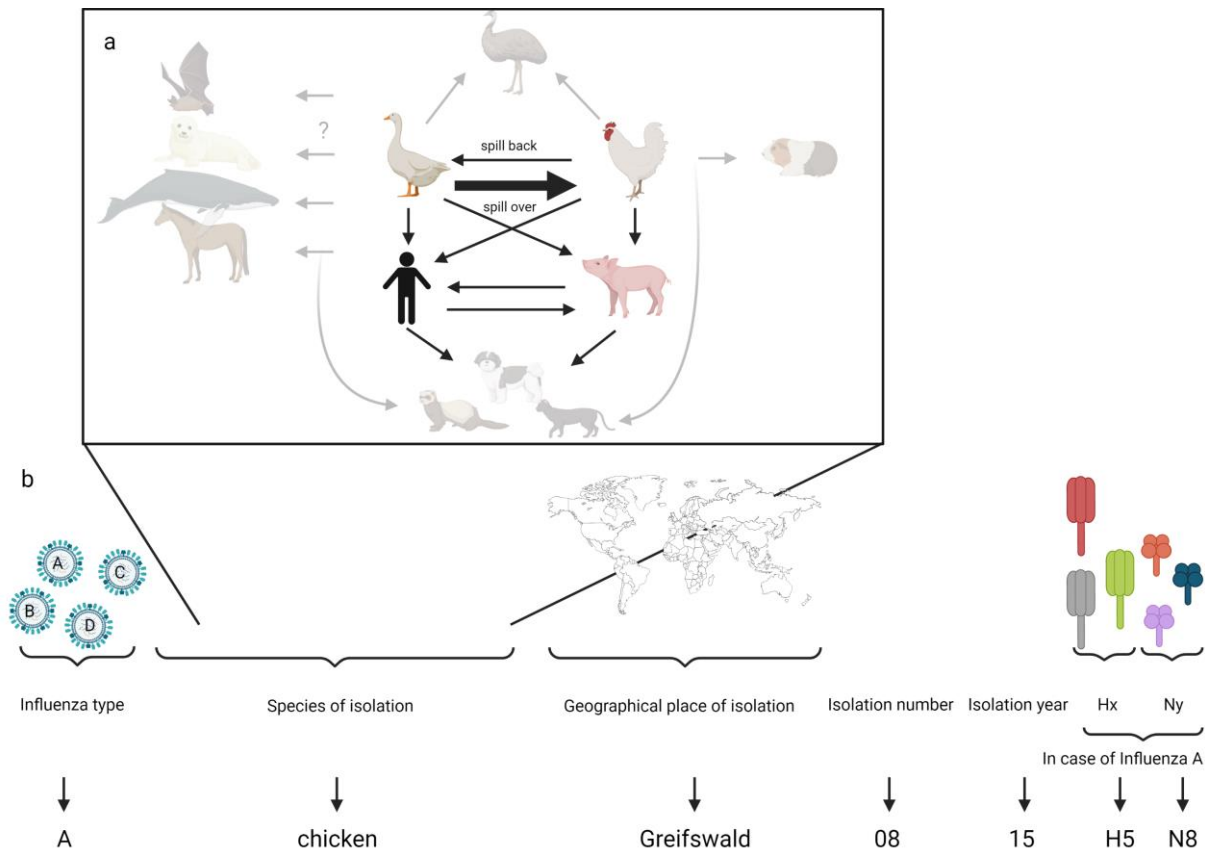


**Figure 1: Schematic description of the features of designation of new influenza virus isolates**

The schematic shows in a) the main inter species transmission pathways and in b), the correct naming of a new influenza isolate is shown schematically, according to [18–20].

### 1.1.2.1 Virus morphology and genome organisation

The influenza virus particles, the individual virions, are variable in shape from spherical to pleomorphic with a rough size of 80 – 120 nm in diameter [21]. There also exist filamentous forms that can achieve a length of several  $\mu\text{m}$  but show a consistent diameter of 80 - 100nm [22]. The single stranded (-ss) RNA genome of negative polarity [23] with a total size of about 14,000 nucleotides [24] is octo-segmented in influenza A and B viruses [25], or spread over seven segments in influenza C and D viruses [23,25,26]. These genes encode non-structural (N=2) and structural virus proteins (N=8) [23,27]. The structural proteins include the polymerase basic protein 1 and 2 (PB1, PB2), and the polymerase acid protein (PA) which form the RNA-depended-RNA polymerase (RdRp) sub-units. The RdRp together with the nucleoprotein (NP) and the viral RNA forms a helical viral ribonucleic complex (RNP) [18]. The matrix proteins (M1, M2), the nucleoprotein (NP) and the two surface glycoproteins haemagglutinin (HA) and neuraminidase (NA) further shape the virion architecture [17]. The

remaining proteins (NS1 and or NEP) are non-structural virus proteins [17]. Despite one publication [28], NS1 does not seem to be present in virions [29]. Furthermore, there are additional proteins originating from *inter alia* mRNA splicing, that are also referred to as accessory proteins like, e.g. PB2-S1, PB1-F2 and PA-X [30]. The HA precursor protein HA0 [17] undergoes a host protease-depending cleavage into the subunits HA1 and HA2 [25]. This cleavage is essential to allow HA-directed fusion of the viral and endosomal membranes during the second step of replication [25]. Without this step, the virus can attach to but cannot replicate in permissive host cells [31]. The disulphide-linked subunits HA1 and HA2 assemble to form a trimer embedded in the lipid virion envelope [32], amounting to about 80% of the protein content in the virion envelope [17]. The neuraminidase forms a tetramer [33] representing 17% envelope protein content [17]. There are 18 different HA-subtypes as well as 11 NA-subtypes known so far [34], of which HA1-16 as well as NA1-9 can be found in aquatic wild birds [35]. H17 and H18 as well as N10 and N11 have been found in a few bat species only [25]. Based on the phylogenetic relationship the HA-subtypes can be further sub-classified into group one (H 1, 2, 5, 6, 8, 9, 11, 12, 13, 16, 17, and 18) and group two (H 3, 4, 7, 10, 14 and 15) [36]. The different NA subtypes can be divided in three groups in total of which only group one (N1, N4, N5 and N8) and group two (N2, N3, N6, N7 and N9) contain influenza A related NA-subtypes while group three harbours NAs of influenza B [37]. Additionally, the matrix protein 2 (M2), an ion channel protein, is integrated with a few copies (up to 3% of envelope protein content) into the virion envelope [17]. The virion envelope is derived from lipid raft and non-lipid raft areas of the host cell's plasma membrane [24,31].

### 1.1.3 Replication

HA in the viral envelope binds to cellular surface receptors [32] composed of a sialic acid (SIA) with an  $\alpha$ 2,3-linkage to penultimate galactose [34] in case of AIV, or an  $\alpha$ 2,6-linkage in human influenza viruses [24]. The major histocompatibility complex class II molecule (MHC-II) serves as a receptor for bat influenza viruses [38] as schematically shown in Figure 2.

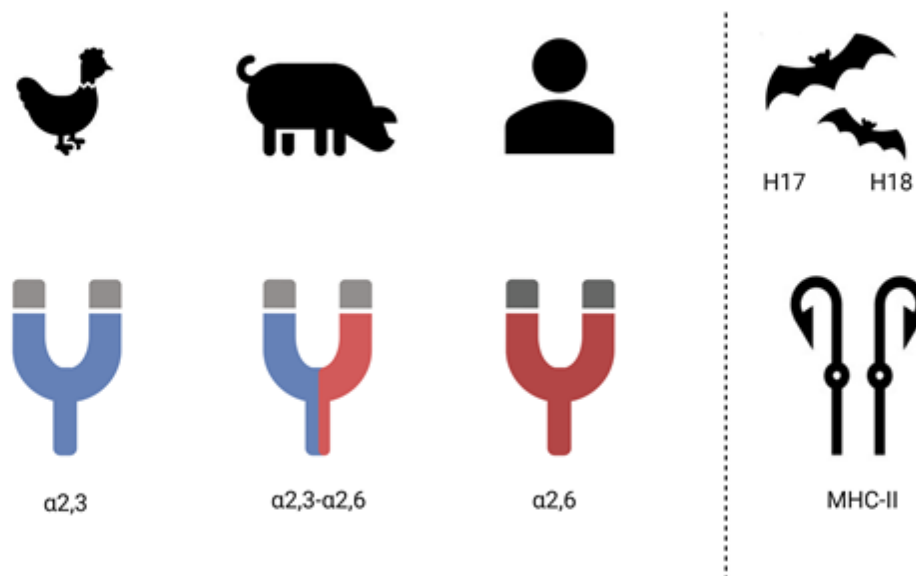


**Figure 2: Influenza-specific cellular receptors in different host species.**

The figure, partly created with BioRender.com, shows the host species-specific differences of the influenza virus receptors. For SIA receptors the linkage to penultimate galactose is important for affinity. Several host species, e.g. the pig, express different types of SIA receptors.

Upon receptor binding endocytosis, mostly clathrin-dependent, is mediated; probably microcytosis is also possible [24,25]. After entry into a cellular endosome the M2 ion channel is activated due to a decreasing pH-value within the endosome [25] and also lowers the pH-value inside the virion. Furthermore, the HA proteins at lowered pH undergo a conformational change to expose the fusion peptide which mediates fusion of virion and endosomal membranes [25]. Through these pores in the fused viral-endosomal membrane the ribonucleoprotein complexes (vRNPs), disassembled from M1 protein are released into the host cytoplasm [25,39] By active transport via cellular importins the RNPs are translocated into the nucleus where transcription by the RdRp in association with further cellular proteins is initiated [40]. The elapsed time between virion attachment until nucleus entry is about one hour. Surface binding is rapidly achieved but the nucleus entry step, which is mainly regulated by adaptor importin- $\alpha$  proteins [17], requires more time [25]. The virus genome replication itself takes place inside the host cell nucleus [25]. Firstly, the vRNA is transcribed into a positive sensed complementary

RNA (cRNA) via RdRp [25]. The 5' methylated cap of a host cell mRNA is cleaved via the viral PB2-endonuclease (cap-snatching). The cap-snatching is essential for the further viral transcription via the RdRp. The host cellular splicing machinery is used to generate different mRNAs from M and NS genome segments to produce M1 and M2, and NS-1 and NEP proteins, respectively. [41] Other accessory proteins, such as PB1-F2, are generated by utilizing alternate initiation codons [42]. Accumulating NP proteins are probably associated with a switch from mRNA to vRNA synthesis [43]. The newly transcribed vRNAs are full length copies which are enwrapped in NP proteins and terminally decorated with a single copy of the three RdRp proteins [25]. The vRNPs leave the nucleus, mediated by the viral nuclear export protein (NEP, leucine-rich-nuclear-export-signal). M1 proteins connect with the C-terminus of the negative sensed vRNPs and the NEP [41,44,25]. The NEP in turn binds on the cellular chromosome region maintenance 1 (CRM1 [45]) and guides the vRNPs out of the nucleus into the cytoplasm. HA and NA surface proteins as well as M2 are transferred to the apical plasma side of polarized cells, where the virus budding takes place [41]. Both M protein splice variants play an important role during the virus budding: M2 is responsible for the viral genome packing and assembly whereas M1 mediates the virus budding [41,46]. The NA aids during the virion release from the cell by cleaving off the SIA receptors [41,46,47].

#### 1.1.4 Genetic flexibility of influenza A viruses

The genetic changes being the motor of influenzaviral evolution are driven by two main mechanisms: (i) replication errors leading to genetic and, if HA and/ or NA proteins are affected, to antigenic drift and (ii) reassortment of genome segments promoting the creation of new genotypes and, if HA and/ or NA genome segments are affected, antigenic shifts [24].

##### 1.1.4.1 Replications errors

The low fidelity (one point mutation per segment and replication round [48]) of the viral RdRp introduces several point mutations within each multiplication round per genome. In theory, from a single virion genome several thousand replicated genomes result that may differ from each other and from the parental genome by one to several mutations. A population of such virions is called a *quasispecies* [48]. Non-synonymous point mutations in viral proteins that are under selective immunological pressure lead to antigenic drift [49].

The interplay between the virus and the host's immune system induces a protective immune response of which neutralizing antibodies targeting mostly the HA protein are an essential part. Antigenic drift, firstly addressed as such in 1965 [50], describes accumulating non-synonymous mutations within antibody binding sites either in the HA or NA or both surface glycoproteins.

Depending of the nature and location of amino acid (AA) mutations within such functional regions neutralizing antibodies may lose affinity to binding these sites and, thus, lose their protective function. Reciprocally, the virus regains replication capacity by escaping these effectors of the host immune system [51–53]. This phenomenon has been detected in influenza A and B viruses and was shown to drive the seasonal pattern of human influenza epidemics [49].

#### 1.1.4.2 Reassortment

RNA-segments exchanges are the result of a co-infections event of one cell by two different influenza A viruses and are defined as reassortment [18]. Reassortment events pose the risk of exchanging different vRNPs from viruses of different host species. This has repeatedly led to new influenza virus strains with human pandemic potential as reassortants with exchanges of either HA, NA and further genome segments were at the basis the major human IAV pandemics in 1957 (H2N2), 1968 (H3N2) and 2009 (H1N1) [18,54]. Reassortments affecting HA subtypes H1 - H3 cause a shift in the antigenic make-up of the virus and have a higher risk for pandemic spread in humans. Other HA subtypes, such as H5, H7 as well as H6, H9 and H10, are causing sporadic infection in humans but have not yet caused extensive human-to-human spread. The latter subtypes are derived from avian sources and need to cross the species barriers to infect humans [55].

#### 1.1.5 Avian influenza disease

##### 1.1.5.1 Clinical signs, infection and transmission routes

Clinical sequelae of an AIV infection in avian hosts can be observed in the respiratory tract as well as in the digestive-, urinary-, and reproductive tracts of avian hosts [56]. LPAIV infections are mostly limited to the respiratory tract but may affect, in laying poultry, the reproductive tract resulting in a drop of egg production [56]. The main clinical signs depend on the viral pathotype as shown in Figure 3.

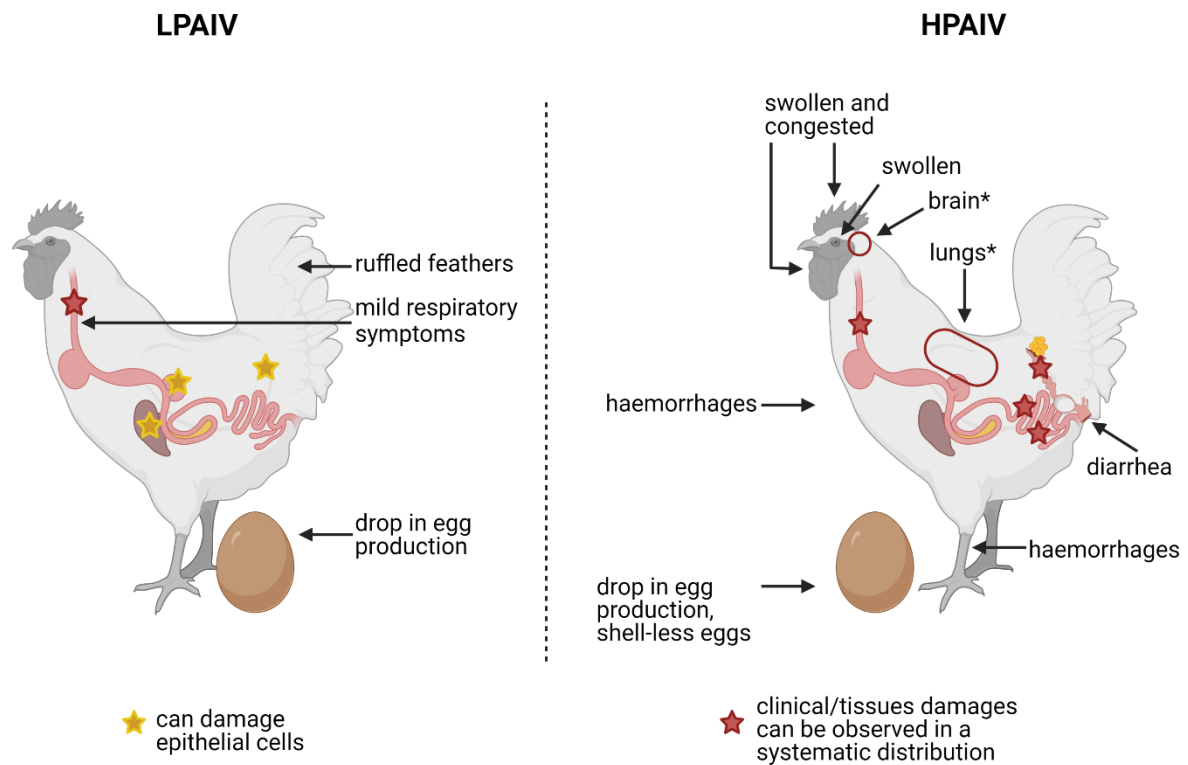


**Figure 3: Main clinical signs of avian influenza infections of different pathogenicity**

Illustration is created with BioRender.com according to [56,57].

The morbidity as well as the mortality rate seems to depend on the virus strain and the infected species [10,58,59]. However, the AA sequence at the HA endoproteolytic cleavage site has a direct influence on the mortality and on the tissue tropism [60]. It is known that LPAIV infections in gallinaceous species might lead to a high morbidity in combination with a low mortality [58]. However, in rare instances, the flock mortality can also reach up to almost 70% for LP (H4N8) virus strains, as reported in the U.S.A. in 1975 [10].

Apart from viral pathogenicity further factors modulate the range of clinical manifestations of AIV infections including co-infections [10], age, species and constitution of the host [56]. Chickens are more vulnerable to an HP infection than ducks [61]. Not all HPAI strains are virulent to all bird species and the morbidity and mortality rate is species-dependent [10]. However, in gallinaceous poultry massive mortality reaching up to 100% is the most significant clinical sign in the affected flock. In waterfowl, symptoms can be milder and range from respiratory symptoms and decline in egg production to haemorrhages of the skin. Sometimes neurological signs can also be observed [10].



Mostly, virus shedding occurs via the cloacal route [9]. However, depending on viral strain and host species virus is shed also via oropharyngeal/ respiratory secretions [9]. The main mode of transmission among avian hosts is via feco-oral chains [62].

#### 1.1.6 Low pathogenicity avian influenza virus (LPAIV)

LPAIV can be defined and characterized via the intravenous pathogenicity index (IVPI). The IVPI is the mean of the categorized clinical signs over 10 days (0 – normal, 1 – sick, 2 – severely sick, 3 – dead) of each of 10 intravenously inoculated 4-8-week-old chickens. An IVPI of 0 means that no animal was ill at any time, and a value of 3 means that all animals died within 24 hours [59]. LPAIV is defined by an IVPI < 1.2 [63,59]. Furthermore, LPAIVs of the subtypes H5 and H7 are characterised by an endoproteolytic cleavage site within the HA that is accessible only by trypsin-like host proteases and, hence, is built with a monobasic AA motif [59,64]. Previously, LPAIVs have been isolated from at least 105 different bird species within 26 different families [65] and were ubiquitously detected in all types of bird husbandry [35]. It is still unclear if all bird species are susceptible to AIV [65].

#### 1.1.7 High pathogenicity avian influenza virus (HPAIV)

HPAIVs reveal an IVPI of > 1.2 or induce mortality of at least 75% within ten days in 4 - 6 weeks old intravenously inoculated chickens [59, 63]. Until today, in nature, only some virus strains of subtypes H5 and H7 showed HPAI properties. Their HA endoproteolytical cleavage site is characteristically altered in that it is presenting multiple basic AA that form a furin-accessible cleavage site [67]. The cleavage site sequence depends on the sub-type and the clade. Eurasian origin H5 LPAIVs usually express the sequence PQRE**TR**/GLF whereas HPAIVs of the goose/Guangdong lineage revealed PQREG**RRKKR**/GLF in clade 1 and PLRE**RRRKR**/GLF for clade 2.3.4 [68]. The bold letters highlight the basic AA that represent the cleavage site motif. LPAIV monobasic cleavage sites are processed by trypsin like proteases only [31]. Multibasic cleavage sites, in contrast, can be cleaved by several cellular host proteases such as furin and other subtilisin-like proteases [68]. The availability of the necessary proteases in different tissues differs: Trypsin-like proteases are confined to the respiratory-, intestinal and reproductive tracts. Whereas furin proteases can be found anywhere in tissues including brain, heart muscle etc. [31]. Thus, replication of LPAIV is confined to tissues where the fitting proteases are expressed, and, hence, a mild clinical picture emerges from replication. In contrast, HPAIV will cause systemic infections and tissue damage with often lethal outcome.

## 1.2 Diagnosis of AI infections

In 1902, CENTANNI [69] already described that embryonated chicken eggs are a suitable substrate for AI virus growth but it was not before the 1930s that BURNET and FERRY [70] used embryonated chicken eggs for virus cultivation [3]. Building on the discovery of agglutination of chicken red blood cells by AIV of LUSH in 1943 [71], the haemagglutination (HA) test was established [3,72]. Since then, there have been many further new developments of diagnostic methods, assignable to roughly three categories (Figure 4): detection of virus growth, serology (detecting humoral immunity of infected hosts) and detection of viral nucleic acids [73,74].

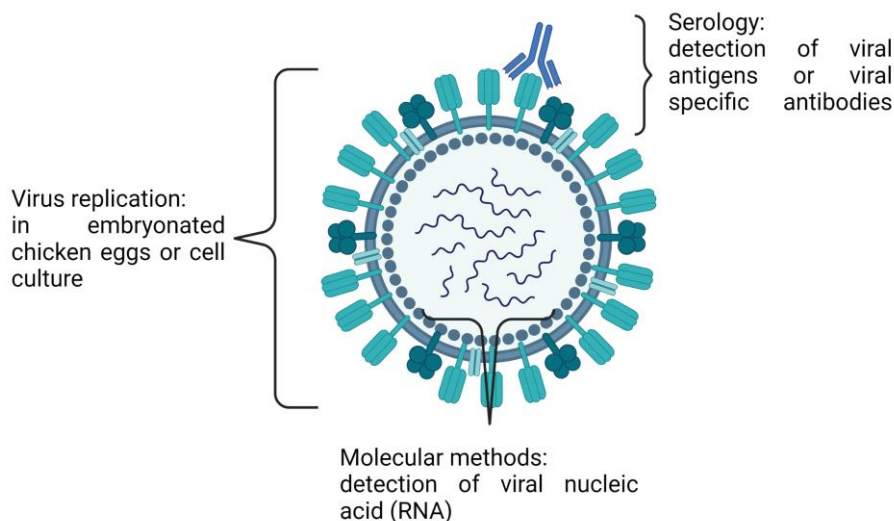


**Figure 4: Virus detection methods**

The figure, created with BioRender.com, shows the main targets of AI-directed laboratory diagnosis.

### 1.2.1 Virus isolation

#### 1.2.1.1 Embryonated chicken eggs

Embryonated chicken eggs (ECE) are an excellent matrix for influenza A virus isolation and cultivation. Usually, the allantois sac of 9 - 11-day old specific pathogen-free ECEs is inoculated with supernatant of clinical swabs or homogenized tissues sample material. The injection hole in the egg shell is then sealed with glue to minimize the risk of contamination. The ECEs are incubated for up to seven days at 37°C and 60% humidity. The ECEs are candled

daily to detect eggs with dead or dying embryos. The eggs are stored at 4°C (at least for four hours or overnight) after death of the embryo or after the incubation period. Amnio-allantoic fluid (AAF) is then extracted from the ECEs and tested for the presence of IAV by HA, or RT-PCR. [75,66]

#### 1.2.1.2 Cell culture

In the late 1940s, ENDERS and colleagues first described the successful cultivation of poliomyelitis as well as the mumps virus in cell cultures [73,76,77]. Today, A549, Madin Darby canine kidney (MDCK), and monkey kidney cells are the main cell types for isolation of infectious human influenza viruses [78]. The sensitivity cell culture virus isolation versus ECE depends on the virus and the cell type [78]. For AIV, no highly sensitive cell culture system is available to date and, consequently, ECE remain the most frequently used system for AIV isolation.

#### 1.2.2 Serology

Due to the high degree of antigenic conservation of NP and M proteins of different IAVs, these proteins are used as the main targets of serological methods aiming at detection of generic humoral immune responses [66]. The enzyme-linked immunosorbent assay (ELISA) is most commonly used for detection of generic antibodies [79]. The system is fast but rather costly [80]. Competitive ELISAs are suitable to analyse samples from different bird species as well as mammals since the antibodies in the sample compete with monoclonal antibodies which are detected species-independently [66]. However, no protective function is assigned to NP- or M-specific antibodies. The majority of antibodies mediating protection is directed against the HA. The haemagglutination inhibition assay (HI) is used to detect such antibodies and can also be used for AIV subtyping purposes [66,79,80]. [80]. Due to the high specificity of the HI, insensitivity might ensue, if badly matching antigens are used [66]. Likewise, the species origin of erythrocytes, used as an indicator system in haemagglutination technologies, can influence assay sensitivity due to varying density and specificity of receptors on the red blood cell membrane [81].

#### 1.2.3 Molecular detection of IAV genome fragments

##### 1.2.3.1 Polymerase-chain-reaction, PCR

PCRs and particularly real time RT-PCRs (RT-qPCR) targeting highly conserved regions of IAV are now routinely used to identify the presence of IAV in clinical and field samples [82]. RT-qPCR was shown to be more sensitive than cell culture [83]. The general principle of each PCR is the repetition of three steps: denaturation, annealing and elongation. During the

denaturation the double stranded deoxyribonucleic acid (DNA) will be melted at high temperature (90 – 97°C). After that, the specific primers (and probe in case of RT-qPCRs) can anneal to the separated DNA-strains at lower temperatures. In the last step, elongation, the heat-stable Taq-DNA-Polymerase duplicates the DNA. [84–86]. For detection of viral RNA, an initial reverse transcription step is required to produce complementary DNA (cDNA) as starting material for the PCR.

Using sub- and pathotype specific primers further rapid sub- and pathotyping can be achieved with RT-qPCRs; these include arrayed sets of RT-qPCRs covering the whole variability of AIV [87].

#### 1.2.3.2 Influenza detection in environmental samples

There are two intrinsic problems with various environmental samples: (i) Presence of biotic (bacteria) and abiotic factors (PCR inhibitors) that interfere with sensitive virus detection systems (RT-qPCR and virus isolation). (ii) Low concentration of viral material requires enrichment, but in parallel to virus enrichment also interfering factors are concentrated in the sample.

Virus detection in large fluid volumes such as surface and sewage water samples poses particular problems. Negatively charged epoxy fiberglass disk filters have frequently been used in virus adsorption-elution methods [88–91]. Virus precipitation or flocculation methods follow a different principle: Viruses suspended in water are forced to accumulate/ flocculate with a precipitation agent into larger pieces, which then fall out of the suspension and can be recovered [92]. Polyethylene glycol (PEG), ion-based agents such as  $Al_2(SO_4)_3$  or  $FeCl_3$  or skimmed milk flocculation are used for precipitation. However, the recovery rate is highly variable and processes may require pH shifts that inactivate virus infectivity [93–97]. Increased use is now made of tangential or dead-end ultrafiltration. In tangential, also called cross-ultrafiltration, the virus suspension flows in parallel to the membrane surface but the virus-free water is drawn off at an angle of 90° to the general direction. Due to the prevailing pressure in the system, an increased turbulent flow velocity is generated, which prevents particles from adhering to the membrane and clogging it. Rather such particles are collected in the concentrated sample fluid [98–101]. In dead-end ultrafiltration, the virus suspension flows across a porous surface, where the virus particles are retained at the pores due to their larger diameter. Therefore, virus particles attached to the membrane need to be released by washing the membrane, generating an eluate. [98–101] The recovery rates of both methods ranged from 66 to 95%, depending on the microorganism being purified [90].

Examples of systematic studies of purification of IAV from environmental water samples are scarce: A field study detected in 4.8% of water samples collected from natural and artificial lakes, surface waters and wetland from the south of Michigan, U.S.A. [98] This study used filtration through a cation ( $Al_3^+$ )-charged filter and an additional ultracentrifugation step. Finally, IAV was detected by PCR targeting the M-gene [102]. In the same range, other studies were able to detect AIV in 0 - 6% of the water samples tested [103–105]. By using 2L water samples collected from locations all over Spain (winter 2007 until autumn 2009) and by precipitating virus particles using PEG6000 AIV was not found by RT-qPCR in any sample [103,105]. On the other hand, a Japanese group managed to detect AIV in six out of 100 50 mL water samples from the Kagoshima prefecture (winter 2012/13). They used the chicken red blood cells precipitation approach. Virus co-precipitated with the erythrocyte were released using neuraminidase treatment and supernatant was inoculated into ECEs. and subtypes H3N8, H4N6, and H4N8 were finally isolated [104,105].

#### 1.2.4 Prevention of AIV infection by biosecurity

Incursion of notifiable AIVs into poultry holdings may occur directly by introducing infected wild birds or poultry. In addition, and maybe more importantly [106], indirect transfer of virus-contaminated fomites, feed or drinking water is important to consider. Several cascades of biosafety measures preventing incursions are described in the legal framework governing notifiable AIV infections of subtypes H5 and H7. [67]

#### 1.2.5 Prevention of AIV infections by vaccination

Vaccination against HPAI can be used to complement biosafety measures where HPAIV is endemic [107]. Prevention by vaccination of clinical signs and economic losses is a main goal of poultry keepers. Prevention of infection and subsequent virus spread is the main epidemiological goal. Successful vaccination programs require careful planning and can be costly [107]. A close antigenic match between the circulating virus in the field and the vaccine strains used is pivotal to ensure high efficacy of the vaccine [108].

### 1.3 Epidemiology of avian influenza

#### 1.3.1 Importance of the reservoir hosts

AI can be divided into two main lineages: the Eurasian and the American. The two lineages are the result of ecological and geographic separation of hosts over a long time. However, connections via overlapping flyways exist across the Bering strait and via Iceland and Greenland in the northern Atlantic [65,109]. Thus, AIV genes with an Asian-Australian origin have already been found in wild bird samples in the U.S.A. [110]. Recently, HPAIVs of subtype

H5N8 have been introduced to North America, in 2014 via the Bering strait and H5N1 in 2021 across the Atlantic, causing in both instances devastating outbreaks in American poultry holdings [111–113]. Wild birds can act not only a long distance vector for AIV but also for other viral or bacterial pathogens like the west Nile virus, drug-resistant enteric bacteria as well as the Lyme disease inducing bacterium *Borrelia burgdorferi* [114].

The highest AIV infection rates within wild bird populations was found in geese and ducks [115]. There may be further important reservoirs and species-specific pools as was shown for the subtypes H13 and H16 which are found in shorebirds such as gulls but not in anseriforme wild birds like geese and ducks [115].

As shown in Figure 1, AIV transmission from wild birds to domestic poultry, so-called spill-over infections lead to primary outbreaks. Onward transmission between holdings can start endemic cycles of infections in poultry populations in a region. Virus can of course be transmitted back from poultry to wild bird populations which is referred to as spillback [20].

#### 1.4 Impact of environmental factors on the epidemiology of avian influenza

##### 1.4.1 Viral tenacity and dispersion in surface water

Release and dispersion of AIV with avian feces in surface waters is considered a main mechanism to establish transmission chains within the reservoir host populations of AIV. Little is known about the fate of water-dispersed AIV particles. At least one study succeeded in detecting and even isolating an H1N8 virus in environmental drinking water samples [116].

A plethora of abiotic factors will influence viral tenacity in the environment. Ultraviolet radiation (UV-A and UV-B) does not seem to have a major influence on the viral infectivity in experimental settings as long as the exposure time is less than 30 minutes [117]. However, other studies indicate that (far-)UV-C radiation is able to reduce the infectivity of IAV in aerosols almost completely within seconds of exposure [118–120]. The reduction impact of UV-C-light also depended on the humidity level.

Furthermore, biotic factors, such as microbes, protozoa, and higher animals (mussels, worms etc.) can have a direct influence on the viral dispersion and tenacity in water. For example, water fleas, zebra mussels and snails were found to accumulate influenza virus in their tissues and reduce net viral loads in water; the effect was mostly attributed to filtering enrichment of viral particles [55,121–123]. At least zebra mussels were able to release virus back into fresh water [124]. On the other hand, and for as yet unknown reasons, the presence of shrimps had a prolonging effect on viral tenacity [55].

In the following the focus is on the influence of abiotic factors temperature, pH, salinity and matrix-specific influences [119].

#### 1.4.2 Temperature

Already in the late 1970s WEBSTER and colleagues [125] noted that influenza A virus remains infectious for more than 30 days if virus-contaminated avian feces or untreated water was stored at 4°C. The viral tenacity decreased to 7 days at 20°C (feces) and to 4 days at 22°C (water) [125]. Further experiments of other groups revealed similar results with some strain-specific variations [91]. HPAIV H5N1 was shown to be stable for more than 100 days at 4°C, if virus-containing protein-stabilized water was used but only for 24 h at 28°C [117].

Temperatures above 70°C are deemed sufficient to fully inactivate viral infectivity within less than a minute [126,127].

#### 1.4.3 Salinity

At fixed pH and temperature values, salinity was found to have an impact on viral tenacity. Tenacity decreased when the salinity concentration increased [123,128]. Strain-specific differences may be attributed to the host cell origin of the virus [128].

#### 1.4.4 pH-value

As already mentioned in 1.1.3, the HA undergoes conformational changes depending on pH value to achieve fusion of endosomal and viral membranes to initiate replication. The pH shift induces refolding of the HA protein and exposure of its fusion domain. Refolding is irreversible. Refolded HA cannot be utilized for receptor binding. Thus, virions exposed to low pH values before attaching to and being endocytosed into host cells are rendered non-infective, i.e. inactivated. The optimal pH value achieving conformational changes ranges from pH 4.6 (lysosomes 4.6 – 5.0) to 6.5 (early endosomes 6.0 – 6.5; late endosome 5.0 – 5.5) and is depending on the host species [129]. Point mutations within the H5N1-HA protein, such as N114K and Y23H (pH optimum increases) or H24Q and K58I (pH optimum decreases) modify the pH optimum for refolding of HA [129,130]. These mutations may also lead to modified environmental perseverance, as described for H5N1 [129]. Higher environmental stability of virions at a temperature of 28°C was shown to be linked with a point mutation in the H5N1 HA (H24Q and K58I) which led to a lower HA activation pH value in the endolysosomal cell environment [129,130]. Due to the fact that the optimal HA activation pH value differs between human (lower pH), swine and avian (higher pH) there is a hint that the avian-origin HA needs to undergo an intermediate stabilisation step in swine before jumping to humans [131]. Results

from [117] indicated that the pH-value itself and not the contact time has the main influence on the infectivity of H5N1. H5N1 kept its infectivity at pH 5,7 and 9 regardless of the exposure time of 6, 12, 18 or 24 hours but outside this range infectivity is irreversibly inactivated. An overview of the impact of some specific abiotic factors is given in Table 2.

**Table 2: Impact of abiotic factors on IA**

Factor	Best conditions	Impact	Reference
Temperature [°C]	4 - 17°C (Diluted AAF)	Higher Temperature (> 28°C) have a negative impact	[132]
Salinity [ppm]	Low; no general information available for the 0 - 20,000 ppm range ≥ 25,000 ppm negative impact for all virus strains (Diluted AAF)	Higher ppm values have a negative impact on the viral persistence	[132]
Relative Humidity [%]	17-25%	Low relative humidity and low temperatures are better than higher	[133]
pH-value	7.4 - 8.2 (Diluted AAF)	HA conformation change	[132]

However, in summary, and as shown in Figure 5, virus infectivity significantly depends on temperature, pH-value and water salinity [91].



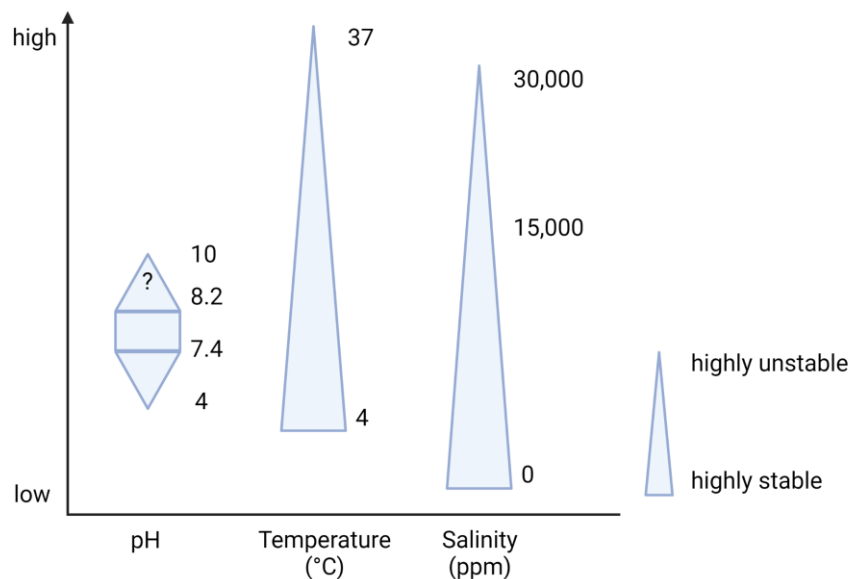


**Figure 5: Tenacity of AIV in surface water with respect to different environmental factors**

According to [91] created with BioRender.com.

### 1.5 Air born transmission of avian influenza virus

Bioaerosols (< 5  $\mu\text{m}$  [48]) comprise all particles of biological origin which are able to be suspended in air [134]. That means that bioaerosols include, among other infectious agents, viruses as well [134]. Due to the fact that livestock production and corresponding farms grow in size and numbers, possible risks of bioaerosols become more aware [134]. The European Union average number of chickens per commercial holding in 2013 was about 43,500 [135]. AIV-RNA could be measured in poultry dust outside of AIV-infected poultry stables [136]. However, some IAV strains were found not to be able to form infectious aerosols [137,138].

If the temperature is under 20°C the AIV-RNA detection rate increases [139]. It is animal experimental proved that IV in general are better transmitted via droplets at 5°C than at 30°C and when the humidity is middle or high [48]. Already between 1983 and 1984 air samples were collected on farms which were coming down with HPAIV in Pennsylvania to investigate epidemiological aspects [140]. Field experiments showed that AIV is present as bioaerosols in the air. The researchers sampled at Hanoi's biggest live poultry market in October 2017 on 10

days (within three weeks) a total air volume of 1200 L per sampler (in total three aerosol samplers). The filtered air as well as the filter cassettes itself were then further treated for RNA extraction and detection. Furthermore, the researchers took swap samples from poultry animals from the market to compare the results. The analysis showed that there is a 90% link between a positive air sample result and a positive swap sample result.[141]

#### 1.5.1.1 Presence and tenacity of AIV in sediments and soils

Although investigations of lake sediments for AIV have been rarely conducted they have shown that virus material can be detected in some sediments and that tenacity of viruses deposited there might be higher than in feces or meat [142]. Sediment analyses could be interesting because excretions from many water bird species over longer period of times are being archived there [142,143]. However, soil and sediments are considered difficult matrices for molecular diagnostic analysis: They have a high density, may contain substances like heavy metal ions, polyphenols and humins which would interfere with RNA isolation and/or PCR enzyme activities [143,144]. Experiments with three (H4N6, H5N1 and H6N8) different LPAIV strains showed, that the viral tenacity, the time span of presence of virus infectivity, depends on the matrix (lake sediment with pH  $7.9 \pm 0.5$  versus duck faeces or duck meat) as well as on the matrix temperature (0, 10, 20 or 30°C) [145]). The results showed that the viruses, with some influence of the specific virus strain, lose up to 90% ( $T_{90}$ ) of their infectivity at 30°C between 2 (duck faeces or meat) to 11 (sediment) days. Lowering the temperature by about 10°C will increase viral perseverance to 3 (H4N6 and H6N8, duck meat) or 7 (H6N8 duck faeces) and up to 18 days (H4N6, sediments). At a temperature of 10°C the  $T_{90}$  time increases up to 12 (H6N8, meat), 21 (H4N6, faeces), and 54 (H6N8, sediments) days. At the lowest temperature (0°C), tenacity was the highest: 81 (H6N8, meat), 75 (H5N1, faeces) and up to 394 days in sediments for H6N8 [145].

#### 1.6 Avian influenza as a zoonotic infection

In principle, IAVs cover a huge host species spectrum, although specific adaptations exist for viruses infecting birds versus mammalian species and human hosts. Host species jumps between the avian and the mammalian world of hosts are regularly encountered as sporadic events. However, only rarely have such events led to the establishment of an adapted, independently circulating lineage in the new host species. In order for an AIV virus to successfully enter and establish itself within the human population, the virus must undergo several changes and adaptations. As shown in Figure 2 avian SIA receptors differ from those of humans. IAV have to be able to access the specific receptors to initiate infection in the

respective host species. The pig, and also some avian species such as quails and turkeys, possess both (human- and avian-like) SIA receptors, which enable these species to act as mixing vessel of IAVs from avian and mammalian hosts. A possible outcome of such mixing leading to new reassortant viruses are influenza pandemics in humans, like the most recent one of 2009 [146,34]. In addition, there are epithelial cells in the lower human respiratory tract that carry  $\alpha$ 2-3 SIA receptors which is why they support AIV replication [147]. Thus, human hosts can be directly infected with AIV, provided an exposure against a large dose of virus, so that some particles reach the lower respiratory tissues.

Moreover, the viruses must adapt to different host body temperatures: While waterfowl has a body temperature of 40°C, humans have a body temperature ranging between 32 (proximal airways) and 37°C (distal airways) [148,149]. A specific AA position in the PB2 protein has been found to regulate the optimum replication temperature of IAV: E627 promotes replication at temperatures above 40°C and is mainly found in avian IAV. K627 in contrast is found predominantly in human IAV and mediates replication at temperatures lower than 37°C [150]. In general, the PB1, PB-2 as well as PA protein forming the RNA-dependent RNA polymerase of IAVs was found to influence virulence and host range [20]. For example, the nuclear import factor importin  $\alpha$  1 regulates binding and transport of IAV RNPs into the cell nucleus in a species-specific way. Mutation D701N of PB2 promotes stronger binding to importin in mammalian cells than in avian cells [151,152].

The antivirally active MxA GPTase poses another obstacle of IAV replication in cells. In humans, MxA effectively prevents replication of non-human IAV. All pandemic IAVs had mutations, mainly in the NP protein, that circumvented the MxA block [153]. Mutations in non-structure protein 1 (NS1) causes the virus to develop resistance to antiviral agents, such as interferon or tumor necroses factor  $\alpha$  [154,147].

The increasing number of (HP) AIV outbreaks increases the risk of species crossing transmission events of H5, H7 and H9 viruses because of a high concentration of virus at the poultry-human interface [55]. Although these viruses are also detected in wild birds, until today, the vast majority of all human-associated infections with HPAIV started via contacts to infected poultry [155,156]. Between 2003 and 2022 (by 22.04.2022), there are at least 863 laboratory-confirmed human cases of HPAIV H5N1 infections reported to the World Health Organization (WHO) [157]. Of these 53% died due to the infection. [157] Until today, there are eleven AIV subtypes which are able to spill over sporadically to humans [17].

### 1.6.1 Recent HPAI epidemics in Europe

During the last decade (2012 - 2022), there were several large waves of HPAI outbreaks sweeping through Europe as outlined in Table 3. Most of these waves were due to HPAIV of the goose/Guangdong lineage of H5 viruses originating in southern China in domestic geese in 1996 [7,158] . Incursion to Europe was predominantly with migratory wild birds during autumn migration along the East Atlantic flyway. Since summer 2021, a trend toward increased detection of HPAIV in wild birds during summer months became visible [159]. This raised fears of an annual entrenchment of these HPAIVs in metapopulations of European wild birds.

**Table 3: Overview of some recent avian influenza epidemics of clade 2.3.4.4b in Europe**

Year/ Season	Strain	Affected countries	Affected wild bird species	Human infection	References
2016/ 2017	HPAIV H5N8	29 European countries (most effected country: France with 484 poultry outbreaks)	At least 12 different species were affected (among others: Common pochard, Tufted duck, Great crested grebe, Eurasian teal, Eurasian wigeon)	12 Not reported	[11,106,160]
2020/ 2021	HPAIV H5N8, H5N1, H5N3, H5N4, H5N5	31 European countries, approx. 22,900,000 heads of poultry were culled from October 2020 until September 2021.	At least 33 different species (mute swans, barnacle geese, red knots, various birds of prey. Furthermore, a few harbour seals and scavenging terrestrial mammals (foxes, otters, mustelids)	7 poultry workers (HP H5N8),	[14,20,161,162]
2021/ 2022	HPAIV H5N1	At least 33 European countries affected, France and Hungary most heavily hit	Same range as 2020/21. In summer 2022 colony-breeding sea birds affected for the first time	One each in the UK and the U.S.A.: HP H5N1	[163,164]

## 2 Study objectives

### 2.1.1 Questions and approach

AIV has the ability to cross species barriers and may infect human hosts. Highly pathogenic variants of AIV induce severe disease and high mortality in many poultry species leading to substantial economic losses. Due to the reservoir function of wild bird populations no final eradication of these agents is feasible. As such, preventive measures are key to protect poultry as well as wild bird populations from reciprocal spill-over infection events. A full understanding of epidemiological features and, in particular, spreading mechanisms of these viruses is mandatory to optimize preventive measures.

Until today, the role of surface water for AIV transmission is not fully explored. This is partly due to the fact that appropriate techniques for concentrating and purifying viruses from water sources are lacking.

This study was designed to address

- (i) improved diagnostic RT-qPCRs for detection of AIV,
- (ii) the design and operation of a filtering system to enrich AIV from natural water sources as a means of active surveillance in order to assess the role of surface and drinking water for virus transmission in infection experiments and in the field,
- (iii) the minimum AIV concentration in surface water to initiate infection of aquatic wild birds.

### 3 Publications

#### **3.1 Improved Subtyping of Avian Influenza Viruses Using an RT-qPCR-Based Low Density Array: ‘Riems Influenza a Typing Array’, Version 2 (RITA-2).**

Kareem E Hassan, [Ann Kathrin Ahrens](#), Ahmed Ali, Magdy F El-Kady, Hafez M Hafez, Thomas C Mettenleiter, Martin Beer, Timm Harder





Viruses

Viruses 2022, 14 (2), 2022

doi: 10.3390/v14020415

Article

# Improved Subtyping of Avian Influenza Viruses Using an RT-qPCR-Based Low Density Array: 'Riems Influenza a Typing Array', Version 2 (RITA-2)

Kareem E. Hassan <sup>1,2</sup>, Ann Kathrin Ahrens <sup>1</sup>, Ahmed Ali <sup>2</sup>, Magdy F. El-Kady <sup>2</sup>, Hafez M. Hafez <sup>3</sup>, Thomas C. Mettenleiter <sup>4</sup>, Martin Beer <sup>1</sup> and Timm Harder <sup>1,\*</sup>

<sup>1</sup> Institute of Diagnostic Virology, Friedrich-Loeffler-Institut, 17493 Greifswald-Insel Riems, Germany; kareem\_eid@yahoo.com (K.E.H.); annkathrin.ahrens@fli.de (A.K.A.); martin.beer@fli.de (M.B.)

<sup>2</sup> Department of Poultry Diseases, Faculty of Veterinary Medicine, Beni-Suef University, Beni-Suef 62511, Egypt; ali.178w@yahoo.com (A.A.); mfelkady@yahoo.com (M.F.E.-K.)

<sup>3</sup> Institute of Poultry Diseases, Free University Berlin, 14163 Berlin, Germany; hafez.mohamed@fu-berlin.de

<sup>4</sup> Friedrich-Loeffler-Institute, 17493 Greifswald-Insel Riems, Germany; thomas.mettenleiter@fli.de

\* Correspondence: timm.harder@fli.de; Tel.: +49-(0)-3-8351-71546

**Abstract:** Avian influenza virus (AIV) variants emerge frequently, which challenges rapid diagnosis. Appropriate diagnosis reaching the sub- and pathotype level is the basis of combatting notifiable AIV infections. Real-time RT-PCR (RT-qPCR) has become a standard diagnostic tool. Here, a total of 24 arrayed RT-qPCRs is introduced for full subtyping of 16 hemagglutinin and nine neuraminidase subtypes of AIV. This array, designated Riems Influenza A Typing Array version 2 (RITA-2), represents an updated and economized version of the RITA-1 array previously published by Hoffmann et al. RITA-2 provides improved integration of assays (24 instead of 32 parallel reactions) and reduced assay volume (12.5 µL). The technique also adds RT-qPCRs to detect Newcastle Disease (NDV) and Infectious Bronchitis viruses (IBV). In addition, it maximizes inclusivity (all sequences within one subtype) and exclusivity (no intersubtypic cross-reactions) as shown in validation runs using a panel of 428 AIV reference isolates, 15 reference samples each of NDV and IBV, and 122 clinical samples. The open format of RITA-2 is particularly tailored to subtyping influenza A virus of avian hosts and Eurasian geographic origin. Decoupling and re-arranging selected RT-qPCRs to detect specific AIV variants causing epizootic outbreaks with a temporal and/or geographic restriction is possible.

**Keywords:** avian influenza; diagnosis; real-time RT-PCR; Newcastle disease virus; infectious bronchitis virus



**Citation:** Hassan, K.E.; Ahrens, A.K.; Ali, A.; El-Kady, M.F.; Hafez, H.M.; Mettenleiter, T.C.; Beer, M.; Harder, T. Improved Subtyping of Avian Influenza Viruses Using an RT-qPCR-Based Low Density Array: 'Riems Influenza a Typing Array', Version 2 (RITA-2). *Viruses* **2022**, *14*, 415. <https://doi.org/10.3390/v14020415>

Academic Editor: Feng Li

Received: 29 December 2021

Accepted: 15 February 2022

Published: 17 February 2022

**Publisher's Note:** MDPI stays neutral with regard to jurisdictional claims in published maps and institutional affiliations.



**Copyright:** © 2022 by the authors. Licensee MDPI, Basel, Switzerland. This article is an open access article distributed under the terms and conditions of the Creative Commons Attribution (CC BY) license (<https://creativecommons.org/licenses/by/4.0/>).

## 1. Introduction

Highly pathogenic avian influenza virus (HPAIV) is the major pathogen associated with substantial economic losses in poultry production. Zoonotic AIV strains, in addition, have caused multiple cases of human infections, sparking influenza pandemic concerns [1]. The influenza A virus genome consists of eight single-stranded RNA gene segments. Two segments encode the major envelope glycoproteins species of these viruses, hemagglutinin (HA) and neuraminidase (NA). These proteins have essential functions in defining host and tissue tropism and influence virulence. The HA, in particular, is a main target of the protective humoral immune response. Based on nucleotide sequence and protein antigenicity of the HA and NA surface glycoproteins, AIVs are classified into 16 different HA (H1–H16) and 9 NA subtypes (N1–N9) [2,3]. The distinctive segmental structure of influenza virus genomes enables reassortment of segments if the same host cell is infected by two (or more) different parental viruses. Theoretically, 144 combinations between HA and NA may result. However, not all of these have actually been detected in nature as there seem to be predilections of certain HA and NA combinations [4]. Moreover, there



is a continuous turnover, with temporal and geographical restrictions, of different AIV subtypes and their variants in the reservoir hosts as in aquatic wild bird populations [5]. Spill-over infections into poultry populations, often starting endemic transmission chains with similar reassortment events, widen the replication basis of these viruses. Error-prone viral genome replication drives genetic drift and further increases genetic and antigenic variability [1,4]. In summary, these processes present a continuous challenge not only for the immune system of the avian hosts but also for accurate and rapid laboratory diagnosis.

Swift and exact diagnosis of AIV infections in poultry populations is pivotal to inform veterinary authorities and steer restriction measures if notifiable AIV subtypes, i.e., H5 and H7, are detected. Adequate control of zoonotic AIV infections in poultry populations is also the most important measure to limit exposure of human populations to these viruses [6]. Aquatic wild birds play a major role in the evolution, maintenance, and spread of AIV. Therefore, optimized surveillance of reservoir populations is important to follow viral evolutionary trajectories [7]. Conventional techniques for AIV diagnosis include virus isolation in embryonated chicken eggs, serological characterization of virus isolates, and animal experiments to define viral pathogenicity [4]. Time until final diagnosis using these methods may take up to two weeks. Minimizing time until diagnosis, therefore, is the main objective of new diagnostic developments. Rapid antigen detection assays based on lateral flow immunochromatography were particularly successful in this respect but lacked sensitivity [8–10] when compared to reverse transcriptase-polymerase chain reaction (RT-PCR) and especially time-saving real-time RT-PCR technologies (RT-qPCR). Thus, RT-qPCRs have become new standards [11–15]. These include RT-qPCRs for generic AIV detection, subtyping, and pathotyping where the latter are targeting the HA cleavage site [16–18].

In 2016, Hoffmann et al. [16] published an assay assembling several subtype-specific RT-qPCRs into a low-density PCR array, designated as the ‘Riems Influenza A Typing Array’ (RITA). RITA enabled AIV RNA detection at subtype level in clinical samples by providing a generic, internally controlled M gene-specific duplex RT-qPCR and a further 31 monoplex TaqMan<sup>®</sup>-based RT-qPCRs to differentiate 14 HA and nine NA subtypes. Although RITA proved suitable for use in routine diagnostic applications, shortcomings in terms of minor cross-reactivities between closely related subtypes (e.g., H2/H5, H7/H10/H15, H1/H6) were noted. These effects caused subtle problems in ruling out co-infections with several AIV subtypes. In addition, the demand to performing in parallel 32 single RT-qPCRs might have a repelling effect on potential users.

In this study, an updated and improved version of RITA (syn. RITA-2) is developed and validated. The new version considers grossly enlarged databases of Eurasian AIV sequences since 2015, when the previous RITA version was designed. Intersubtypic cross-reactions have been abrogated by re-designing primers and probes so as to select target locations that were less conserved between the subtypes. Many primers and probes have been newly established so as to also meet the growing demands for full inclusivity of all Eurasian virus sequences of a certain subtype available in public databases. The revised version also achieved a higher degree of assay integration by using multiplexing of RT-qPCRs more stringently. Space on the array was economized to accommodate four instead of three clinical samples per 96-well array plate and to include all 16 HA and nine NA AIV subtypes in addition to an influenza A generic RT-qPCR. Also, targets for other important avian pathogens, Newcastle Disease virus (NDV) and Infectious Bronchitis virus (IBV), have been added to the design for differential diagnostic means. In addition, we show how the RITA-2 array can be used as an “assay mine” and single reactions be decoupled and recombined into much smaller arrays tailored to routine diagnosis during HPAIV epizootics.

## 2. Materials and Methods

### 2.1. Viruses

RNA extracted from 428 influenza viral strains representing 16 HA and nine NA subtypes pre-typed (either serologically or by sequencing) at the National Reference Laboratory for Avian Influenza, Friedrich-Loeffler-Institut (NRL-AI, FLI, Isle of Riems, Germany) were used for analytical validation of the newly developed assays. Table 1 provides a condensed overview of the subtypes used and their species of origin. In addition, fifteen reference isolates each for IBV and NDV viruses were used for re-evaluation of previously established IBV and NDV RT-qPCR assays (Table S1).

**Table 1.** Collection of influenza A virus strains of different host origin and differing subtypes (hemagglutinin, HA, and neuraminidase, NA) used for evaluation of real-time RT-PCRs.

Subtype	Number of Samples	Host				
		Avian	Human	Porcine	Equine	Unknown
H1	63	10	17	32		4
H2	20	19	1			
H3	52	25	11	15	1	
H4	20	20				
H5	53	53				
H6	67	67				
H7	42	40			1	1
H8	5	5				
H9	43	29				14
H10	32	30		2		
H11	14	12			1	1
H12	1	1				
H13	10	10				
H14	1	1				
H15	1	1				
H16	4	4				
HA, total	428	327	29	49	3	20
N1	144	93	17	30		4
N2	125	88	11	12		14
N3	29	29				
N4	10	10				
N5	6	5				1
N6	28	23		4		1
N7	38	34		3	1	
N8	37	36			1	
N9	11	9	1		1	
NA, total	428	327	29	49	3	20

### 2.2. Clinical Material

Oropharyngeal and cloacal swabs collected from diseased or freshly dead birds were submitted to the NRL-AI. Egyptian samples consisted of pools of 15 to 20 swabs from each flock of poultry and were collected from duck, chicken, and turkey farms in Egypt during

2018 and from Egyptian chicken flocks during early 2019 (47 samples in total). Samples were suspended in 2 mL of phosphate-buffered saline (PBS), pH 7.0–7.4, and clarified by centrifugation at 4000 rpm for 10 min at the Department of Poultry Diseases (Beni-Suef University, Beni Suef, Egypt). About 200 µL of clarified supernatant were uploaded on Whatman® FTA® Cards (Merck, Darmstadt, Germany) and sent to NRL-AI at FLI, Germany. In addition, oro-nasal and cloacal swabs collected from clinically healthy duck flocks from Bangladesh during 2019 were included (13 samples in total) as well as routine diagnostic samples submitted for diagnosis during HPAI epizootics in Germany ( $n = 62$ ; Table S2).

### 2.3. Primers and Probes

Primers and probes reported for version 1 of the RITA array were double-checked against the EpiFlu database of GISAID (<http://platform.gisaid.org>), the International Nucleotide Sequence Data Collaboration IRD (<http://www.fludb.org>) sequence databases or against comprehensive alignments of HA and NA sequences built from these. Sequences were handled using the Geneious software, version 11.1.7 [19]. Alignment and identity matrix analyses were generated using MAFFT [20] and manually edited with AliView [21]. The focus of searches and comparisons was on sequences added to the databases since 2015. The chemical properties of preselected oligos were analyzed by the OligoCalc software [22]. Oligos were synthesized by Metabion GmbH (Martinsried, Germany) and Eurogentec (Liège, Belgium). Oligos were solubilized to produce stock solutions of 100 pmol µL<sup>-1</sup> and stored at -20 °C until use. For use in PCRs, stock solutions were diluted to give a final concentration of 5–20 pmol µL<sup>-1</sup> depending on individual reactions as shown in Table 2.

Table 2. The final design of primers and probes used for assembling the RITA-2 array.

Subtype	Designation	Sequence 5'→3'	Amount <sup>1</sup>	Reference
Pan AI assay	M1-F	AGA TGA GYC TTC TAA CCG AGG TCG	20.0 µL	[4,15]
	M1-FAM	FAM-TCA GGC CCC CTC AAA GCC GA-BHQ1	2.5 µL	
	M1-R1	TGC AAA AAC ATC TTC AAG TYT CTG	15.0 µL	
	M1-R2	TGC AAA GAC ACT TTC CAG TCT CTG	15.0 µL	
	M1-R3	TGC AAA I(Inosine)AC ATC YTC AAG TYT CTG	7 µL	
H1 assay	H1-F1	CCA TCT GTA TAG GCT AYC AT	20 µL	This study <sup>2</sup>
	H1-F2	AAA CAT YCC TTC CRT TCA ATC	20 µL	
	H1-FAM1	FAM-TAC AGA CAC TGT YGA CAC DGT GCT-BHQ1	5 µL	
	H1-FAM2	FAM-TTC ATT GAA GGR GGR TGG ACA GGA AT-BHQ1	5 µL	
	H1-R1	GTG AGT CAC RGT YAC ATT CTT	20 µL	
H2 assay	H1-R2	GAG CAA GGI TCY GGT TAT G	20 µL	This study <sup>2</sup>
	H2-F	CTA AST GTR CCW GAA TGG TC	40 µL	
	H2-R	GAG GTG TTT CAR TTC YTC RTA	40 µL	
H3 assay	H2-FAM	FAM-TGT GCT ACC CAG GYA GTT TCA ATG A-BHQ1	8 µL	This study <sup>2</sup>
	H3-F1	CCT CGR GGC TAY TTC AAR AT	15 µL	
	H3-F2	AGA CTG GAT CYT RTG GAT TTC	15 µL	
	H3-F3	CTG GGR CAC CAT GCA GT	15 µL	
	H3-FAM1	FAM-TGC ATC TGA YCT CAT TAT YGA RCT TTT-BHQ1	4 µL	
	H3-FAM2	FAM-ACR CAA AGC AAA AAG CAT GAT ATG GC-BHQ1	4 µL	
	H3-FAM3	FAM-ACA GGG AAA ATA TGC ARC AAT CCY CA-BHQ1	4 µL	
	H3-R1	ATT TGG RGT GAT RCA TTC AGA	15 µL	
H4 assay	H3-R2	CTC AAA TGC AAA TGK TGC AYC	15 µL	This study <sup>2</sup>
	H3-R3	TGT GCA GTC YCT TCC ATC	15 µL	
	H4-F1	ACYCAGGRTACAAGGACA	20 µL	
	H4-F2	GGA CAT CAT YCT YTG GAT TTC	20 µL	
	H4-FAM	FAM-TCC ATA TCA TGC TTY TTG CTY GTA GC-BHQ1	4 µL	
	H4-R	CAA GCC CAC AAA AYR AAG G	40 µL	

Table 2. Cont.

Subtype	Designation	Sequence 5'→3'	Amount <sup>1</sup>	Reference
H5 assay	H5-HA1-F	GAT TYT AAA RGA TTG TAG YGT AGC	20 µL	This study <sup>2</sup>
	H5-FAM3-RC	FAM-CGC ACA TTG GRT TYC CRA GGA GCC-BHQ1	6 µL	
	H5-HA1-R1	CTC TCY ACC ATG TAR GAC CA	15 µL	
	H5-HA1-R2	CTC TCY ACT ATG TAR GAC CA	15 µL	
	H5-F2	GTT CCC TAG YAY TGG CAA TCA T	20 µL	
	H5-FAM2	FAM-CTG GTC TAT YTT TRT GGA TGT GCT CC-BHQ1	6 µL	
H6 assay	H5-R2	AAT TCT ARA TGC AAA TTC TGC AYT G	15 µL	This study <sup>2</sup>
	H6-F1	TTG GYG TGT ATC AAA TYC TTK C	20 µL	
	H6-F2	TTG RCG TGT ATC AAA TAC TTG C	20 µL	
	H6-FAM	FAM-AGR CTG CTC GAY ACC GTA CTA TAA A-BHQ1	10 µL	
H7 assay	H6-R	TTGA RCY ATT TGA ACA CAT CCA	40 µL	This study <sup>2</sup>
	H7-F	CAA CTG AAA CRG TRG ARC G	45 µL	
	H7-FAM	FAM-CCC AGG ATY TGC TCA ARA GGR AAA A-BHQ1	10 µL	
	H7-R1	CAG GAG YCC ACA TTG ACC	15 µL	
	H7-R2	CAG WAG YCC ACA TTG ACC	15 µL	
H8 assay	H7-R3	TTC TAG GAA TTG GTC ACA TTG	15 µL	This study <sup>2</sup>
	H8-F	CCA CCT AYA AAA TTC TCA GCA	40 µL	
	H8-FAM	FAM-TGC CAA GCA RAG ACT GGC CGC CA-BHQ1	4 µL	
H9 assay	H8-R	ARA CCT CCA GCA AYC AGG A	40 µL	This study <sup>2</sup>
	H9-F1	CAA TGG GGT TYG CTG CCT	20 µL	
	H9-F2	CAA TGG GRK TTG CTG CCT	20 µL	
	H9-FAM	FAM-TTY TGG GCC ATG TCI AAT GGR TC-BHQ1	6 µL	
H10 assay	H9-R	TTA TAT ACA RAT GTT GCA YCT G	40 µL	[23]
	H10-F	CAA CTC AGR CAG AAT GCW GA	40 µL	
	H10-FAM	FAM-TGC ATG GAG AGY ATA AGR AAC AAC AC-BHQ1	6 µL	
H11 assay	H10-R	CTT CYT CTC TGT AYT GTG AAT G	40 µL	This study <sup>2</sup>
	H11-F	GGA CAT ATG AYC ACA ARG AAT T	40 µL	
	H11-FAM	FAM-ACT GTC RAT TTA CAG CTG CAT YGC A-BHQ1	8 µL	
H12 assay	H11-R	ATG CAA ATG GTA CAT CTA CAT G	40 µL	This study <sup>2</sup>
	H12-F	CAT CTA CAG CAG YGT YGC	40 µL	
	H12-FAM	FAM-ACT GCT CAT GAT TAT TGG GGG TTT CA-BHQ1	12 µL	
H13 assay	H12-R	GAA AGT ACA ACG AAC ATT TCC A	40 µL	This study <sup>2</sup>
	H13-F1	CTT AAG CAC AAA CTC ATC AGA A	15 µL	
	H13-F2	CTG AGC ACC AAT TCA TCA GA	15 µL	
	H13-F3	CTT AAG CAC AAA CTC ATC AGA A	15 µL	
	H13-FAM1	FAM-CKA ACC ACA CRG GAA CAT AYT GTT C-BHQ1	5 µL	
	H13-FAM2	FAM-CAC ACI GGA ACA TWC TGT TCA ATC A-BHQ1	5 µL	
H14 assay	H13-R1	CTG GCA CAG GCA GGG TT	20 µL	This study <sup>2</sup>
	H13-R2	CCY ACA ATC CAT CCT TCA AA	20 µL	
	H14-F	CCC AAT ATA GGA AGT AGA CC	40 µL	
H15 assay	H14-HEX	HEX-AAG CAT CTA CTG GAC YCT AGT AAA CC-BHQ1	6 µL	This study <sup>2</sup>
	H14-R	CTT CTT GTC ACT TYT AAG CAC	40 µL	
	H15-F	CAS CTT TCT CCG CTC TAA TG	40 µL	
H16 assay	H15-FAM	FAM-CAC TGG GAA TAC AGA GTG ATG CAC AA-BHQ1	3 µL	This study <sup>2</sup>
	H15-R	AAR CAT TCC CCT TCA CAT GA	40 µL	
H16 assay	H16-F	ARY TGA AGA CTG AAG ACA ATG T	40 µL	This study <sup>2</sup>
	H16-HEX	HEX-CTG GTA GGW CTC ATA CTY GCA TTT AT-BHQ1	6 µL	
	H16-R	CCA CTG CTG CAT GCC CA	40 µL	

Table 2. Cont.

Subtype	Designation	Sequence 5'→3'	Amount <sup>1</sup>	Reference
N1 assay	N1-F	GRC CTT GYT TCT GGG TKG A	40 µL	This study <sup>2</sup>
	N1-FAM	FAM-CAA TYT GGA CYA GTG GRA GYA GCA T-BHQ1	6 µL	
	N1-R	ACC GTC TGG CCA AGA CCA	40 µL	[16]
N2 assay	N2-F1	AGTC TGG TGG ACY TCA AAY AG	20 µL	[16]
	N2-F2	CAG AGT RTG GTG GAC ITC	20 µL	[23]
	N2-FAM	FAM-CAT CAG GCC ATG AGC CTG TYC CAT-BHQ1	4 µL	
	N2-R	TTG CGA AAG CTT AYA TNG VCA T	40 µL	
	N3-F	GCA AYA GTA TAG TTA CYT TCT G	40 µL	This study <sup>2</sup>
N3-FAM	FAM-AGA CAA TGA ACC TGG ATC GGG VAA-BHQ1	3 µL		
N3-R1	TTA CTT GGG CAT RAA CCC AAT	20 µL		
N4 assay	N3-R2	GTT GGM ACC RTC WGG CCA	20 µL	This study <sup>2</sup>
	N4-F1	GAC TAG YGG TAG TAG YAT TGC	20 µL	
	N4-F2	AGT AGY ATT GCR TTY TGT GGT GTT	20 µL	[16]
	N4-HEX	HEX-TGG TCR TGG CCY GAT GGC GCT CT-BHQ1	6 µL	This study <sup>2</sup>
N4-R	CGA AAA ATY ACT TGT CTA TGT CAA	40 µL		
N5 assay	N5-F1	CCT TCA GAA TGC AGR ACY TT	20 µL	This study <sup>2</sup>
	N5-F2	CAA ATA ATA CAG TAA ARG ACA GAA G	20 µL	
	N5-HEX	HEX-TAA TGA GCG TRC CAT TGG GAT CCT C-BHQ1	6 µL	
	N5-RR	TAG CAG ACC AYC CRA CGG A	40 µL	[16]
	N6-F1	GGT GAM AAT GAA YCC AAA YCA	15 µL	
N6 assay	N6-F2	AAT GAA YCC AAA YCA RAA GAT AA	15 µL	This study <sup>2</sup>
	N6-F3	GAA AAT GAA TCC AAA TCA RAA GRT A	15 µL	
	N6-FAM	FAM-CAT YTC AGC IAG GAR TRA CAC TAT C-BHQ1	12 µL	
	N6-R1	CTT RTA RTG RAG TCC GAT GTT	15 µL	[16]
	N6-R2	GAT TCC TAT YAG SAG GCT TAC	15 µL	
	N6-R3	GAT TCC TAT YAG SAI ICT TAC	15 µL	
	N7-F1	GTT GAA TTA ATW AGA GGA AGR CC	20 µL	
N7 assay	N7-F2	AGA GGC YAA ATA YGT RTG GTG	20 µL	This study <sup>2</sup>
	N7-FAM	FAM-CCT ATG TGG RAG CCC ATT CCC AGT-BHQ1	3 µL	
	N7-R	GA TYT GTG CCC CAT CRG GGA	40 µL	[16]
N8 assay	N8-F1	TCC ATG YTT TTG GGT TGA RAT GAT	15 µL	[16]
	N8-F2	CTG ATC TCT CTT ACA GGG TTG	15 µL	This study <sup>2</sup>
	N8-F3	TCC ATG YTT TTG GGT IGA AAY GAT	15 µL	[16]
	N8-FAM1	FAM-TCH AGY AGC TCC ATT GTR ATG TGT GGA GT-BHQ1	6 µL	[16]
	N8-FAM2	FAM-TGC CCA GTG ACA CTC CAA GAG GGG AA-BHQ1	6 µL	This study <sup>2</sup>
	N8-R1	GCT CCA TCR TGC CAY GAC CA	20 µL	[16]
	N8-R2	GTG CAT GAA CCG ACA AAT TGA G	20 µL	This study <sup>2</sup>
N9 assay	N9-F	AGY ATA GTA TCR ATG TGT TCC AG	40 µL	[14]
	N9-FAM	FAM-TTC CTR GGA CAA TGG RAC TGG CC-BHQ1	3 µL	[16]
	N9-R	GTA CTC TAT TYT AGC CCC RTC	40 µL	This study <sup>2</sup>
NDV assay	NDF	GAG CTA ATG AAC ATT CTT TC	12.5 µL	[23]
	NDR	AAT AGG CGG ACC ACA TCT G	12.5 µL	
	ND-FAM1	FAM-TCA TTC TTT ATA GAG GTA TCT TCA TCA TA-BHQ1	4 µL	
	ND-FAM2	FAM-TCA TAC ACT ATT ATG GCG TCA TTC TT-BHQ1	4 µL	

Table 2. Cont.

Subtype	Designation	Sequence 5'→3'	Amount <sup>1</sup>	Reference
IBV assay	IBV-F1	CAG TCC CDG ATG CNT GGT A	25 µL	[24]
	IBV-F2	CAG TCC CDG ACG CGT GGT A	25 µL	
	IBV-F3	GCT TTT GAG CCT AGC GTT	5 µL	
	IBV-FAM1	FAM-ACT GGA ACA GGA CCD GCC GCT GAC CT-BHQ1	6 µL	
	IBV-FAM2	FAM-CAC CAC CAG AAC CTG TCA CCT C-BHQ1	2 µL	
	IBV-R1	CCT TWS CAG MAA CMC ACA CT	25 µL	
	IBV-R2	GCC ATG TTG TCA CTG TCT ATT G	5 µL	
IC-2	EGFP-1-F	GAC CAC TAC CAG CAG AAC AC	5 µL	[25]
	EGFP-10-R	CTT GTA CAG CTC GTC CAT GC	5 µL	
	EGFP-HEX	HEX-AGC ACC CAG TCC GCC CTG AGC A-BHQ1	3.75 µL	

<sup>1</sup> A stock mix of 200 µL was produced for each assay; the amount in µL of a 100 pmol µL<sup>-1</sup> solution of each primer and probe for the stock mix is given here. 0.1 × TE buffer was then added up to a final volume of 200 µL. Finally, 1 µL of the stock mix was used per PCR reaction. <sup>2</sup> Positions shown in red have changed in comparison to the RITA-1 array. Oligonucleotides shown completely in red have been newly designed in this study. IC—Internal control system based on an RNA run-off transcript of a fragment of the EGFP gene [25].

#### 2.4. RNA Extraction

Viral RNA was extracted from infected MDCK cell cultures supernatants or allantoic fluids of embryonated chicken eggs using the NucleoMag<sup>®</sup>VET Kit (Macherey-Nagel GmbH & Co. KG, Düren, Germany) according to the manufacturer's instructions. Clinical material (swab samples) was extracted manually using the Qiagen Viral RNA kit (Qiagen, Hilden, Germany) or by the Qiagen MagAttract Kit operated on a KingFisher Biosprint96 device (Qiagen). Samples sent on FTA cards were extracted as described by [26], using the QIAamp Viral RNA Mini Kit (Qiagen). Nucleic acids were eluted in 70 µL of nuclease-free water, and aliquots of 10 µL were stored at −20 °C until use.

#### 2.5. Plate Design

The layout of the RITA-2 array aimed at economizing space by integrating several targets into duplex PCR reactions. As depicted in Figure 1a, the layout allows the testing of four samples simultaneously on one plate. Batches of plates ready-for-use were prepared and stored at −20 °C by pipetting 1 µL of primer-probe stock mixes into the fixed positions as shown in Figure 1a before freezing.

In the same way, strips of eight or four wells were prepared with single PCR reactions decoupled from the RITA-2 design and recombined with previously published pathotyping RT-qPCRs H5-LP, H5-HP Pan, H5-HP 2.3.4.4 [17] or H7-LP and H7-HP [18] (Figure 1b).

#### 2.6. Set-Up of RT-qPCR Reactions

RT-qPCRs were run on a Bio-Rad CFX 96 real-time PCR machine (Bio-Rad, Munich, Germany) in the 96-well format using the AgPath-ID One-Step kit (Applied Biosystems, Foster City, CA, USA) and non-skirted, low profile, white qPCR 96-well plates (RT-PL96-OPWSA, Eurogentec, Liège, Belgium). For 8- and 4-well designs (Figure 1b) also 0.2 mL 8-Tube PCR Strips (low profile, white #TLS0851, Bio-Rad, Munich, Germany) were used. A heterologous internal control system (IC-2) was used to check the performance of reverse transcription and PCR amplification [26]. Details of the reaction mix set-up are shown in Table 3, whereas × should be understood as multiplication sign. Primer-probe stock mixes had already been pipetted into plates at fixed positions, as shown in Figure 1. Fully prepared plates were sealed and kept frozen at −20 °C until use. Plates were prepared in batches of 20–40 plates. The total PCR volume of a single reaction comprised 12.5 µL to which 2.5 µL of extracted RNA was added. CFX96 machines were programmed as follows: Reverse transcription 45 °C for 10 min, initial denaturation 95 °C for 10 min, 45 cycles of denaturation 95 °C for 15 s, annealing/reading (of FAM and HEX channels) 56.5 °C for 20 s, and elongation 72 °C for 30 s. The C<sub>q</sub> threshold was set to <40.

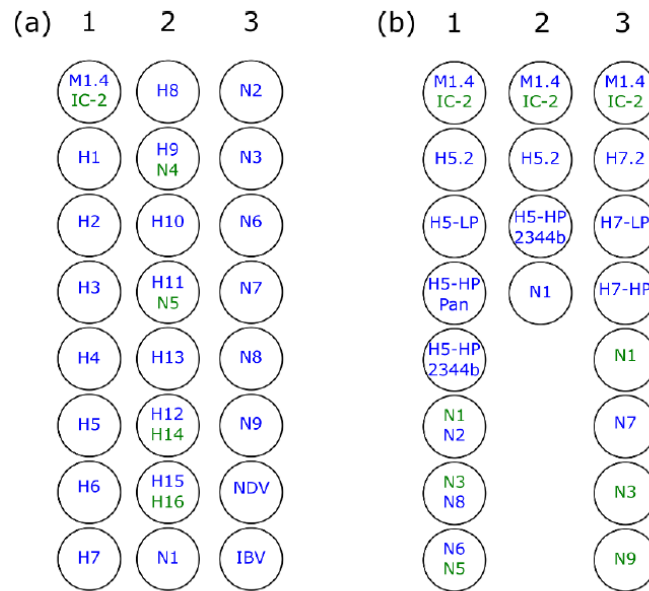


**Figure 1.** (a) 24-well plate layout (1–3) of the RITA-2 array allowing simultaneous testing of four clinical samples on a whole 96-well plate. Some reactions were decoupled from the RITA-2 format and newly recombined with additional reactions in eight- and four-well format for use in routine diagnostics tailored for epizootic outbreaks of notifiable AIV (b) 1- Eight-well layout for sub- and pathotyping of Eurasian H5 viruses, 2- Four-well layout for sub- and pathotyping of viruses encountered during the current (autumn 2021) HPAIV H5N1 epizootic, 3- Eight well layout for sub- and pathotyping of Eurasian H7 viruses. Subtype color indicates the type of reporter dye, blue—FAM, green—HEX.

**Table 3.** Reaction volumes used for individual and arrayed RT-qPCRs.

RNA/Masternix AgPath-ID™ One-Step RT-PCR	Single Reaction	24 Reactions (1 Sample)	96 Reactions (4 Samples)
	1×	26×	100×
RNase free water	2.25 µL	58.5 µL	225 µL
2× RT-PCR Buffer	6.25 µL	162.5 µL	625 µL
RT-PCR Enzyme Mix	0.5 µL	13 µL	50 µL
Primer-Probe mix <sup>1</sup>	1 µL	26 µL	100 µL
Sample RNA	2.5 µL	65 µL	2.5 µL/well
<b>Total volume</b>	<b>12.5 µL</b>	<b>299 µL</b>	<b>1000 µL</b>
Template	2.5 µL/well	2.5 µL/well	2.5 µL/well

<sup>1</sup> Primer-probe mixes had already been pipetted into plates at fixed positions as shown in Figure 1.

### 2.7. Preparation of Positive Controls

Different plate batches were evaluated by a set of four positive controls, each consisting of RNA of five different viruses, as shown in Table 4. RNA of individual viruses was mixed in RNA safe buffer [16] (0.05% *v/v* Tween 20, 0.05% *w/v* sodium azide, 50 ng µL<sup>-1</sup> of carrier RNA [poly(A) homopolymer; Amersham Biosciences, Piscataway, NJ, USA]) to ensure a C<sub>q</sub> value of 28–32 in the M-PCR. PTCs were frozen at −80 °C until use. The

identification of strains used to compile the PTCs is given in Supplementary Materials Table S2. Each batch of plates was also checked with a no-template control.

Table 4. Identity of virus isolates used as positive controls for RITA-2 batch evaluations.

Positive Control	Subtype	Strain	Cq Value/Reaction
PTC-1	H1N1	A/Mallard/Germany/R193/09	23–25
	H5N6	A/White stork/Germany/AR251/2018	21–23
	H9N2	A/Chicken/Egypt/AR538/2017	22–25
	H13N8	A/Larus ridibundus/Germany/R2064/2006	24–26
	IBV-1	AI20298/2019	23–25
PTC-2	H2N3	A/Mallard/Germany/Wv677/04	23.65–25
	H6N2	A/Turkey/Mass/3740/65	22–24
	H10N7	A/Mallard/Germany/1490/09	22–24
	H14N5	A/Mallard/Gurjev/263/82	26–27
	IBV	AI20298/2019	23–25
PTC-3	H3N8	A/Mallard/Germany/R1648/07	23–25
	H7N7	A/Greylag goose/Germany/AR942/2015	22–24
	H11N9	A/Mallard/Föhr/Wv1499-1503/03	22–24
	H15N9	A/Shearwater/West Australia/2576/79	22–24
	NDV-1	ND/Lentogenic/713/2016	22–24
PTC-4	H4N6	A/Mallard/Germany/R485/3/08	21–23
	H8N4	A/Anas platyrhynchos/Germany/R2167/2009	22–24
	H12N5	A/Duck/Alberta/60/76	21–23
	H16N3	A/Herring gull/Germany/R2788/06	23–25
	NDV-2	ND/Velogenic	22–24

### 2.8. Statistical Analyses

Statistical analyses for sensitivity, specificity, intra-, and inter-assay variation were performed using the SigmaPlot software, version 11 (Systat Software Inc., Duesseldorf, Germany). Spearman's rank correlation and Student's t-test were employed.  $p < 0.05$  was considered significant.

## 3. Results

### 3.1. Evaluation and Selection of Oligonucleotide Sets

In silico analyses of comprehensive sequence alignments for each HA and NA subtype of Eurasian origin revealed, for the majority of subtypes, a within-subtype variation that was too wide to be covered by a single set of primers and probe; inclusion of sequences of American or Australian origin grossly increased such variation. Therefore, it was decided, as a continuation of the array strategy of RITA-1, to restrict oligonucleotide selection to Eurasian viruses. In order to avoid a large number of degenerate positions, two (e.g., H1, H5, N8) and even three separate sets (H3) of primers and probes had to be designed to cover the full width of sequence variation of these subtypes (Table 2). The PCRs were du- or triplexed within each subtype and probes specific for the same subtype labeled with the same reporter dye. As indicated by the red color of nucleotides in Table 2, the majority of oligonucleotides used in RITA-1 had to be modified or fully replaced to qualify for inclusion into RITA-2. Primer and probe sets were tested extensively against selected reference isolates of the matching and closely related subtypes with several rounds of



optimization. The final selection was then successfully tested against all homosubtypic isolates as listed in Table 1.

### 3.2. Extended Target Spectrum of RITA-2

To economize space on the final PCR array, RT-qPCRs specific for several different subtypes were duplexed using FAM and HEX reporter dyes (Figure 1a: M/IC2; H9/N4; H11/N5; H12/H14; H15/H16); care was taken to combine subtypes that have not been detected so far in nature to avoid competition during amplification.

While RITA-1 provided no reactions to identify subtypes H14 and H15, these have now been added to RITA-2. Figure 2 shows that these assays have a sensitivity comparable to the generic M-PCR. In addition, the H15 assay did not cross-react to the closely related subtypes H7 and H10. Unfortunately, only a single reference isolate was available each for AIV subtypes H14 and H15.

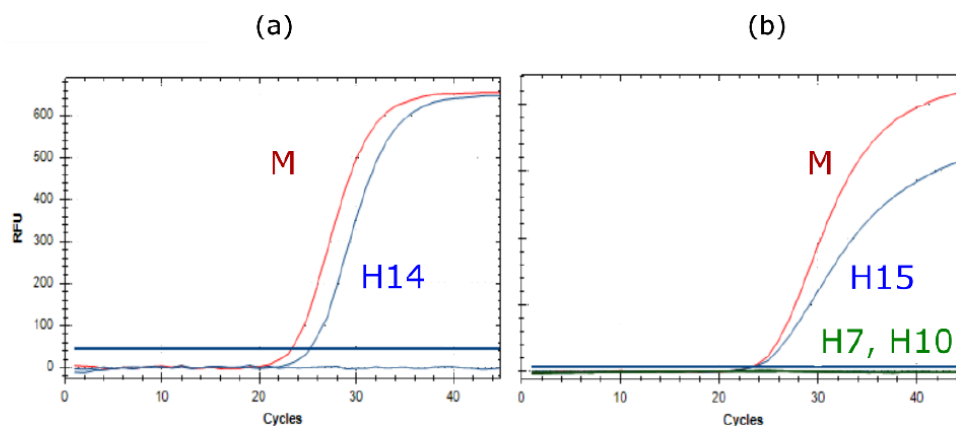


Figure 2. RT-qPCRs specific for avian influenza virus subtypes (a) H14 (A/Mallard/Gurjev/263/82), and (b) H15 (A/Shearwater/West Australia/2576/79), in comparison to influenza A virus-generic M-PCR (red, in (a,b)). Subtypes H7 and H10 (green in (b)), closely related to H15 did not cross-react.

According to recent data from Egypt, poultry flocks showing respiratory disease and increased mortality were often found to suffer from co-infections of AIV with NDV and/or IBV [23,24]. Likewise, viral isolates were found to harbor a mix of AIV, NDV, and/or IBV [27–29]. In addition, NDV and IBV infections are among the most important differential diagnoses of HPAI in poultry. Therefore, in RITA-2, NDV- and IBV-specific RT-qPCRs have been included. Rather than designing new assays, approved published methods have been adopted here (Table 2).

Routine use of RITA-1 for subtyping clinical samples isolates revealed a lower sensitivity of several subtype-specific assays compared to the generic M-PCR. Examples are shown in Figure 3. Re-designing primers and/or probes or selecting completely new target regions re-established sensitivity of the RITA-2 assays to the level of the M-PCR.

### 3.3. Analytical Sensitivity

All subtype-specific assays were evaluated with all the available matched subtypes and compared to the generic M-PCR. A wide range of isolates regarding time, place of origin, and host species was used. The analyses showed that most of the subtype-specific assays attained the level of sensitivity of the M-PCR as indicated by correlation coefficients  $> 0.93$  (Figure 4). For some assays (H2, H6, H11, N2, N7), however, a statistically significant ( $p < 0.05$ ) lower sensitivity of up to 3 Cq value on average was calculated. For H1, H3, and N1 subtypes, the host species origin was found to modulate sensitivity (Figure 5),

and targets of non-avian origin were detected with significantly lower sensitivity due to mismatches in primers and/or probes. The H1 subtypes of human and swine-origin were particularly negatively affected. In order to address these findings in routine diagnostic settings, clinical samples with a viral load of Cq > 35 (as measured by a generic influenza A virus RT-qPCR) were not assigned to examination in the RITA-2 array.

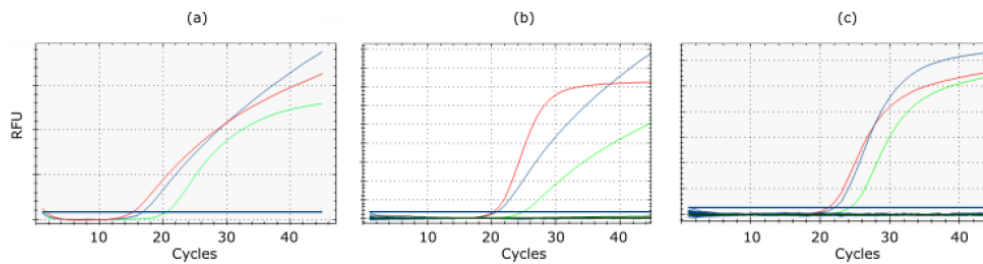


Figure 3. Improved sensitivity of RT-qPCRs specific for avian influenza virus subtypes (a) H3 (A/Mallard/Germany/R1648/07 [H3N8]), (b) N2 (A/Chicken/Egypt/AR538/2017 [H5N2 hp]), and (c) N4 (A/Mallard /Germany/R2167/2009 [H8N4]) in RITA-2 (blue) compared to RITA-1 (green). Generic M-specific amplification curves are shown in red.

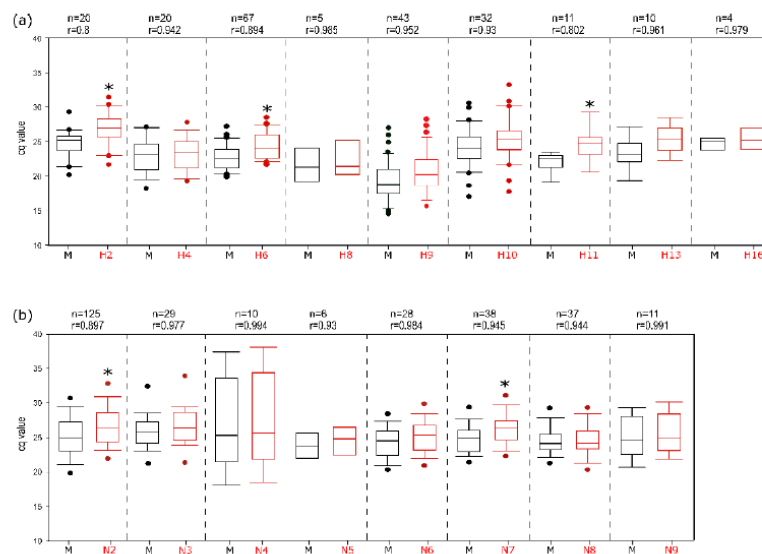


Figure 4. Subtype-specific analytical sensitivity of the RITA-2 array compared to the generic M-RTqPCR assay. (a) HA subtypes 2, 4, 6, 8, 9, 10, 11, 13, and 16; for subtypes H14 and H15, only a single isolate was available (s. Figure 2). (b) NA subtypes 2–9. *n*—Number of isolates tested, *r*—Spearman's rank correlation coefficient, \*—statistically significant difference between the Cq values of the generic and the subtype-specific RT-qPCRs. Dots define outliers.

Notifiable AIV of subtypes H5 and H7 received specific dedication (Figure 6): RITA-2 assays detected RNA of these subtypes with high sensitivity, independently of the pathotype and the clade of H5 viruses of the goose/Guangdong lineage.

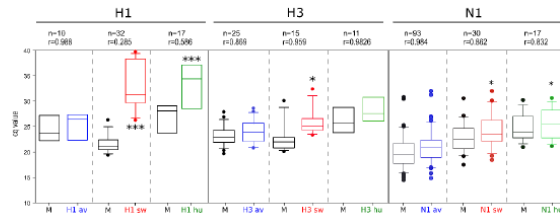


Figure 5. Influence of host origin of virus isolates on the analytical sensitivity of the RITA-2 array. *n*—Number of isolates tested, *r*—Spearman’s rank correlation coefficient, \*—Statistically significant difference. \*\*\*—Highly significant difference; av, sw, hu—avian (blue), swine (red), human (green) host origin. Dots define outliers.

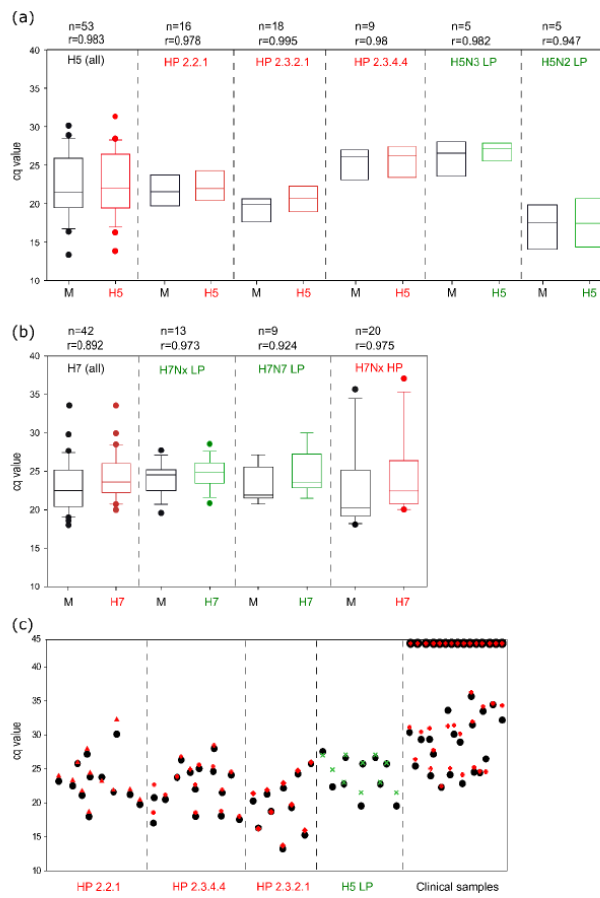


Figure 6. Analytical sensitivity of the RITA-2 array for notifiable avian influenza viruses of HA subtypes H5 (a) and H7 (b), stratified by phylogenetic lineage and pathotype (HP—red, LP—green) and (c) pairwise comparison of Cq values for individual isolates or clinical samples (including H5-negative ones) obtained by generic M-PCR (black dot) and the H5 subtype-specific RITA-2 assay (colored symbols). *n*—number of tested isolates, *r*—Spearman’s rank correlation coefficient.

### 3.4. Analytical Specificity

In RITA-1, several assays revealed minor intersubtypic cross-reactions, particularly between subtypes H1/H6, H2/H5, and H7/H10/H15 which are known to be genetically closely related. Therefore, special care was taken to re-design primers and probes to avoid such cross-reactions. Based on published phylogenetic panoramas for the HA and NA subtypes [30,31], a selected pattern of closely related subtypes was used to validate analytical specificity.

As shown in Figure 7, upper left panel, RITA-1 produced a highly specific signal for H2 when tested with an H2 isolate but also an H5 virus gave a (significantly weaker) positive signal in the H2 assay; the same was seen vice versa for the H5 assay. The problem was even more complex for H7 viruses, which are closely related to subtypes H10 and H15: In RITA-1, an H7 virus gave a highly specific signal in the H7 assay, but also H10 and H15 viruses tested (false-) positive in the H7 assay (Figure 7, lower left panel). Similarly, an H10 virus produced a weakly positive specific signal in the H7 assay. In RITA-2, these cross-reactions no longer exist (Figure 7, right panels). Similar results were obtained for all assays tested against the pattern of closely related subtypes. Thus, the RITA-2 array has increased in specificity.

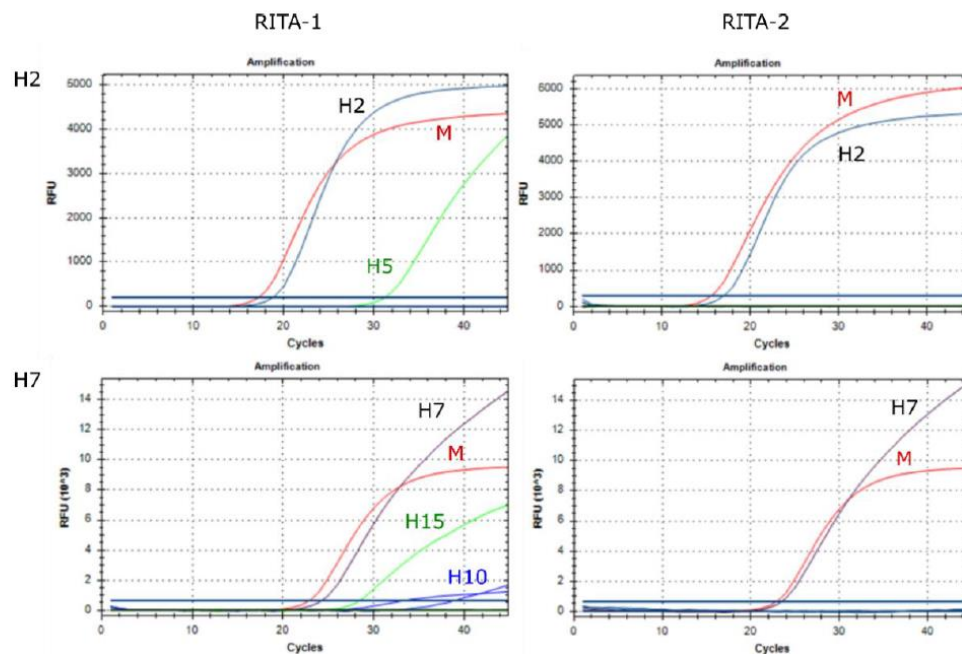


Figure 7. Intersubtypic cross-reactions of RITA-1 are resolved in re-designed RITA-2 assays. Here the following strains were used: H2 (A/Mallard/Germany/Wv677/04 [H2N3]), H5 (A/White stork/Germany/AR251/2018 [H5N6 hp]), H7 (A/Greylag goose/Germany/AR942/2015 [H7N7]), H10 (A/Mallard/Germany/1490/09 [H10N7]) and H15 (A/Shearwater/West Australia/2576/79 [H15N9]).

### 3.5. Assay Robustness

Duplicate runs of selected reference samples for all 16 HA and nine NA assays plus IBV and NDV targets on the same plate were used to evaluate intraassay variation. Inter-assay variation was investigated using two different thermal cyclers and two different

plates for the same selected samples on two different days. As shown in Tables S3 and S4, the standard deviations and covariances calculated suggest excellent assay robustness.

### 3.6. Performance Characteristics with Clinical Samples

The diagnostic performance of RITA-2 was evaluated with a set of 60 clinical samples from poultry originating from Egypt and Bangladesh. RITA-2 succeeded in differentiating subtypes and detecting IBV and/or NDV with high sensitivity and specificity, as shown in Table 5. In RITA-2, all subtypes specified for these samples by other RT-PCRs and/or sequence analysis were confirmed (H5, H9, N1, N8, and N2). Some of these samples were also tested by RITA-1 but failed to detect the H9 subtype at lower viral loads. RITA-2 takes advantage of a set of primers and probes that we updated previously [23], which enabled detection of recent H9N2 viruses of the G1 lineage circulating in northern Africa with much higher sensitivity than an older H9 protocol [32]. Also, mixed infections of different AIV subtypes were detected; these results extended to co-infections with IBV and NDV in two samples, as depicted in Figure 8.

Table 5. Comparison of the results of clinical samples obtained with RITA-2 and by sequencing or subtyping with other RT-PCRs. Results for sample originating from Germany are shown in Table S2.

Country	Species	No. of Farms	RITA-2	Subtyping/ Other PCRs	Sequencing
Egypt	Chicken	2	H5, N8	H5, N8	H5 HP, N8 [22]
Egypt	Turkey	2	H5, N8	H5, N8	H5 HP, N8 [22]
Egypt	Ducks	1	H5, N8	H5, N8	H5 HP, N8
Egypt	Ducks	7	H5, N8	H5, N8	H5 HP
Egypt	Chicken	3	H9, N2	H9, N2	H9, N2 [22]
Egypt	Chicken	2	H5, N1	H5, N1	H5, N1 [22]
Egypt	Duck	5	H5, N8	H5, N8	H5 HP
Egypt	Chicken	5	H5, H9, N8, N2	H5, H9, N2	H5 HP [22]
Egypt	Chicken	3	H5, N2	H5, N2	H5 HP, N2 [22]
Egypt	Chicken	2	H5, H9, N8, N2	H5, H9, N8, N2	H5, H9, N8, N2 [10]
Egypt	Chicken	1	H5, H9, N8, N2, IBV, NDV	H5, H9, N8, N2, IBV, NDV	H5, H9, N8, N2, IBV [10]
Egypt	Chicken	1	H5, N8, IBV, NDV	H5, N8, IBV, NDV	H5, N8, IBV [10]
Bangladesh	Duck	13	H4, N6	H4, N6	H4, N6 [23]

In addition, we decoupled single assays from the RITA-2 array and re-arranged smaller arrays of eight or four wells (Figure 1b) comprising RT-qPCRs for: (i) generic AIV detection, (ii) H5 or H7 sub- and pathotyping, and (iii) fitting NA subtyping. This step was taken to guarantee high throughput of a demanding daily sample size during HPAI epizootics experienced in Europe 2016/17 and 2020/21. We analyzed a total of 63 clinical samples from the recent 2020/21 HPAI H5 epizootic in Europe (Supplementary Materials Table S3) and show that careful selection of single assays decoupled from RITA-2 allowed a full diagnosis regarding H5 sub- and pathotype as well as (in most cases) the NA subtype with a grossly reduced turn-around time as compared to the full RITA-2 or single RT-qPCRs and nucleotide sequencing for pathotyping.

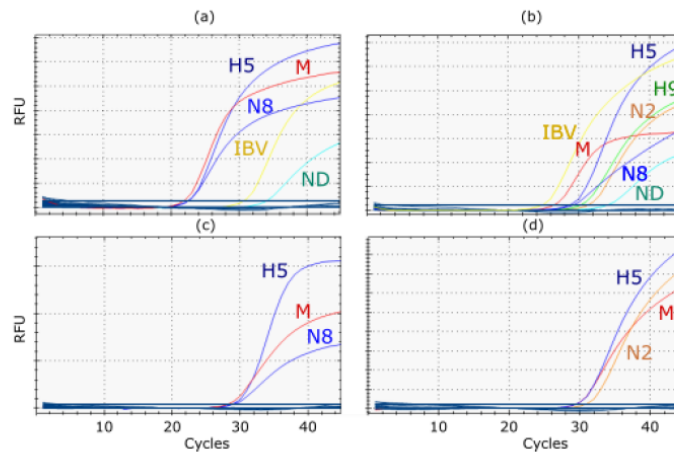


**Figure 8.** Examples of RITA-2 analysis of clinical (cloacal swab) samples from poultry flocks in Egypt detecting mixed infections of several AIV subtypes (a) Mixed infection with AIV H5N8, IBV and NDV; (b) Mixed infection with AIV H5, H9, N2, N8 IBV and NDV; (c) Mono-infection with AIV H5N8; (d) Mono-infection with AIV H5N2.

#### 4. Discussion

Diagnostic tools for avian influenza viruses (AIV) are constantly challenged due to reassortment and genetic drift of these viruses. Recently, RT-qPCRs have been established as standards for rapid and sensitive diagnosis [4]. Due to the rapid evolutionary diversification of the AIV sequence cloud, particularly affecting the HA segment, subtyping RT-qPCRs are under exceptionally high pressure to adapt to the fluctuations of such clouds. Ideally, assays should be inclusive for all sequences published for a single subtype and, at the same time, exclusive for all sequences not clustering with this subtype. Suitably conserved but subtype-specific target sequences in the HA and NA genome segments become limited in reciprocal relation to the growing number of sequences in databases, as our in-silico study of comprehensive alignment sets has revealed.

To re-establish high sensitivity and specificity of arrayed influenza virus subtype-specific RT-qPCRs for recently circulating viruses, we re-designed primers and probes previously published by Hoffmann et al. [16] and re-assembled those PCRs into an economized PCR array, termed RITA-2. An acceptable balance between a highly sensitive broad reactivity and full subtype specificity was finally achieved using multiplexed Taqman<sup>®</sup> based technology. The use of two fluorescent marker dyes allowed integration of PCRs and reduced the set of previously 32 subtyping PCRs of RITA-1 to 24 in RITA-2. In addition, two further AIV subtypes (H14, H15) and targets for NDV and IBV, two important differential diagnoses of AIV infections in poultry, were accommodated into the array. The assay provides considerable versatility and robustness as all 24 wells for a single sample can be pipetted using a multichannel pipette and a single master mix per sample. The plates can be prepared in advance in batches with primers and probes pipetted into the correct positions and stored at  $-20^{\circ}\text{C}$ . A storage time of nine months in our hands did not lead to a loss of sensitivity. Cutting the plates if the full range of four samples per plate is not required can be accomplished as well. Reducing the total volume of the RT-qPCR reactions from 25  $\mu\text{L}$  (RITA-1) to 12.5  $\mu\text{L}$  per reaction further adds to cost reduction in RITA-2.

A continuing emergence of AIV variants characterized the evolution of highly pathogenic (HP) AIV of the Chinese Gs/GD lineage over the last two decades. NA subtype switching and an accelerated diversification of HA sequences leading to an intricate fragmentation into various phylogenetic clades, subclades, and lineages have been a hallmark of these

viruses [33]. Appropriate diagnostic tools should be able to detect such diverse viruses, and the H5 assay implemented in RITA-2 achieves this goal as demonstrated by detecting representative HPAI H5 viruses from at least four recent clades (Figure 6a). Severe epizootic outbreaks of Gs/GD HP H5 viruses have been witnessed in Europe during the winter seasons of 2016/17 (mainly H5N8), 2020/21 (mainly H5N8, but also N1, N3, N4, and N5), and 2021/22 (mainly H5N1) [34,35]. Single subtyping assays of RITA-2 and pathotyping RT-qPCR published by Naguib et al. and Graaf et al. [17,18] were customized and rearranged into 8- and 4-well arrays (Figure 1b, Table S2). In cases such as the mentioned HPAI epizootics, when most AIV-positive samples are expected to be dominated by a certain sub- and pathotype, smaller arrays can be used to save time and costs to establish a final diagnosis (Table S2).

Mixed infections with different influenza A virus subtypes are a prerequisite of reassortment. In addition, co-infections of AIV and other viral avian pathogens with clinical impact have recently been found at increasing frequency in poultry in countries like Egypt [23,24,27–29] and Bangladesh [36]. In Egypt, such co-infection gave rise to a diffuse clinical picture, termed “respiratory disease complex” in gallinaceous poultry [27]. We show here that RITA-2 detects mixed infections in clinical samples even if these targets are present in grossly different concentrations (Figure 8). Separating the amplification reaction into distinct wells obviates competition effects which would decrease the sensitivity of detecting minor targets. To detect mixed infections, it is essential to understand better the viral infection dynamics in individual birds and populations. Reassortment events “*in statu nascendi*” can be followed using RITA-2, and has led previously to the detection of a new HPAIV subtype, H5N2, in Egypt [11]. Sensitive virus isolation techniques would essentially cover at least the same range of viruses (AIV, NDV, IBV), but often certain viruses outcompete others in such mixtures [28,29]. This would lead to a skewed impression of the actual co-infections. Next-generation sequencing focusing on a true metagenomics approach would be adequate to uncover the full range of co-infecting pathogens in a sample [34]. However, such technology is still costly and less suitable than RT-qPCR for routine diagnostic laboratories. The capabilities of RITA-2 to detect mixed infection might also be useful when analyzing the purity of virus strains based on clinical isolates that are used as diagnostic antigens in serological assays or for (autologous) vaccine production.

Emerging new subtypes and drift variants of influenza A viruses pose an ultimate challenge to their diagnostic detection by sequence-based techniques such as RT-qPCR. There is extensive natural sequence variation between AIV subtypes circulating in wild birds and poultry in the Americas and Oceania compared to Eurasia [30,31]. In silico analyses of the available sequence information did not allow the selection of a global “one-fits-all” type of RT-qPCR for all the different subtypes. Therefore, like RITA-1, the new version-2 remains restricted to the analysis of viruses and samples obtained from wild birds and poultry of Eurasia and Africa. Nevertheless, it should be possible to design a similar array for the corresponding American or Oceanian lineages. Sequence variation was also related to the host origin of the viruses and negatively affected the sensitivity of detection. In particular, the H1 assay was not sensitive enough to ensure proper detection of H1 viruses in clinical samples of swine and human origin. Other, more sensitive assays have been published that should be used for those species instead [37]. Unlike H1 viruses, H3 viruses were detected more efficiently also from swine and humans; this is likely due to the use of three multiplexed RT-qPCRs targeting a larger spectrum of H3 sequences. The re-designed N1 assay was able to pick up the N1 subtype from the swine and human origin samples.

## 5. Conclusions

RITA-2 constitutes an important technical update and improved development compared to RITA-1. It also provides functional progress through the combination of RT-qPCR for differential diagnoses of AIV infections; this serves needs to disentangle complex mixtures of viral co-pathogens (NDV, IBV) synergistically acting in respiratory disease of

viruses [33]. Appropriate diagnostic tools should be able to detect such diverse viruses, and the H5 assay implemented in RITA-2 achieves this goal as demonstrated by detecting representative HPAI H5 viruses from at least four recent clades (Figure 6a). Severe epizootic outbreaks of Gs/GD HP H5 viruses have been witnessed in Europe during the winter seasons of 2016/17 (mainly H5N8), 2020/21 (mainly H5N8, but also N1, N3, N4, and N5), and 2021/22 (mainly H5N1) [34,35]. Single subtyping assays of RITA-2 and pathotyping RT-qPCR published by Naguib et al. and Graaf et al. [17,18] were customized and rearranged into 8- and 4-well arrays (Figure 1b, Table S2). In cases such as the mentioned HPAI epizootics, when most AIV-positive samples are expected to be dominated by a certain sub- and pathotype, smaller arrays can be used to save time and costs to establish a final diagnosis (Table S2).

Mixed infections with different influenza A virus subtypes are a prerequisite of reassortment. In addition, co-infections of AIV and other viral avian pathogens with clinical impact have recently been found at increasing frequency in poultry in countries like Egypt [23,24,27–29] and Bangladesh [36]. In Egypt, such co-infection gave rise to a diffuse clinical picture, termed “respiratory disease complex” in gallinaceous poultry [27]. We show here that RITA-2 detects mixed infections in clinical samples even if these targets are present in grossly different concentrations (Figure 8). Separating the amplification reaction into distinct wells obviates competition effects which would decrease the sensitivity of detecting minor targets. To detect mixed infections, it is essential to understand better the viral infection dynamics in individual birds and populations. Reassortment events “*in statu nascendi*” can be followed using RITA-2, and has led previously to the detection of a new HPAIV subtype, H5N2, in Egypt [11]. Sensitive virus isolation techniques would essentially cover at least the same range of viruses (AIV, NDV, IBV), but often certain viruses outcompete others in such mixtures [28,29]. This would lead to a skewed impression of the actual co-infections. Next-generation sequencing focusing on a true metagenomics approach would be adequate to uncover the full range of co-infecting pathogens in a sample [34]. However, such technology is still costly and less suitable than RT-qPCR for routine diagnostic laboratories. The capabilities of RITA-2 to detect mixed infection might also be useful when analyzing the purity of virus strains based on clinical isolates that are used as diagnostic antigens in serological assays or for (autologous) vaccine production.

Emerging new subtypes and drift variants of influenza A viruses pose an ultimate challenge to their diagnostic detection by sequence-based techniques such as RT-qPCR. There is extensive natural sequence variation between AIV subtypes circulating in wild birds and poultry in the Americas and Oceania compared to Eurasia [30,31]. In silico analyses of the available sequence information did not allow the selection of a global “one-fits-all” type of RT-qPCR for all the different subtypes. Therefore, like RITA-1, the new version-2 remains restricted to the analysis of viruses and samples obtained from wild birds and poultry of Eurasia and Africa. Nevertheless, it should be possible to design a similar array for the corresponding American or Oceanian lineages. Sequence variation was also related to the host origin of the viruses and negatively affected the sensitivity of detection. In particular, the H1 assay was not sensitive enough to ensure proper detection of H1 viruses in clinical samples of swine and human origin. Other, more sensitive assays have been published that should be used for those species instead [37]. Unlike H1 viruses, H3 viruses were detected more efficiently also from swine and humans; this is likely due to the use of three multiplexed RT-qPCRs targeting a larger spectrum of H3 sequences. The re-designed N1 assay was able to pick up the N1 subtype from the swine and human origin samples.

## 5. Conclusions

RITA-2 constitutes an important technical update and improved development compared to RITA-1. It also provides functional progress through the combination of RT-qPCR for differential diagnoses of AIV infections; this serves needs to disentangle complex mixtures of viral co-pathogens (NDV, IBV) synergistically acting in respiratory disease of



poultry. It is clear that the assay compositions arrayed here will remain subjects to change. AIV in general and Gs/GD viruses, in particular, remain a highly mobile and moving target for sequence-based diagnostic tools. Continuous reference to updated sequence databases and appropriate adaptation of primers and probes are inevitable permanent tasks. An additional functional step forward compared to RITA-1 is provided by the combination of selected RT-qPCR assays with pathotyping RT-qPCR so as to serve the needs of rapid diagnosis of HA and NA subtypes and of the pathotype in HPAI epidemics with a temporal and/or geographic restriction.

**Supplementary Materials:** The following supporting information can be downloaded at: <https://www.mdpi.com/article/10.3390/v14020415/s1>, Table S1. Identity of Infectious Bronchitis and Newcastle Disease virus isolates used to validate specific RT-qPCRs; Table S2. Analysis of clinical samples obtained during active or passive monitoring of wild birds and poultry in Germany, 2020–21. Table S3. Summary statistics of intra- and interassay variations of the RITA-2 array; Table S4. Raw data of inter- and intra-assay variations.

**Author Contributions:** Conceptualization, T.H. and M.B.; methodology, K.E.H. and A.K.A.; software, A.A.; validation, K.E.H. and A.K.A.; formal analysis, K.E.H. and A.K.A.; investigation, K.E.H., A.A. and A.K.A.; resources, T.C.M. and M.B.; data curation, T.H.; writing—original draft preparation, K.E.H., A.K.A. and T.H.; writing—review and editing, T.H. and M.F.E.-K.; visualization, K.E.H.; supervision, T.C.M., M.B., H.M.H. and M.F.E.-K.; project administration, T.H.; funding acquisition, M.F.E.-K., K.E.H. and T.C.M. (for A.K.A.). All authors have read and agreed to the published version of the manuscript.

**Funding:** This research was funded by a grant to K.E.H. from the Egyptian Ministry of Higher Education (Mission sector) and by a grant to A.K.A. from the Federal German Environment Agency (Umweltbundesamt), grant number FKZ 3718 62 236 0.

**Institutional Review Board Statement:** No segments of the study required ethical approval. Clinical samples were not collected specifically for this study but were obtained from routine diagnostic submissions.

**Data Availability Statement:** All data pertinent to this study are presented in tables and figures in the main text or in the Supplementary Materials.

**Acknowledgments:** We gratefully acknowledge the technical support provided by Aline Maksimov and Diana Parlow, Friedrich-Loeffler-Institute, and the willingness of several veterinarians in Bangladesh, Egypt, and Germany to submit clinical sample material.

**Conflicts of Interest:** The authors declare no conflict of interest.

## References

1. Webster, R.; Govorkova, E. Continuing challenges in influenza. *Ann. N. Y. Acad. Sci.* **2014**, *1323*, 115–139. [\[CrossRef\]](#)
2. Ma, W.; Gramer, M.; Rossow, K.; Yoon, K.-J. Isolation and genetic characterization of new reassortant H3N1 swine influenza virus from pigs in the midwestern United States. *J. Virol.* **2006**, *80*, 5092–5096. [\[CrossRef\]](#)
3. Fouchier, R.A.M.; Munster, V.; Wallensten, A.; Bestebroer, T.M.; Herfst, S.; Smith, D.; Rimmelzwaan, G.F.; Olsen, B.; Osterhaus, A.D.M.E. Characterization of a novel influenza A virus hemagglutinin subtype (H16) obtained from black-headed gulls. *J. Virol.* **2005**, *79*, 2814–2822. [\[CrossRef\]](#)
4. Spackman, E.A. Brief Introduction to Avian Influenza Virus. *Methods Mol. Biol.* **2020**, *2123*, 83–92.
5. Horimoto, T.; Kawaoka, Y. Influenza: Lessons from past pandemics, warnings from current incidents. *Nat. Rev. Microbiol.* **2005**, *3*, 591–600. [\[CrossRef\]](#)
6. Poovorawan, Y.; Pyungporn, S.; Prachayangprecha, S.; Makkoeh, J. Global alert to avian influenza virus infection: From H5N1 to H7N9. *Pathog. Glob. Health* **2013**, *107*, 217–223. [\[CrossRef\]](#)
7. Machalaba, C.C.; Elwood, S.E.; Forcella, S.; Smith, K.M.; Hamilton, K.; Jebara, K.B.; Swayne, D.E.; Webby, R.J.; Mumford, E.; Mazet, J.A.K.; et al. Global avian influenza surveillance in wild birds: A strategy to capture viral diversity. *Emerg. Infect. Dis.* **2015**, *21*, e1–e7. [\[CrossRef\]](#)
8. Chan, K.H.; Lam, S.Y.; Puthavathana, P.; Nguyen, T.D.; Long, H.T.; Pang, C.M.; Chan, K.M.; Cheung, C.Y.; Set, W.H.; Peiris, J.S. Comparative analytical sensitivities of six rapid influenza A antigen detection test kits for detection of influenza A subtypes H1N1, H3N2 and H5N1. *J. Clin. Virol.* **2007**, *38*, 169–171. [\[CrossRef\]](#)
9. Marché, S.; van den Berg, T. Evaluation of rapid antigen detection kits for the diagnosis of highly pathogenic avian influenza H5N1 infection. *Avian Dis.* **2010**, *54*, 650–654. [\[CrossRef\]](#)

10. Chua, T.H.; Ellis, T.M.; Wong, C.W.; Guan, Y.; Ge, S.X.; Peng, G.; Lamichhane, C.; Maliadis, C.; Tan, S.W.; Selleck, P.; et al. Performance evaluation of five detection tests for avian influenza antigen with various avian samples. *Avian Dis.* **2007**, *51*, 96–105. [[CrossRef](#)]
11. Hassan, K.E.; King, J.; El-Kady, M.; Afifi, M.; Abozeid, H.H.; Pohlmann, A.; Beer, M.T.H. Novel Reassortant Highly Pathogenic Avian Influenza A(H5N2) Virus in Broiler Chickens, Egypt. *Emerg. Infect. Dis.* **2020**, *26*, 129–133. [[CrossRef](#)]
12. Brown, I. Advances in molecular diagnostics for avian influenza. *Dev. Biol.* **2006**, *124*, 93–97.
13. Suarez, D.L.; Das, A.; Ellis, E. Review of rapid molecular diagnostic tools for avian influenza virus. *Avian Dis.* **2007**, *51*, 201–208. [[CrossRef](#)]
14. Kalthoff, D.; Bogs, J.; Harder, T.; Grund, C.; Pohlmann, A.; Beer, M.; Hoffmann, B. Nucleic acid-based detection of influenza A virus subtypes H7 and N9 with a special emphasis on the avian H7N9 virus. *Euro Surveill.* **2014**, *19*, 20731. [[CrossRef](#)]
15. Hoffmann, B.; Harder, T.; Lange, E.; Kalthoff, D.; Reimann, I.; Grund, C.; Oehme, R.; Vahlenkamp, T.W.; Beer, M. New real-time reverse transcriptase polymerase chain reactions facilitate detection and differentiation of novel A/H1N1 influenza virus in porcine and human samples. *Berl. Munch. Tierarztl. Wochenschr.* **2010**, *123*, 286–292.
16. Hoffmann, B.; Hoffmann, D.; Henritzi, D.; Beer, M.; Harder, T.C. Riems influenza a typing array (RITA): An RT-qPCR-based low density array for subtyping avian and mammalian influenza A viruses. *Sci. Rep.* **2016**, *6*, 27211. [[CrossRef](#)]
17. Naguib, M.; Graaf, A.; Fortin, A.; Luttermann, C.; Wernery, U.; Amarín, N.; Hussein, A.H.; Sultan, H.; Al Adhadi, B.; Hassan, M.K.; et al. Novel real-time PCR-based patho- and phylogeny of potentially zoonotic avian influenza A subtype H5 viruses at risk of incursion into Europe in 2017. *Euro Surveill.* **2017**, *22*, 30435. [[CrossRef](#)]
18. Graaf, A.; Beer, M.; Harder, T.C. Real-time reverse transcription PCR-based sequencing-independent pathotyping of Eurasian avian influenza A viruses of subtype H7. *Virol. J.* **2017**, *14*, 137. [[CrossRef](#)]
19. Kearse, M.; Moir, R.; Wilson, A.; Stones-Havas, S.; Cheung, M.; Sturrock, S.; Buxton, S.; Cooper, A.; Markowitz, S.; Duran, C.; et al. Geneious Basic: An integrated and extendable desktop software platform for the organization and analysis of sequence data. *Bioinformatics* **2012**, *28*, 1647–1649. [[CrossRef](#)]
20. Katoh, K.; Standley, D.M. MAFFT multiple sequence alignment software version 7: Improvements in performance and usability. *Mol. Biol. Evol.* **2013**, *30*, 772–780. [[CrossRef](#)]
21. Larsson, A. AliView: A fast and lightweight alignment viewer and editor for large datasets. *Bioinformatics* **2014**, *30*, 3276–3278. [[CrossRef](#)]
22. Kibbe, W. OligoCalc: An online oligonucleotide properties calculator. *Nucleic Acids Res.* **2007**, *35*, W43–W46. [[CrossRef](#)]
23. Hassan, K.E.; El-Kady, M.F.; El-Sawah, A.A.A.; Luttermann, C.; Parvin, R.; Shany, S.; Beer, M.; Harder, T.C. Respiratory disease due to mixed viral infections in poultry flocks in Egypt between 2017 and 2018: Upsurge of highly pathogenic avian influenza virus subtype H5N8 since 2018. *Transbound. Emerg. Dis.* **2021**, *68*, 21–36. [[CrossRef](#)]
24. Naguib, M.M.; El-Kady, M.F.; Lüscho, D.; Hassan, K.E.; Arafa, A.-S.; El-Zanaty, A.; Hassan, M.K.; Hafez, H.M.; Grund, C.; Harder, T.C. New real time and conventional RT-PCRs for updated molecular diagnosis of infectious bronchitis virus infection (IBV) in chickens in Egypt associated with frequent co-infections with avian influenza and Newcastle Disease viruses. *J. Virol. Methods* **2017**, *245*, 19–27. [[CrossRef](#)]
25. Hoffmann, B.; Depner, K.; Schirmmeier, H.; Beer, M. A universal heterologous internal control system for duplex real-time RT-PCR assays used in a detection system for pestiviruses. *J. Virol. Methods* **2006**, *136*, 200–209. [[CrossRef](#)]
26. Abdelwhab, E.M.; Lüscho, D.; Harder, T.C.; Hafez, H.M. The use of FTA® filter papers for diagnosis of avian influenza virus. *J. Virol. Methods* **2011**, *174*, 120–122. [[CrossRef](#)]
27. Hassan, K.E.; Ali, A.; Dahshan, A.-H.M.; El-Sawah, A.A.; Shany, S.A.S.; El-Kady, M.F. Prevalence of avian respiratory viruses in broiler flocks in Egypt. *Poult. Sci.* **2016**, *95*, 1271–1280. [[CrossRef](#)]
28. Samy, A.; Naguib, M.M. Avian Respiratory Coinfection and Impact on Avian Influenza Pathogenicity in Domestic Poultry: Field and Experimental Findings. *Vet. Sci.* **2018**, *5*, 23. [[CrossRef](#)]
29. Shehata, A.A.; Sedeik, M.E.; Elbestawy, A.R.; Zain El-Abideen, M.A.; Kilany, W.H.; Ibrahim, H.H.; Ali, A. Co-infections, genetic, and antigenic relatedness of avian influenza H5N8 and H5N1 viruses in domestic and wild birds in Egypt. *Poult. Sci.* **2019**, *98*, 2371–2379. [[CrossRef](#)]
30. Liu, S.; Ji, K.; Chen, J.; Tai, D.; Jiang, W.; Hou, G.; Chen, J.; Li, J.; Huang, B. Panorama Phylogenetic Diversity and Distribution of Type A Influenza Virus. *PLoS ONE* **2009**, *4*, e5022. [[CrossRef](#)]
31. Zhuang, Q.; Wang, S.; Liu, S.; Hou, G.; Li, J.; Jiang, W.; Wang, K.; Peng, C.; Liu, D.; Guo, A.; et al. Diversity and distribution of type A influenza viruses: An updated panorama analysis based on protein sequences. *Virol. J.* **2019**, *16*, 85. [[CrossRef](#)]
32. Monne, I.; Ormelli, S.; Salviato, A.; De Battisti, C.; Bettini, F.; Salomoni, A.; Drago, A.; Zecchin, B.; Capua, I.; Cattoli, G. Development and validation of a one-step real-time PCR assay for simultaneous detection of subtype H5, H7, and H9 avian influenza viruses. *J. Clin. Microbiol.* **2008**, *46*, 1769–1773. [[CrossRef](#)]
33. Harfoot, R.; Webby, R. H5 influenza, a global update. *J. Microbiol.* **2017**, *55*, 196–203. [[CrossRef](#)]
34. King, J.; Harder, T.; Conraths, F.J.; Beer, M.; Pohlmann, A. The genetics of highly pathogenic avian influenza viruses of subtype H5 in Germany, 2006–2020. *Transbound. Emerg. Dis.* **2021**, *68*, 1136–1150. [[CrossRef](#)]
35. European Food Safety Authority; Adlhoch, C.; Fusaro, A.; Gonzales, J.; Kuiken, T.; Marangon, S.; Niqueux, E.; Staubach, C.; Terregino, C.; Aznar, I.; et al. Avian influenza overview February–May 2021. *EFSA J.* **2021**, *19*, 6951.

36. Parvin, R.; Begum, J.A.; Chowdhury, E.H.; Islam, M.R.; Beer, M.; Harder, T.C. Co-subsistence of avian influenza virus subtypes of low and high pathogenicity in Bangladesh: Challenges for diagnosis, risk assessment and control. *Sci. Rep.* **2019**, *9*, 8306. [[CrossRef](#)]
37. Henritzi, D.; Zhao, N.; Starick, E.; Simon, G.; Krog, J.S.; Larsen, L.E.; Reid, S.M.; Brown, I.H.; Chiapponi, C.; Foni, E.; et al. Rapid detection and subtyping of European swine influenza viruses in porcine clinical samples by haemagglutinin- and neuraminidase-specific tetra- and triplex real-time RT-PCRs. *Influenza Respir. Viruses* **2016**, *10*, 504–517. [[CrossRef](#)]

## Supplemental Material

**Table S1.** Identity of Infectious Bronchitis and Newcastle Disease virus isolates used to validate specific RT-qPCRs.

Virus species	Strain	Patho-/Genotype
ND	ND/713/2016	Lasota vaccine/Lentogenic, 2
	A/Chicken/Egypt/AR518/2017	Lentogenic, 2
	A/Chicken/Egypt/AR593/2018	Lentogenic, 2
	ND/NR730/2016	Velogenic, 7b
	A/Chicken/Egypt/AR551/2018	Velogenic, 7b
	A/Chicken/Egypt/AR563/2018	Velogenic, 7b
	A/Chicken/Egypt/AR589/2018	Velogenic, 7b
	A/Chicken/Egypt/AR549/2018	Velogenic, 7b
IBV	AI20298/2019	4/91 IBV vaccine/793B
	A/Chicken/Egypt/AR545/2018	Egyptian variant 2
	A/Chicken/Egypt/AR63/2018	Egyptian variant 2
	A/Chicken/Egypt/AR593/2018	Egyptian variant 2
	A/Chicken/Egypt/AI20290/2019	Egyptian variant 2
	A/Chicken/Egypt/ AI20293/2019	Egyptian variant 2
	A/Chicken/Egypt/ AI20297/2019	Egyptian variant 2

**Table S2.** Analysis of clincial samples obtained during active or passive monitoring of wild birds and poultry in Germany, 2020-21.

Sample id.	Species	Subtype <sup>1</sup>	Pathotype	H5-8	H7-8	RITA-2	Cq
2020A01301	Mallard	H1N1		HxN1	HxN1	H1N1	26.46
2020A01399	Mallard	H1N2		HxN2	HxNx	H1N2	30.62
2020A01045	Mallard	H2N5		HxNx	HxNx	H2N5	35.53
2020A01071	Mallard	H3N8		HxN8	HxNx	H3N8	31.13
2020A100046	Tufted duck	H5N1	LP	H5LPN1	nt	H5N1	25
2020A103671	Greyleg goose	H5N1	HP	H5N1	nt	H5N1	33.05
2021A101598	Greyleg goose	H5N1	HP	H5(HP, 2344b)N1	nt	H5N1	32.36
2021A101602	Chicken	H5N1	HP	H5(HP, 2344b)N1	nt	H5N1	15.69
2021A101605	Barnacle goose	H5N1	HP	H5(HP, 2344b)N1	nt	H5N1	26.81
2021A103752	Barnacle goose	H5N1	HP	H5(HP, 2344b)N1	nt	H5N1	24.16
2021A103933	Chicken	H5N1	HP	H5(HP, 2344b)N1	nt	H5N1	18.24
2021A103934	Chicken	H5N1	HP	H5(HP, 2344b)N1	nt	H5N1	20.99
2020A101397	Mallard	H5N2	LP	H5(LP)N2	nt	H5N2	29.07
2020A101462	Mute swan	H5N3	LP	H5LPN3	nt	H5N3	31.75
2020A103422	Red knot	H5N3	HP	H5(HP, 2344b)N1	nt	H5N3	28.23
2021A100094	Red knot	H5N3	HP	H5	nt	H5N3	32.63
2021A100382	Common buzzard	H5N3	HP	H5(HP, 2344b)N3	nt	H5N3	25.09
2021A100394	Red knot	H5N3	HP	H5(HP, 2344b)N3	nt	H5N3	26.05
2021A101068	Red knot	H5N3	HP	H5(HP, 2344b)N3	nt	H5N3	22.90
2021A101736	Peregrine falcon	H5N3	HP	H5(HP, 2344b)N3	nt	H5N3	23.12
2021A101497	Gull	H5N4	HP	H5(HP, 2344b)Nx <sup>2</sup>	nt	H5N4	33.05
2021A101498	Mute swan	H5N4	HP	H5(HP, 2344b)Nx <sup>2</sup>	nt	H5N4	27.05
2021A101743	Tufted duck	H5N4	HP	H5(HP, 2344b)Nx <sup>2</sup>	nt	H5N4	35.93
2021A101766	Peregrine falcon	H5N4	HP	H5(HP, 2344b)Nx <sup>2</sup>	nt	H5N4	33.76
2020A102166	Common buzzard	H5N5	HP	H5(HP, 2344b)Nx <sup>2</sup>	nt	H5N5	16.28
2020A102246	Eurasian wigeon	H5N5	HP	H5(HP, 2344b)Nx <sup>2</sup>	nt	H5N5	31.59
2020A102255	Bean goose	H5N5	HP	H5(HP, 2344b)Nx <sup>2</sup>	nt	H5N5	21.75
2020A102419	Chicken	H5N5	HP	H5(HP, 2344b)Nx <sup>2</sup>	nt	H5N5	28.05
2020A102170	White-tailed sea eagle	H5N5/N8	HP	H5(HP, 2344b)N8	nt	H5N5/N8	27.04
2020A102196	Barnacle goose	H5N5/N8	HP	H5(HP, 2344b)N8	nt	H5N5/N8	20.89
2020A100326	Turkey	H5N8	HP	H5(HP, 2344b)N8	nt	H5N8	21.20
2020A100350	Turkey	H5N8	HP	H5(HP, 2344b)N8	nt	H5N8	23.14
2020A102315	Curlew	H5N8	HP	H5(HP, 2344b)N8	nt	H5N8	19.93
2020A103043	Crescent sandpiper	H5N8	HP	H5(HP2344b)N8	nt	H5N8	24.78
2020A103056	Mallard	H5N8	HP	H5(HP, 2344b)N8	nt	H5N8	24.57
2020A103433	Turkey	H5N8	HP	H5(HP, 2344b)N8	nt	H5N8	21.35
2021A100092	Barnacle goose	H5N8	HP	H5(HP, 2344b)N8	nt	H5N8	21.66
2021A100383	Greyleg goose	H5N8	HP	H5(HP, 2344b)N8	nt	H5N8	22.98
2021A100385	Laughing gull	H5N8	HP	H5(HP, 2344b)N8	nt	H5N8	25.63
2021A100386	Kestrel	H5N8	HP	H5(HP, 2344b)N8	nt	H5N8	22.98
2021A101495	Barnacle goose	H5N8	HP	H5(HP, 2344b)N8	nt	H5N8	27.32
2021A101737	Peregrine falcon	H5N8	HP	H5(HP, 2344b)N8/N3	nt	H5N8	30.87
2021A101742	Eagle owl	H5N8	HP	H5(HP, 2344b)N8	nt	H5N8	28.60
2021A101752	Great cormorant	H5N8	HP	H5(HP, 2344b)N8	nt	H5N8	32.06
2021A102466	Mute swan	H5N8	HP	H5(HP, 2344b)N8	nt	H5N8	20.78
2020A102379	Barnacle goose	H5N8/N5	HP	H5(HP, 2344b)N8	nt	H5N8/N5	24.93
2020A102279	Eurasian wigeon	H5Nx	HP	H5(HP, 2344b)N8	nt	H5Nx	30.55
2021A100432	Turkey	H6N1		HxN1	HxN1	H6N1	27.88
2021A102559	Dwarf chicken	H7N3	LP	nt	LP H7N3	nt	28.32
2021A102560	Dwarf chicken	H7N3	LP	nt	LP H7N3	nt	28.52
2021A102561	Dwarf chicken	H7N3	LP	nt	LP H7N3	H7N3	28.52
2021A103100	Domestic duck	H7N3	LP	nt	LP H7N3	H7N3	32.69
2020A103228	Mallard	H7N7	LP	nt	LP H7N7	H7N7	27.70
2020A102242	Mallard	H8N4		nt	HxNx	H8N4	32.58
2020A101400	Mallard	H9N1		HxN1	nt	H9N1	29.42
2020A101047	Mute swan	H9N8		HxN8	HxNx	H9N8	32.23
2020A101893	Mallard	H10N6		HxN6	HxNx	H10N6	29.14
2020A101055	Mallard	H11(?)N9		nt	HxN9	H11N9	29.54
2020A101499	Mute swan	H11N1		HxN1	HxN1	H11N1	24.48
2020A103651	Mallard	H12N2		HxN2	HxNx	H12N2	32.30
2020A101401	WeiBohturako	H12N5		HxN5	HxNx	H12N5	25.39
2020A102738	Herring gull	H13N2		HxN2	nt	H13N2	23.84

<sup>1</sup> – Subtype determined according to single RT-qPCRs and/or partial HA/NA sequencing.

<sup>2</sup> – N4 and N5 RT-qPCRs had not been included in the H5-8 array when these samples were tested.

nt – not tested.

Cq – threshold value obtained with the generic M-RTqPCR included in the RITA-2 assay

**Table S3.** Summary statistics of intra- and interassay variations of the RITA-2 array.

Subtype	Intra-assay variation				Inter-assay variation		
	Day one		Day two		Mean	SD	CV%
	SD	CV%	SD	CV%			
H1	0.007	0.036	0.007	0.036	19.47	0.023	0.122
H2	0.007	0.035	0.007	0.035	19.69	0.018	0.092
H3	0.014	0.082	0.028	0.164	17.17	0.044	0.258
H4	0.007	0.037	0.056	0.303	18.65	0.034	0.182
H5	0.007	0.021	0.014	0.043	32.64	0.012	0.038
H6	0.007	0.024	0.098	0.344	28.67	0.075	0.263
H7	0.007	0.049	0.007	0.049	14.24	0.058	0.407
H8	0.035	0.149	0.056	0.238	23.69	0.046	0.196
H9	0.007	0.038	0.014	0.077	18.30	0.009	0.052
H10	0.070	0.361	0.007	0.036	19.54	0.045	0.234
H11	0.021	0.114	0.014	0.076	18.49	0.015	0.081
H12	0.014	0.082	0.028	0.165	17.08	0.021	0.126
H13	0.014	0.072	0.056	0.291	19.39	0.033	0.173
H14	0.007	0.036	0.007	0.036	19.17	0.023	0.124
H15	0.007	0.025	0.028	0.102	27.62	0.035	0.130
H16	0.014	0.082	0.021	0.124	17.09	0.020	0.120
N1	0.069	0.319	0.014	0.065	21.62	0.068	0.318
N2	0.056	0.261	0.014	0.065	21.60	0.033	0.155
N3	0.021	0.108	0.042	0.216	19.60	0.046	0.236
N4	0.042	0.228	0.007	0.038	18.59	0.026	0.141
N5	0.049	0.264	0.021	0.113	18.68	0.046	0.249
N6	0.028	0.151	0.070	0.380	18.63	0.059	0.320
N7	0.056	0.390	0.063	0.439	14.47	0.051	0.353
N8	0.035	0.174	0.028	0.140	20.18	0.033	0.163
N9	0.021	0.124	0.056	0.331	17.07	0.040	0.236
ND	0.007	0.028	0.021	0.086	24.43	0.042	0.173
IBV	0.077	0.295	0.028	0.107	26.27	0.072	0.276

**Table S4.** Raw data of inter- and intra-assay variations.

Subtype	Day one			Day two		
	Cq value	Cq value	Mean	Cq value	Cq value	Mean
H1	19.45	19.46	19.45	19.50	19.49	19.49
H2	19.70	19.71	19.70	19.68	19.67	19.67
H3	17.13	17.15	17.14	17.23	17.19	17.21
H4	18.65	18.64	18.64	18.70	18.62	18.66
H5	32.65	32.66	32.65	32.63	32.65	32.64
H6	28.64	28.63	28.63	28.79	28.65	28.72
H7	14.30	14.29	14.29	14.20	14.19	14.19
H8	23.65	23.70	23.67	23.76	23.68	23.72
H9	18.31	18.30	18.30	18.29	18.31	18.3
H10	19.61	19.51	19.56	19.53	19.52	19.52
H11	18.51	18.48	18.49	18.50	18.48	18.49
H12	17.08	17.10	17.09	17.09	17.05	17.07
H13	19.38	19.40	19.39	19.35	19.43	19.39
H14	19.19	19.20	19.19	19.15	19.16	19.15
H15	27.65	27.66	27.65	27.62	27.58	27.6
H16	17.10	17.12	17.11	17.10	17.07	17.08
N1	21.62	21.72	21.67	21.59	21.57	21.58
N2	21.56	21.64	21.60	21.59	21.61	21.6
N3	19.62	19.65	19.63	19.54	19.60	19.57
N4	18.57	18.63	18.60	18.58	18.59	18.58
N5	18.75	18.68	18.71	18.64	18.67	18.65
N6	18.69	18.65	18.67	18.65	18.55	18.6
N7	14.53	14.45	14.49	14.51	14.42	14.46
N8	20.23	20.18	20.20	20.15	20.19	20.17
N9	17.11	17.08	17.09	17.10	17.02	17.06
ND	24.40	24.39	24.39	24.45	24.48	24.46
IBV	26.38	26.27	26.32	26.25	26.21	26.23

**3.2 Investigating environmental matrices for use in avian influenza virus surveillance  
– surface water, sediments and avian fecal samples**

Ann Kathrin Ahrens, Hans-Christoph Selinka, Claudia Wylezich,  
Hubert Wonnemann, Ole Sindt, Hartmut H. Hellmer, Florian Pfaff, Dirk Höper,  
Thomas C. Mettenleiter, Martin Beer and Timm C. Harder

Microbiology Spectrum

Microbiology Spectrum March/April 2023, 11 (2)

doi: [10.1128/spectrum.02664-22](https://doi.org/10.1128/spectrum.02664-22)





# Investigating Environmental Matrices for Use in Avian Influenza Virus Surveillance—Surface Water, Sediments, and Avian Fecal Samples

Ann Kathrin Ahrens,<sup>a</sup> Hans-Christoph Selinka,<sup>b</sup> Claudia Wylezich,<sup>a</sup> Hubert Wonnemann,<sup>c</sup> Ole Sindt,<sup>c</sup> Hartmut H. Hellmer,<sup>d</sup> Florian Pfaff,<sup>a</sup> Dirk Höper,<sup>a</sup> Thomas C. Mettenleiter,<sup>e</sup> Martin Beer,<sup>a</sup> Timm C. Harder<sup>a</sup>

<sup>a</sup>Institute of Diagnostic Virology, Friedrich-Loeffler-Institut, Greifswald-Isle of Riems, Germany

<sup>b</sup>Section II 1.4 Microbiological Risks, German Environment Agency (UBA), Berlin, Germany

<sup>c</sup>State Laboratory of Schleswig-Holstein, Neumuenster, Germany

<sup>d</sup>Climate Sciences, Physical Oceanography of the Polar Seas, Alfred Wegener Institute, Bremerhaven, Germany

<sup>e</sup>Friedrich-Loeffler-Institut, Greifswald-Isle of Riems, Germany

**ABSTRACT** Surveillance of avian influenza viruses (AIV) in wild water bird populations is important for early warning to protect poultry from incursions of high-pathogenicity (HP) AIV. Access to individual water birds is difficult and restricted and limits sampling depth. Here, we focused on environmental samples such as surface water, sediments, and environmentally deposited fresh avian feces as matrices for AIV detection. Enrichment of viral particles by ultrafiltration of 10-L surface water samples using Rexeed-25-A devices was validated using a bacteriophage  $\phi 6$  internal control system, and AIV detection was attempted using real-time RT-PCR and virus isolation. While validation runs suggested an average enrichment of about 60-fold, lower values of 10 to 15 were observed for field water samples. In total 25/36 (60%) of water samples and 18/36 (50%) of corresponding sediment samples tested AIV positive. Samples were obtained from shallow water bodies in habitats with large numbers of waterfowl during an HPAIV epizootic. Although AIV RNA was detected in a substantial percentage of samples virus isolation failed. Virus loads in samples often were too low to allow further sub- and pathotyping. Similar results were obtained with environmentally deposited avian feces. Moreover, the spectrum of viruses detected by these active surveillance methods did not fully mirror an ongoing HPAIV epizootic among waterfowl as detected by passive surveillance, which, in terms of sensitivity, remains unsurpassed.

**IMPORTANCE** Avian influenza viruses (AIV) have a wide host range in the avian metapopulation and, occasionally, transmission to humans also occurs. Surface water plays a particularly important role in the epidemiology of AIV, as the natural virus reservoir is found in aquatic wild birds. Environmental matrices comprising surface water, sediments, and avian fecal matter deposited in the environment were examined for their usefulness in AIV surveillance. Despite virus enrichment efforts, environmental samples regularly revealed very low virus loads, which hampered further sub- and pathotyping. Passive surveillance based on oral and cloacal swabs of diseased and dead wild birds remained unsurpassed with respect to sensitivity.

**KEYWORDS** avian influenza, surveillance, surface water, sediment, environment, filtration, feces

Avian influenza viruses (AIV) are influenza A viruses within the *Orthomyxoviridae* family. Their genome consists of eight segments of single-stranded RNA of negative orientation (1–3). Based on the two surface glycoproteins, hemagglutinin (HA) and neuraminidase (NA), which are embedded in a host cell-derived lipid envelope, AIV are

**Editor** Daniel R. Perez, University of Georgia

**Copyright** © 2023 Ahrens et al. This is an open-access article distributed under the terms of the [Creative Commons Attribution 4.0 International license](https://creativecommons.org/licenses/by/4.0/).

Address correspondence to Timm C. Harder, [tim.harder@fli.de](mailto:tim.harder@fli.de).

The authors declare no conflict of interest.

[This article was published on 26 January 2023 with incomplete information in the legends of Fig. 2, 4, and 5. The missing information was added and Fig. 4 was slightly reformatted in the current version, posted on 21 February 2023.]

**Received** 3 August 2022

**Accepted** 19 December 2022

**Published** 26 January 2023

grouped into 16 HA and 9 NA subtypes, whereas 2 further influenza A virus subtypes, H17N10 and H18N11, have been detected in bats only (4, 5).

AIV of HA subtypes H5 or H7 are further differentiated by their pathogenicity in chickens: high-pathogenicity (HP) AIV causes systemic infections leading to massive morbidity and mortality in chickens. HPAIV infection can cause high mortality also in other bird species. HPAIV infections in poultry have caused drastic economic losses worldwide, particularly after the emergence in Southeast Asia in 1996 and the subsequent global spread of the so-called goose/Guangdong lineage of H5 HPAIV (6). In contrast, infections with low-pathogenicity AIV (LPAIV) are usually focused on the gastrointestinal tract and induce a much milder course of infection. Frequently, they even remain asymptomatic, especially in populations of wild water birds of the orders *Anseriformes* (ducks, geese, swans) and *Charadriiformes* (gulls, terns, waders), which constitute the most important natural reservoirs of AIVs worldwide (7).

In contrast to mammalian influenza A virus infections, which essentially rely on respiratory infection and droplet-driven transmission, fecal-oral transmission plays a key role in the epidemiology of AIV (7–9). Many waterfowl species use shallow water habitats for foraging and resting. If infected birds congregate in such water bodies, AIVs could then be excreted in surface water through fecal contamination. This may turn such waters into a highly efficient source of infection (10). Once present in water, AIV can drift with currents, sink into sediments, or may otherwise be diluted and inactivated by various abiotic and biotic factors. Yet, the tenacity of AIV in surface water and in sediments is remarkably high for a virion whose infectivity depends on an intact lipid envelope (11–15). In addition, very few viral particles resuspended in surface water can be sufficient to start an infection, as recently shown by experimental infection studies in mallards (*Anas platyrhynchos*) (10). This highlights the putative importance of surface water as a transmission medium of AIV.

Surveillance of AIV in wild water bird populations is important for early warning purposes in protecting poultry populations from incursions of HPAM (16–18). However, some waterbird species are highly endangered, and disturbance of their habitats should be avoided. This limits the sampling opportunities of the birds themselves. Instead, environmental matrices such as surface water that are potentially virus contaminated have been the focus of recent surveillance strategies (19, 20). The counterproductive effect of a dilution of the virus in larger water bodies or by currents needs to be considered when aiming at surface water as a surveillance target. Enrichment of viral particles therefore is an important step in increasing the sensitivity of detection. The spectrum of previously described methods focused on filtration (size or charge exclusion) often combined with ultracentrifugation or precipitation (21).

Charged filters have been found suitable for AIV enrichment from water (22). In general, negatively charged filters led to higher AIV recovery rates (22). Another method to concentrate AIV from smaller water volumes took advantage of formaldehyde-stabilized chicken erythrocytes for AIV binding; erythrocytes express sialic acid receptors utilized by influenza viruses to attach to permissive host cells (23). In addition, other methods such as ultracentrifugation, chromatography, and PEG precipitation were described for influenza A virus purification from cell culture supernatants but not from surface water (24–26). No general best-practice enrichment technology has been identified so far. The use of elution buffers to release particles from filter membranes grossly influenced downstream processing methods for the detection of AIV and poses a common dilemma: Detergents, alcohols, and aldehydes are expected to inactivate viral infectivity rapidly and would exclude virus isolation techniques in cell or egg cultures. However, using less harsh elution buffers might impair the recovery of viruses from filter membranes.

Here, we revisited previous attempts at AIV enrichment from surface water and sediments from various water bodies and types of surface water (fresh, brackish, salt). We combined and validated ultrafiltration techniques with several postfiltration enrichment steps and real-time RT-PCR detection. Environmental water, avian fecal samples, and wild bird carcasses were obtained from regions and during times of a high incidence of HPAIV H5N1 in the anseriform wild bird population. Despite our optimization attempts of active environmental surveillance, passive surveillance on diseased and

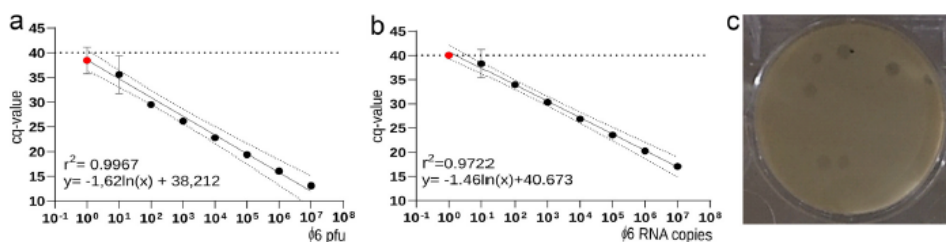


**FIG 1** Performance characteristics of a TaqMan-based real-time RT-PCR (pair 3) for the detection of an M gene-specific fragment of bacteriophage  $\phi 6$ . RT-qPCR was assessed versus phage infectivity (PFU; a) and versus runoff RNA transcript copies of the target (b). Arithmetic averages and variation of triplicate experiments are shown. Red dots depict dilutions in which only 1 out of 3 replicates yielded  $C_t$  values  $<40$  defined as the threshold. (c) Typical results of the six-well plaque assay for bacteriophage  $\phi 6$ .

dead birds remained superior in terms of early detection and measuring population infection trends with HPAIV.

## RESULTS

**Establishment and validation of bacteriophage  $\phi 6$  as an internal surrogate marker of enveloped RNA viruses in surface water filtration and concentration experiments.** Here, we established an infectivity titration system in six-well soft agar plates on basis of plaque-forming units (PFU; Fig. 1), which was complemented by a sensitive, copy-based reverse transcription-quantitative PCR (RT-qPCR). Out of nine different primer pairs (pairs 1 to 9) and two (pairs 3 and 5) TaqMan probes (Table S1 in the supplemental material), the most sensitive one (pair 3) was selected. Figure 1 summarizes the performance characteristics of the optimum  $\phi 6$  TaqMan RT-qPCR. As shown for other dsRNA viruses (27), an initial denaturation step of extracted RNA samples at 95°C for 5 min followed by a snap-cooling step improved PCR sensitivity by at least 1.5  $\log_{10}$  steps (not shown). The RT-qPCR tested with  $\log_{10}$  dilutions of RNA runoff transcripts and RNA extracted from infectious phage particles revealed limits of detection at 10 RNA copies or PFU per reaction, respectively. On the basis of these results, 10 L of surface water was spiked with infectious  $\phi 6$  phage particles as an internal control of enrichment and purification manipulations equivalent to  $2.5 \times 10^{12}$  RNA copies in total.

Downscaling the plaque assay used to determine  $\phi 6$  infectivity titers from standard petri dishes to a six-well plate format had no effect on the test sensitivity (not shown).

**Comparison of filtration and concentration efficacy of Vivaflow and Rexeed ultrafiltration systems using spiked water samples.** Characteristics of two ultrafiltration devices, Rexeed and Vivaflow, were compared. In each case, 10 L of Baltic Sea surface water, taken during the summer months of 2020 from the harbor basin at the FU located on a shallow outlet on the southern coast of the Baltic Sea (54°8'40.428" N; 13° 29' 0.021" E), was spiked with infectious  $\phi 6$  phage particles equivalent to  $2.5 \times 10^{12}$  RNA copies. In addition, 100  $\mu$ L of MDCK-II-grown supernatant containing AIV of subtype H9N2 at a titer of  $5.62 \times 10^7$  TCID<sub>50</sub> mL<sup>-1</sup> was added as a positive target control in validation runs. After addition of the two controls, the 10-L samples were stirred for 30 min at room temperature to achieve homogenous particle distribution.

For standardization, both filtration systems were tested repeatedly (Vivaflow,  $n = 2$ ; Rexeed,  $n = 12$ ). The Rexeed columns were tested with two different elution buffers: 0.2% PBS with ( $n = 8$ ) or without 0.001% Tween 80 detergent ( $n = 4$ ). For Rexeed, the maximal flow rate reached 268.46 mL/min ( $\pm 15.09$  mL/min) versus 45.2 mL/min ( $\pm 6.0$  mL/min) for Vivaflow. Thus, the Rexeed system had processed the 10-L samples on average in 40 min; elution adds another 10 min completing the full cycle in less than 1 h. Aliquots of the original 10-L samples as well as the eluate (Rexeed) and the concentrate (Vivaflow), respectively, each of 150 mL, were tested for viral loads by RT-qPCR and for infectivity by virus isolation in embryonated chicken eggs (AIV H9N2, two to four samples per method) or  $\phi 6$ -plaque assay, respectively (Table 1; Table S2).

**TABLE 1** Validation of two ultrafiltration devices (Vivaflow, Rexeed) for enrichment of enveloped RNA virions (bacteriophage  $\phi 6$ , avian influenza virus H9N2) from surface water samples<sup>a</sup>

Target	Parameter	Vivaflow (n = 2)	Rexeed PBS (n = 8)	Rexeed PBST (n = 4)
$\phi 6$				
10 L	$C_q$	31.98	29.81	31.72
150 mL	$C_q$	27.80	23.49	25.66
Delta $C_q$	$C_q$	4.18 ( $\pm 0.51$ )	6.32 ( $\pm 1.05$ )	6.06 ( $\pm 0.35$ )
10 L	RNA copies	$1.91 \times 10^4$	$9.58 \times 10^4$	$2.43 \times 10^4$
150 mL	RNA copies	$4.73 \times 10^5$	$1.44 \times 10^7$	$2.74 \times 10^6$
Factor	n	$2.99 \times 10^1$ ( $\pm 1.1 \times 10^1$ )	$1.93 \times 10^2$ ( $\pm 1 \times 10^2$ )	$1.27 \times 10^2$ ( $\pm 3.37 \times 10^1$ )
10 L	PFU	$2.09 \times 10^5$	$4.05 \times 10^7$	$9.0 \times 10^5$
150 mL	PFU	$9.07 \times 10^2$	$8.29 \times 10^8$	$1.31 \times 10^7$
Factor	n	$1.26 \times 10^{-2}$ ( $1.26 \times 10^{-2}$ )	$4.64 \times 10^1$ ( $\pm 7.2 \times 10^1$ )	$1.49 \times 10^1$ ( $\pm 4.1 \times 10^0$ )
H9N2				
10 L	$C_q$	30.91	30.99	31.18
150 mL	$C_q$	27.62	25.54	26.08
Delta	$C_q$	3.29 ( $\pm 0.13$ )	5.45 ( $\pm 0.65$ )	5.11 ( $\pm 1.83$ )

<sup>a</sup>Values in parenthesis indicate the standard deviation. Samples were spiked with known amounts of  $\phi 6$  and AIV isolate H9N2. Target detection was by specific RT-qPCRs ( $C_q$  values and, for  $\phi 6$ , corresponding RNA copies are shown) and by virus isolation (plaque assay for  $\phi 6$ ; qualitative isolation in ECE for H9N2). Elution buffers were with (PBST) or without (PBS) supplementation of Tween 80.

As summarized in Table 1, for both spike systems, bacteriophage  $\phi 6$  and AIV H9N2, a basic value in RT-qPCRs of around quantification cycle ( $C_q$ ) 30 was achieved when analyzing aliquots of the original 10-L samples (details for each run separate are depicted in Table S2). Each of the ultrafiltration devices yielded an enrichment of viral RNA. Independent of the elution buffer, the Rexeed system led to a higher concentration than the Vivaflow system when comparing delta  $C_q$  values ( $\phi 6$  and H9N2) and enrichment factors of RNA copies ( $\phi 6$ ). With respect to the different elution buffers of the Rexeed system, marginally higher enrichment factors were obtained by the 0.2 $\times$  PBS buffer without Tween although yields varied considerably between different runs compared to the Tween buffer protocol. Interestingly, elution with either 0.2 $\times$  PBS or 0.2 $\times$  PBS+ 0.001% Tween 80 yielded infectious virus both with  $\phi 6$  and H9N2. Tween-containing elution buffer led to reduced recovery rates for  $\phi 6$ , although infectious H9N2 was recovered from both elution buffer types (Table 1). In the Vivaflow system,  $\phi 6$  infectivity was lost to a great extent while qualitative virus isolation for H9N2 still yielded positive results.

Based on these validation data, as well as on technical considerations, including ease of handling and reduction of time and costs (Table S3), the Rexeed system using PBS elution buffer without Tween supplement was found superior and used in all examination of field samples. The Vivaflow system was excluded also on basis of technical terms due to the frequent blocking of filters.

**Attempts at postfiltration enrichment increasing AIV RNA recovery.** We attempted to further concentrate nucleic acids from the 150 mL of Rexeed filtration eluates comparing solid-phase extraction of dissolved organic matter filtration ( $n = 3$ ), as described in reference 28, and particle-associated ultrafiltration ( $n = 3$ ) using eluate aliquots of 100 mL each. With SPE-DOM, all RNA and infectivity present in the eluate were consistently lost and seemed to be fully adsorbed to the filter material (not shown). Ultrafiltration, in contrast, led to the recovery of particles testing positive by RT-qPCR but no quantitative gain in recovery rates could be verified compared to Rexeed filtration alone (not shown). Based on these results, field water samples were subsequently processed using solely the Rexeed system without applying any postfiltration enrichment procedures (compare Fig. 2).

**Examination of surface water and sediment samples from the field.** 44 surface water samples were examined for the presence of AIV-specific RNA following Rexeed-assisted ultrafiltration. All field water samples were spiked with  $\phi 6$  phage particles as an internal marker of enrichment efficacy. By  $\phi 6$ -specific RT-qPCR and plaque formation assay, recovery rates were controlled and shown to yield variable enrichment efficacies, which on average were lower than validation runs (enrichment factor 10 to 15 versus 60; Fig. 3). This indicates a certain robustness of the Rexeed-assisted

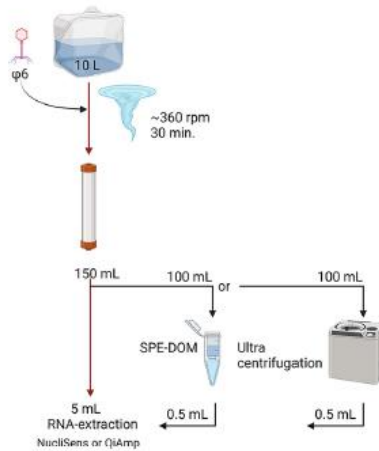


**FIG 2** Flow diagram for influenza A virus and bacteriophage  $\phi 6$  particle enrichment from surface water samples using Rexeed columns and postfiltration measures (ultrafiltration and centrifugation), tested during validation (black arrows) and finally applied (red arrows). Created with BioRender.com.

ultrafiltration procedures with water samples of different origin (fresh, salt and brackish water). However, the higher content of floating particles/sediment in the majority of samples might have reduced recovery rates. As a positive control for the detection of AIV, a sample was obtained from a small water pool of 100 L used by 10 mallards during an HPAIV H5N8 infection experiment (10). This sample, expectedly, yielded a high virus load ( $C_q$  26.47) after ultrafiltration, sufficient for full sub- and pathotyping (Table 2, sample 57). True field samples were obtained from various locations in Sweden ( $n = 1$ ; bird trap on the island of  $\text{\O}$ land, Baltic Sea, Sweden), Germany ( $n = 33$ ), and the Antarctic Weddell Sea ( $n = 5$ ) (Table 2, Fig. 4, and Fig. S1). Shallow water bodies on the island of Koos, Germany, at the southern coast of the Baltic Sea, were sampled repeatedly over a period of 19 weeks. Five additional samples were taken from open water bodies on holdings of poultry ( $n = 2$ ) or kept birds ( $n = 2$ ), which experienced acute HPAIV outbreaks during a period of a high incidence of HPAIV infections in wild birds in the respective regions in northern Germany (Fig. 4, stars).

In 27 out of 44 true field water samples (61%), AIV-specific RNA could be detected. The  $C_q$  values ranged from 33.7 to 39.67 signaling low virus loads. RNA isolated from nine sample eluates revealed PCR inhibitory effects and had to be retested at a 1:10

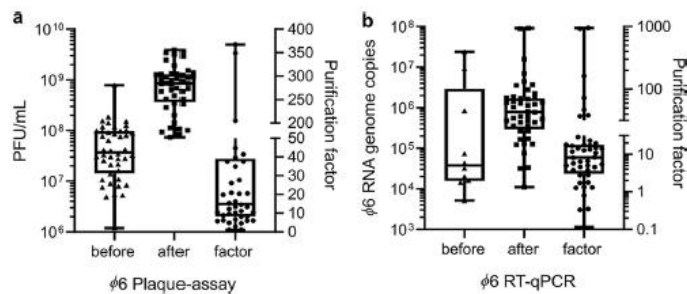


**FIG 3** Recovery rates of bacteriophage  $\phi 6$  spiked into field samples of surface water as a measure of enrichment efficacy by Rexeed-assisted ultrafiltration. Infectivity (a) was measured by plaque formation assay (PFU/mL; left scale) and by RT-qPCR (b; RNA copies; left scale) before and after filtration. Corresponding enrichment factors were calculated (a and b; right scales).

**TABLE 2** Analyses for presence of avian influenza viruses of Rexeed-filtrated surface water samples and corresponding sediment samples from different sources<sup>a</sup>

Sampling site <sup>b</sup>	Sample no. and type <sup>c</sup>	Water				Sediment			
		AI RT-qPCR before Rexeed	AI RT-qPCR after Rexeed <sup>d</sup>	Subtype	Pathotype	AIRT-qPCR	Subtype	Pathotype	
1	1	Neg	37.08	Not H5/H7	n.e.	32.07	H2, H4, H5, H6, N3, N9	Not typable	
6a	2	35.87	33.70*	H6, N2, not H5/H7	n.e.	Neg	n.e.	n.e.	
6b	3	Neg	36.68*	Not H5/H7	n.e.	Neg	n.e.	n.e.	
3	5	36.06	35.55	H5	Neg	34.92	H5	Not typable	
8	6	Neg	35.02*	Not H5/H7	n.e.	Neg	n.e.	n.e.	
6b	7	n.e.	Neg	n.e.	n.e.	40.19	H5	n.e.	
2	12	38.02	37.68	Not H5/H7	n.e.	35.32	H5, H6, N3, N9	H5-LP, H5-2.3.4.4b	
6a	13	n.e.	Neg	n.e.	n.e.	37.36*	Not H5/H7	n.e.	
6b	14	Neg	37.51	H5	Not typable	34.15*	Not H5/H7	n.e.	
8	15	n.e.	Neg	n.e.	n.e.	34.53*	Not H5/H7	n.e.	
7	17	n.e.	35.76*	Not H5/H7	n.e.	35.13*	Not H5/H7	n.e.	
4	18	Neg	36.56*	Not H5/H7	n.e.	Neg	n.e.	n.e.	
6b	19	Neg	35.70*	Not H5/H7	n.e.	37.37*	Not H5/H7	n.e.	
6a	20	n.e.	39.67	Not H5/H7	n.e.	Neg	n.e.	n.e.	
6b	22	n.e.	Neg	n.e.	n.e.	Neg	n.e.	n.e.	
6a	23	n.e.	Neg	n.e.	n.e.	Neg	n.e.	n.e.	
5	25	Neg	36.03	Not H5/H7	n.e.	Neg	n.e.	n.e.	
8	26	Neg	35.45	Not H5/H7	n.e.	37.05*	Not H5/H7	n.e.	
7	27	n.e.	37.79	Not H5/H7	n.e.	36.54	Not H5/H7	n.e.	
6b	28	n.e.	Neg	n.e.	n.e.	35.77	Not H5/H7	n.e.	
6a	29	n.e.	Neg	n.e.	n.e.	Neg	n.e.	n.e.	
6b	30	n.e.	Neg	n.e.	n.e.	37.15	H5, H7	Not typable	
6a	31	n.e.	Neg	n.e.	n.e.	38.12*	Not H5/H7	n.e.	
7	32	n.e.	Neg	n.e.	n.e.	35.04	Not H5/H7	n.e.	
4	33	n.e.	Neg	n.e.	n.e.	Neg	n.e.	n.e.	
6a	34	Neg	38.51	Not H5/H7	n.e.	Neg	n.e.	n.e.	
6b	35	Neg	35.57*	Not H5/H7	n.e.	Neg	n.e.	n.e.	
6b	44	Neg	36.73	Not H5/H7	n.e.	Neg	n.e.	n.e.	
6a	45	Neg	36.37	Not H5/H7	n.e.	Neg	n.e.	n.e.	
8	46	38.23*	35.34	Not H5/H7	n.e.	33.92	Not H5/H7	n.e.	
6a	47	Neg	36.27	Not H5/H7	n.e.	Neg	n.e.	n.e.	
6b	48	Neg	39.64	Not H5/H7	n.e.	Neg	n.e.	n.e.	
7	49	Neg	35.44	Not H5/H7	n.e.	36.93	Not H5/H7	n.e.	
8	50	Neg	36.37	Not H5/H7	n.e.	Neg	n.e.	n.e.	
A	4	Neg	36.98*	H5	Not typable	Neg	n.e.	n.e.	
B	16	Neg	37.82	Not H5/H7	n.e.	34.62*	Not H5/H7	n.e.	
C	21	Neg	39.1	Not H5/H7	n.e.				
D	24	Neg	34.84*	Not H5/H7	n.e.				
M, G	57	32.79*	26.24	H5, N8	HP-2.3.4.4b				

<sup>a</sup>Neg,  $C_q \geq 40$ ; n.e., not examined; M, sample from mallard infection experiment (10).

<sup>b</sup>See Table 4 and Fig. 4 for numbering of sampling site and type of water sample.

<sup>c</sup>Water sample type is indicated by no shading (fresh), light-gray shading (brackish), or dark-gray shading (salt).

<sup>d</sup>Asterisks represent 1:10 dilution.

dilution (Table 2, marked by an asterisk). From these samples, virus loads up to 3.3  $C_q$  values higher are to be expected lowering the range to arithmetically  $C_q$  30.4 for sample 2. For four samples, subtyping by RT-qPCR was successful. This included sample 2 showing the highest virus load that contained AIV of subtype H6N2. Three further samples generated a positive signal for subtype H5, but no corresponding NA subtype could be assigned. Likewise, pathotyping by RT-qPCR did not produce valid results due to the low virus loads. Interestingly, all five samples from HPAIV outbreak holdings tested positive for AIV of which two were also subtyped as H5. None of the ocean water samples collected in the Antarctic Weddell Sea yielded a positive signal (data not shown). Virus isolation was unsuccessful.

For a subset of 36 water samples, corresponding sediments were available. 18 sediment samples (50%) tested positive in the generic RT-qPCR with average  $C_q$  values of

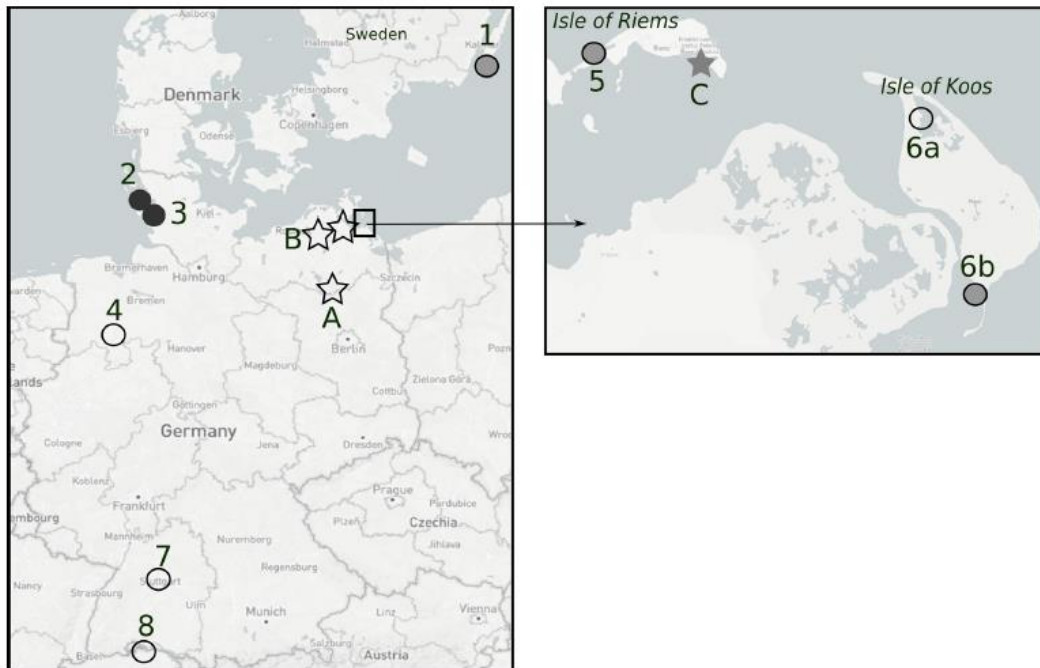


**FIG 4** Geographic locations of sampling sites for surface water and corresponding sediments. Dots, scheduled samples taken on a routine base; stars, HPAI outbreak samples. Shading of symbols represents water sample type: no shading, fresh; gray shading, brackish; black, salt. (Maps © Mapbox [[www.mapbox.com/about/maps](http://www.mapbox.com/about/maps)] and © OpenStreetMap [[www.openstreetmap.org/about/](http://www.openstreetmap.org/about/)].)

35.9 (range, 32.07 to 38.04). For the matched surface water samples, 25 out of 36 (69%) tested AI positive by RT-qPCR (36.6, range, 33.07 to 38.78), but no significant differences in average  $C_q$  values were evident (Table 2). Fourteen samples were congruently positive, and four were negative in water and sediment extracts. Twelve samples tested positive in water only and seven were positive in sediments only. For each type, eight samples revealed PCR inhibitory factors. Subtyping was possible for four and five of the matched water and sediment samples, respectively. The range of subtypes detected appeared to be broader for the sediment type (Table 2). Six different HA (2, 4, 5, 6, 7, and 9) and three different NA (3, 6, and 9) were detected in sediments whereas in water samples HA5 and 6 and N2 were distinguished. Pathotyping was possible in a single sediment sample only. As with the water samples, no AIV was isolated from any of the sediment samples.

**Metagenome sequencing of a field water sample.** RNA extracted from water sample 5 was subjected to a metagenome sequencing approach because of its comparatively high virus load for H5 with a  $C_q$  value of 33.55 (Table 2). The data set obtained from the generic sequencing workflow yielded 5,749,075 reads in total. The generic approach of the metagenome analysis of the sample primarily showed a broad spectrum of viruses ( $n = 2,877$ ), bacteria ( $n = 1,623,636$ ), archaea ( $n = 9,807$ ), and eukaryotes ( $n = 4,020,940$ ) present in the sample. Members of a total of 29 different virus families could be detected. The internal marker bacteriophage  $\phi 6$  was highly represented (1,039 reads, 0.02%) likely due to the specific spiking of the sample. However, the generic approach failed to generate any AIV-specific reads despite the positive results of the generic and H5-specific RT-qPCRs. Using a baits-based enrichment approach, however, 288 AIV reads (0.08%) were detected in the sequencing data set of 359,114 reads in total. A blastn analysis (<https://blast.ncbi.nlm.nih.gov/Blast.cgi>) assigned all of those reads to

**TABLE 3** Results of active (environmental avian fecal samples) and passive surveillance (swabs of avian carcasses) for avian influenza viruses in three anseriform bird species during epizootics of HPAIV H5 along the Wadden Sea coast of the German Federal State of Schleswig-Holstein<sup>a</sup>

Species	Time	Environmental fecal samples			Swabs (carcasses)	
		Total/AI <sup>b</sup>	Subtype	Pathotype	Total/AI <sup>b</sup>	Sub- and pathotype
<i>Branta leucopsis</i>	12/20	20/0			8/6	HP H5Nx (2), HP H5N5 (1), HP H5N8 (4)
	01/21	390/4	H9N2 (3), H5N2 (1)			
	02/21	390/24	H5Nx (2), H5N6 (1), Not H5/H7 (17), H7 (1), H5 (1), n.e. (2)		6/6	HP H5N8 (6)
	03/21	580/33	Not H5/H7 (29), H5 (1); [H9, N2, H5, N3] (1), [H9, N2, H10, H5 (1)]	H5-LP (1), 2.3.4.4b (1)	5/5	HP H5N1 (1), HP H5N8 (4)
	11/21	125/3		H5-HP (1), 2.3.4.4b	6/6	HP H5N1 (6)
	12/21	100/2			5/4	HP H5N1 (4)
	01/22	25/0			10/9	HP H5N1 (9)
	02/22	50/2	Not H5/H7 (2)		9/8	HP H5N1 (5)
	03/22	25/3	H5 (2)	2.3.4.4b (1)	11/9	HP H5N1 (9)
	Sum <i>Branta leucopsis</i>		1,705/71		65/56	53
	<i>Branta bernicla</i>	01/21	20/2	H3N8 (2)		
02/21		20/2	Not H5/H7 (1), n.e. (1)			
03/22		75/4	Not H5/H7 (2), N1 (1), N8 (1)	H5-HP-2.3.4.4b (2)	1/1	HP H5N1 (1)
Sum <i>Branta bernicla</i>		115/8		1/1	1	
<i>Mareca penelope</i>	12/20	20/3	H4N6 (2), n.i. (1)		1/0	
	01/21	85/0				
	02/21	25/0				
	03/21	70/4	Not H5/H7 (3), H5 (1)			
	11/21	50/2				
	12/21	50/1				
	03/22				2/0	
Sum <i>Mareca penelope</i>		300/10		3/0		
Sum all		2,120/89		68/57	54	

<sup>a</sup>Over the complete sampling time (November 2020 until April 2022), 12% of the suspected passive surveillance sampled were AIV negative and 15% were negative for HPAIV. n.i., not identifiable; n.e., not examined.

<sup>b</sup>Positive for AIV RNA by generic RT-qPCR.

subtype H5N8. A full AI virus genome, however, could not be assembled from those reads. Likewise, pathotyping based on HA sequences was not possible. Sequences were submitted to NCBI and are available under accession numbers [OP615145–OP615148](https://doi.org/10.1093/oxford.oi.oi.oi.oi.oi.oi).

**Examination of environmental fecal wild bird samples.** Environmental avian fecal samples were tested as another leg of AIV wild bird surveillance. Here, a region and time were chosen for a high incidence of HPAIV H5 clade 2.3.4.4b among populations of anseriform wild birds along the Wadden Sea coast of the German Federal State of Schleswig-Holstein from November 2020 to April 2022. Fecal samples were collected by ornithologically experienced rangers of the Wadden Sea national park. To correlate fecal samples and corresponding bird species, sampling was restricted to sites where large flocks of barnacle (*Branta leucopsis*) and brent geese (*Branta bernicla*) or Eurasian wigeons (*Mareca penelope*) were spotted immediately before sampling. At the same time and region, but not necessarily at the same spots, carcasses of the three species were retrieved and oropharyngeally and cloacally swabbed. Results of AIV RT-qPCRs performed on fecal samples and swabs are summarized in Table 3. A considerable proportion of fecal samples (52%) but not of swabs revealed the presence of PCR inhibitors and had to be reexamined in a 1:10 dilution. A total of 2,120 fecal samples and 115 carcasses were finally examined. From that total, 83.8% of all carcasses tested positive for AIV ( $C_q$  26.4 ± 5.2), and 79.4% of the carcasses tested positive for HPAIV H5 of clade 2.3.4.4b with, on average, high viral loads ( $C_q$  24.8 ± 5.2). A total of 89 fecal samples (4.2%) harbored AIV-specific RNA with viral loads ranging from  $C_q$  31.1 to 39.3; 26



samples could be subtyped revealing a broad spectrum of subtypes as listed in Table 3. Among them, viruses of subtypes H5 ( $n = 13$ ) and H7 ( $n = 1$ ) were also present. Pathotyping was successful for six fecal samples identifying HPAIV H5 of clade 2.3.4.4b in five and LPAIV H5 in one sample.

## DISCUSSION

HPAIV of the gs/GD lineage remains a threat to poultry populations worldwide. In Europe, seasonal reoccurrence during the winter months in migratory wild bird populations and subsequent spread to and among poultry holdings have been observed (8, 29). In Germany, since 2016/2017, there is a trend toward an increasing number of cases in wild birds and poultry (30). In parallel, a tendency for the year-round presence of HPAIV in the wild bird population in northern Europe has been reported (31). As a response to the year-round high incursion pressure of HPAIV, enhanced biosecurity measures for poultry holdings included restricted outdoor rearing and trading activities. Improved early warning for HPAIV incursion pressure is expected to limit the period of restrictive biosecurity measures. Here, we examined whether environmental samples can be used to support strategies of individual wild bird samplings. We validated a hollow-fiber ultrafiltration system to enrich AIV from surface water bodies. The results were compared to the analysis of corresponding sediments and environmentally deposited avian fecal samples.

Since the discovery of viruses, filtration for viral enrichment from liquid media has been important (32). However, these techniques were mostly designed to concentrate virus from cell culture supernatants or other smaller volumes such as clinical samples. Here, we used 10 L of surface water, which is easy to collect and ship to the laboratory by general services. Sample collection was mainly directed to smaller shallow water bodies within aquatic bird habitats. With respect to the enrichment effect, the Rexeed device proved to be the best method. The bacteriophage  $\phi 6$  was indispensable as an internal control during validation runs and is useful also in the control of field samples with various loads of suspended sediment matter. An astonishingly high percentage of about 60% gave positive results for AIV-specific RNA by RT-qPCR. However, the virus load ( $C_q$  range from 33.7 to 39.67) detected usually was close to the limit of detection and postfiltration methods failed to further enrich virus particles. The type of water sample (i.e., fresh, brackish, or salt) apparently had no influence on detectability (Table 2). Also, water samples obtained from water bodies at confirmed HPAI outbreak areas revealed only low virus RNA loads, comparable to previous studies (33). Several samples had to be examined after dilution due to the presence of PCR inhibitory substances. This severely restricted downstream analyses for sub- and pathotype determination. Consequently, only some samples could be further sub- or pathotyped. Other groups (e.g., reference 34) recommended using 2 M NaCl and 2 mM ethylenediamine tetra-acetic acid to minimize PCR inhibitors in difficult samples, but this has not been applied here to keep the number of steps and preparation time as low as possible. Also, AIV isolation was generally unsuccessful although validation runs suggested that infectious AIV can be recovered qualitatively, and spiked infectious bacteriophage  $\phi 6$  was regularly recovered from field samples (Fig. 3). Metagenomic sequencing approaches confirmed that the RNA recovered from the Rexeed columns is generally suitable for a large array of downstream investigations. However, low viral RNA loads again limited the success of further genotyping AIV since an additional myBaits-directed sequencing approach was required to enrich AIV nucleic acids nevertheless allowing at least sub- and pathotyping.

Given the very low virus loads recovered in the eluates, the use of larger sampling volumes might be appropriate. However, a substantial effect (gain of at least 1  $\log_{10}$  step of virus load) would require volumes  $>100$  L. Since sending such volumes is difficult and costly, pumping surface water through the Rexeed device on a sampling spot would be required. Notwithstanding the fact that handling larger volumes requires increased technical support including a source of electricity in the field and skilled staff, we did not evaluate the suitability of Rexeed columns for such large sample volumes.

The success of detecting and characterizing AIV in surface water samples correlated

with the initial virus load in the sampled water body. This was evident also by examining a sample from a 100-L water pool used for at least 2 days without changing the water by 10 HPAIV-infected mallards during an infection experiment. Virus detection and sub- and pathotyping were readily possible in the pooled sample.

Sediments of shallow water bodies had previously been successfully used to detect AIV RNA (35). Sedimentation of virus particles with other floating matter over time actually resembles a first enrichment step from water columns. Here, we examined 36 sediment samples matching with water samples from the same spot. In half of them, AIV RNA was detected but at the same low virus loads as in water samples. Nevertheless, subtyping attempts by RT-qPCRs revealed a larger spectrum of subtypes compared to the water column. This may reflect deposits of different AIV subtypes over time in sediments versus representation of more current AIV strains in the water column. In addition, matching qualitative results of corresponding water and sediment samples were limited indicating again that two different reservoirs of AI viruses are likely represented by these matrices. Although virus isolation failed for sediment samples, it cannot be excluded that AI viruses deposited in sediment retain infectivity and that sediments could serve as an environmental reservoir of infectivity. RNA extraction from sediments proved to be highly time consuming (at least 8 h) and not suitable for high-throughput analyses. The limited elution volume of about 30  $\mu$ L generated by the method used here grossly restricts downstream diagnostic investigations.

With respect to the above-mentioned restrictions of using water and sediment samples for AIV surveillance, we included in our analysis environmentally deposited fresh avian fecal samples collected in the same region and during the same period. Although sampling was restricted to very few species including the barnacle goose, which was the main victim of the HPAIV wild bird epizootics since 2020 in Germany, only a minority (71/1705; 4.16%) of fecal samples from that species harbored AIV-specific RNA even during the peak of the epizootic, and only 10 samples could be determined as H5, of which just 3 were accessible to pathotyping as LP ( $n = 1$ ) or HP-2.3.4.4b ( $n = 2$ ), respectively. As with water and sediment samples, low viral RNA loads hampered downstream analyses. The presence of PCR inhibitory substances in the fecal matter likely contributed to the low viral loads detected. The use of different RNA extraction buffers claimed to reduce the inhibitory effects of fecal samples did not help to increase yields of viral RNA (not shown). In contrast, analysis of swabs collected from dead barnacle geese at the same time and from the same region revealed the presence of HPAIV H5Nx of clade 2.3.4.4b in 82.81% of carcasses analyzed. The limited usefulness of environmentally deposited avian feces for active AIV surveillance has been pointed out repeatedly (36, 37), and our current results confirm this. Several independent factors may contribute such as failure to collect sufficient fecal material, low cloacal excretion of AIV, and presence of inhibitory substances (porphyrins from chlorophyll, gut microbiota).

Despite over 100 years of practical work on virus purification via filtration devices, highly sensitive and technically undemanding methods for broad-spectrum viral surveillance applications are still scarce. Here, we confirmed previous reports that it is generally possible to detect AIV in environmental water and sediment samples. Yet, the viral loads are generally too low for virus isolation or further sub- and pathotyping purposes. Specific receptor-binding approaches such as those described in reference 38 have recently been found to be potentially more sensitive, also when smaller water volumes were investigated. Such techniques should be explored further. Alternative targets, such as environmentally deposited avian fecal samples, are laborious during collection and were shown to suffer from similar limitations as the water samples. Moreover, the spectrum of viruses detected by such active surveillance methods did not fully mirror an ongoing HPAIV epizootic among anseriform wild birds as detected by passive surveillance, which, in terms of sensitivity, remains unsurpassed.

## MATERIALS AND METHODS

**Use of bacteriophage  $\phi$ 6 as surrogate of influenza A viruses in environmental samples.** The bacteriophage  $\phi$ 6 of the *Cystoviridae* family resembles AIV by featuring a lipid envelope, a spherical shape of 75-nm diameter, and a segmented 13.4-kB RNA genome. However, in contrast to AIV,  $\phi$ 6 carries a

double-stranded RNA genome. The bacteriophage  $\phi 6$  replicates in a plant-specific bacterium and is considered a BSL-1 agent (39). These features render  $\phi 6$  an interesting surrogate of influenza A viruses in validation experiments using environmental samples.

**(i) Bacterial media and buffers.** Medium 545 (tryptone soya broth [TSB]) was prepared as described by the DSMZ (German Collection of Microorganisms and Cell Cultures, Braunschweig, Germany) (40). The bouillon was supplemented with bacterial agar (Bact Agar Solidifying Agent; no. 214010; BD Diagnostics, East Rutherford, NJ, USA). For soft agar, 7.5 g per L broth was added and 15 g for solid agar. Phage buffer (49 mM  $\text{Na}_2\text{HPO}_4$ , 22 mM  $\text{KH}_2\text{PO}_4$ , 86 mM NaCl, 1 mM  $\text{MgSO}_4$ , and 1 mM CaCl<sub>2</sub>) was used for cultivation of bacteriophage  $\phi 6$ , as mentioned in reference 41. Salt-peptone buffer was used for dilution of  $\phi 6$  in titration experiments (no. OXTV5016D; Oxoid Deutschland, Wesel, Germany).

**(ii) Culture of *Pseudomonas syringae*.** *Pseudomonas syringae* (DSMZ-21482) was received from DSMZ as a freeze-dried sample. For cultivating, the sample was mixed with 0.5 mL TSB liquid medium and 0.25 mL was plated and incubated overnight on TSB agar. A single bacterial colony was then transferred into 25 mL TSB bouillon and incubated for 20 h at 25°C and 222 rpm. Glycerine was then added to the bacterial suspension to a final concentration of 20% (vol/vol), and aliquots were stored at -80°C as a stock from which "working-aliquots" were grown as described.

**(iii) Culture of bacteriophage  $\phi 6$ .** The *pseudomonas* phage  $\phi 6$  (DSMZ-21518) was obtained from DSMZ. The bacteriophage was grown in cultures of its specific host bacterium *Pseudomonas syringae*. Generally, all culturing steps took place at 25°C for 20 h on an orbital shaker at 222 rpm. The bacteriophage  $\phi 6$  was shipped on filter paper; half of the paper was placed onto a TSB-agar plate. In a reaction tube, 0.1 mL *Pseudomonas syringae* working solution (see below), 0.1 mL phage buffer, and 4 mL TSB-soft agar were mixed, poured over the paper on the plate, and incubated at 25°C. The next day, a single plaque colony was identified and transferred into 50  $\mu\text{L}$  of phage buffer, mixed, and pipetted into 42 mL of a liquid culture of *Pseudomonas syringae* and incubated for 20 h at 25°C at 222 rpm. The bacteriophage-containing supernatant was recovered by centrifugation ( $5,594 \times g$ , 30 min) and passed through a 0.45- $\mu\text{m}$  filter. The filtrate was supplemented with glycerine to 20% (vol/vol), aliquoted, and stored at -80°C until further use.

**(iv) Titration of  $\phi 6$  infectivity.** Classical plaque assays were used. A *Pseudomonas syringae* working stock (0.5 mL) was cultivated overnight in 300 mL TSB media, at 25°C and 222 rotations per minute (rpm). Then, 10 mL of the overnight bacterial suspension was diluted 1:5 in TSB media to start a fresh log-growth phase for 4 further hours. At an optical density ( $\text{OD}_{600}$ ) of 1.2 to 1.4, the suspension was ready to be used for the plaque assay. Phage suspensions were serially diluted 10-fold in salt-peptone buffer. Of each dilution step, 400  $\mu\text{L}$  of the sample, 1,000  $\mu\text{L}$  of hand-warm TSB soft agar, and 400  $\mu\text{L}$  of *Pseudomonas* suspension ( $\text{OD}_{600}$  1.2 to 1.4) were mixed. A total of 450  $\mu\text{L}$  of this mixture were then pipetted into 1 well of a 6-well plate on top of 2.5 mL of solidified TSB agar. Triplicates of each dilution step and sample were used. A  $10^{-9}$   $\phi 6$  dilution containing  $19 (\pm 7.4)/0.1$  mL plaque-forming units (PFU) was used as a titrated positive control. As negative controls, salt-peptone buffer without  $\phi 6$  and bacteria only was used. After solidification of the soft agar layer, the plates were incubated upside down at 25°C for 22 h. Dilutions with  $\leq 120$  plaques were quantified with the naked eye, and PFU per volume were calculated.

**(v)  $\phi 6$ -Specific real-time quantitative RT-PCR.** Nine pairs (pairs 1 to 9) of primers were selected from conserved regions within the M-segment of  $\phi 6$  and evaluated using a SYBR green RT-qPCR kit (SensiFAS SYBR No-ROX one-step kit; no. BIO-72001; Bioline Reagents Ltd., UK) at different annealing temperatures (50, 53, 56, and 60°C) in a three-step PCR-Program and at 60°C annealing for a two-step amplification program on a Bio-Rad Cfx1000 thermocycler (Bio-Rad Laboratories, Inc, Munich, Germany). Serial 10-fold dilutions of a stock of  $\phi 6$  RNA were used as a template for validation runs, and PCR products were also checked by agarose gel electrophoresis.

For two primer pairs (pairs 3 and 5) yielding specific products at high sensitivity, FAM-labeled TaqMan probes were designed (Metabion International AG, Planegg, Germany, or IDT, Leuven, Belgium; Table S1). RT-qPCRs were assembled using the AgPath-ID one-step RT-PCR kit (Applied Biosystems; AM1005). Each 25  $\mu\text{L}$  PCR contained 5  $\mu\text{L}$  of  $\phi 6$  RNA template. According to previous experiences with PCRs of viral double-stranded RNA (27), each RNA sample was subjected to an initial melting step (95°C for 5 min) whereafter the RNA was shock-cooled on a 96-well plate rack precooled in the -80°C freezer before being added to the RT-qPCR mix. Cycling conditions on a CFX96 Real-Time-System C1000 Thermal Cycler (Bio-Rad, Munich, Germany) comprised of reverse transcription at 45°C for 10 min, Taq activation at 95°C for 10 min, followed by 43 cycles of 95°C for 15 s, 56°C for 20 s, and 72°C for 30 s.

**(vi)  $\phi 6$ -Specific T7-runoff transcripts.** A 95-bp-long  $\phi 6$  fragment was chosen to generate a T7-runoff transcript as a positive control and to determine genome copy number. The fragment was ligated into the pCR 2.1-TOPO vector (K450002; Thermo Fisher Scientific, Waltham, MA, USA), and subsequently DH10B Competent Cells (EC0113; Thermo Fisher Scientific) were transformed with the plasmid. One hundred microliters of the transformation mixture was spread on an ampicillin-supplemented LB plate with IPTG and X-Gal for blue-white selection and incubated overnight. The next day, white bacterial colonies were picked and plasmids were prepared and sequenced with the M13-F and M13-RV primers. A plasmid harboring a fragment with an integer sequence inserted in the correct orientation was expanded, and plasmid DNA was recovered with the Qiagen Plasmid Midi kit (no. 12141; Qiagen, Hilden, Germany). Subsequently, 5  $\mu\text{g}$  of the Midi prep plasmid DNA was linearized using KpnI (New England Biolabs, Ipswich, MA, USA). Linearized DNA was cleaned using the QIAquick Nucleotide Removal kit (no. 28306; Qiagen). For *in vitro* transcription, the Ribomax Large Scale RNA Production System (no. P1300; Promega, Walldorf, Germany) was used. Priming was achieved with a T7 primer. After completion of the *in vitro* transcription, the preparation was digested using DNase Max (no. 15200-50; Qiagen). The RNA

**TABLE 4** Characteristics of water and sediment sampling locations

Sampling site ID <sup>a</sup>	Name	Longitude	Latitude	Water body	Water type <sup>b</sup>	Size (km <sup>2</sup> )	Maximum depth (m) <sup>c</sup>
1	Öland, Sweden	56.19505388	16.40021843	Baltic Sea, shallow inlet	Brackish	4	459 (inlet: 2 m)
2	Wadden Sea, Germany	54.52323015	8.863123177	North Sea, Wadden Sea	Salt	57,500	10
3	Wadden Sea, Germany	54.32637344	8.978028613	North Sea, Wadden Sea	Salt	57,500	10
4	Lake Duemmer, Germany	52.51297182	8.363835947	Lake	Fresh	14	1,4
5	Isle of Riems, Germany	54.18209948	13.35165043	Baltic Sea, shallow inlet	Brackish	514	14
6a	Isle of Koos, Germany, pond	54.17812491	13.40298791	Pond	Fresh	0,20	0,5
6b	Isle of Koos, Germany, beach area	54.16425804	13.41179628	Baltic Sea, shallow inlet	Brackish	514	14
7	Lake Max-Eyth, Germany	48.83135805	9.212351778	Lake	Fresh	0,17	2,3
8	Lake Constance, Germany	47.73414934	8.969084606	Lake, shallow inlet	Fresh	536	251 (inlet: 2 m)
A	Amt Röbel-Müritz, Germany	53,37700785	12.60598935	Fire pond	Fresh	100 m <sup>2</sup>	2
B	Amt Laage, Germany	53.92883034	12.34628184	Fire pond	Fresh	100 m <sup>2</sup>	1
C	County Greifswald, Germany	54.09577118	13.38036172	Southern Baltic Sea, shallow inlet 2	Brackish	514	14
D	Grimmen, Germany	54.1129066	13.04327085	Fire pond	Fresh	100 m <sup>2</sup>	2

<sup>a</sup>See Fig. 4 for depiction of site on map; A to D, samples originating from HPAI outbreak holdings; holding C is the site of a mallard sentinel station (60). The numbering corresponds with the sample IDs given in Table 2.

<sup>b</sup>Fresh, brackish, and salt (sea) water categorization is according to salt concentration: <1.000 ppm, 1.000 ≤35.000 ppm, and ≥35.000 ppm.

<sup>c</sup>All samples were taken in "rubber boots-depth" (50 cm) indicating sampling spots close to the riverbank.

concentration was measured by Nanodrop. The genomic copy number of generated  $\phi 6$  RNA runoff transcripts was calculated by using the <http://endmemo.com/bio/dnacopynum.php> calculator (42).

**Influenza A viruses.** AIV were obtained from the virus collection kept at the German National Reference Laboratory for Avian Influenza at Friedrich-Loeffler-Institut, Greifswald-Isle of Riems, Germany. Strain A/Greyllag goose/Germany-MV/AR10080/2016 (H9N2) was grown in MDCK-II cells in a T25 cell-culture flask in the presence of TPCK-trypsin (2  $\mu$ g/mL, final). Cultures were incubated for 48 h when extensive cytopathic effects had disrupted the cell monolayer. Following a freeze/thaw cycle the supernatant was clarified, aliquoted, and stored at  $-80^{\circ}\text{C}$ .

**(i) Isolation and titration of influenza A viruses in cell culture and embryonated eggs.** Field samples to be analyzed for AIV infectivity were passed through a 0.45- $\mu\text{m}$  filter (Millex-MCE 50S Filtereinheit, 45  $\mu\text{m}$ ; no. Millipore SLHA0335S; Merck KGaA, Darmstadt, Germany) to reduce bacterial contamination. A total of five 11-day-old embryonated specified pathogen-free-chicken eggs (ECE; VALO, Cuxhaven, Germany) were inoculated each with 0.2 mL of the filtered sample into the allantoic cavity. The eggs were incubated for up to 6 days at  $37^{\circ}\text{C}$  and candled daily for embryonic death. Eggs containing dead embryos, and all eggs at day 6 postinoculation, were chilled to  $4^{\circ}\text{C}$  for at least 16 h before allantoic fluid (AAF) was harvested and tested for hemagglutination as described previously (43). In addition, RNA was extracted from selected AAFs and tested by influenza A virus generic RT-qPCR (see below). Infectivity titers were measured and calculated according to reference 44.

Furthermore, MDCK-II cell cultures (CRL-2936) were used for virus isolation, amplification, and titration of AIV infectivity in parallel. Methods have been outlined in reference 10.

**(ii) Influenza A virus-specific RT-qPCRs.** Extracted RNAs (see below) were tested for the presence of AIV by targeting in real-time RT-qPCR generally conserved regions of the M or NP genome segments (45, 46). An internal control (IC-2) as described in reference 47 was added to each sample during the RNA extraction process. Samples that showed an inhibition of the IC-2 amplification were reexamined at a 1:10 dilution. Samples testing positive for AIV-specific RNA were sub- and pathotyped by RT-qPCRs as described previously (48–51).

**Collection and processing of environmental samples.** Samples of 10 L of surface water were collected between November 2020 and October 2021 from various locations in Germany (Fig. 4). Characteristics of the sampling site and water type are presented in Table 4. The surface water was recovered and transported in 10-L canisters (no. 216-5333; VWR International GmbH, Darmstadt, Germany). To collect water, the canisters were dipped just below the water's surface. Antarctic water samples were taken via pumping (Fig. S1). Water samples from Germany were either shipped in a Styrofoam box within 24 h after collection or immediately transferred to the lab, depending on the site. When accessible at the water sampling site, sediments (scooped out the sediment at the water extraction site) were collected as well. RNA from sediment samples was extracted as described in reference 52 and analyzed for AIV. The fecal samples were treated in the same way as those from active monitoring.

A further 10-L sample originated from a water pool used in experimental AIV infection studies of mallards (10). This sample was taken on day 6 of the infection experiment, when the majority of mallards were excreting HPAIV of subtype H5N8, clade 2.3.4.4b, at high titers. During February 2021, ocean water samples were obtained by pumping from coastal areas of the Antarctic Weddell Sea as shown in Fig. S1 (sampling permission no. II 2.2-94033/176 in combination with no. II 2.8-94033/168). These samples were intended as a kind of negative control due to the expected high dilution effect.

**(i) Surface water filtration using the Vivaflow 200 device.** The Vivaflow 200 system utilizes tangential cross-flow filtration in combination with a cassette filter unit design. The additional equipment for the Vivaflow 200 filtration included Masterflex peristaltic pump (no. VFP001), Masterflex Easy Load pump head (size 15; no. VFA013), Tygon pumping tube (size, 15, 4.8 × 1.6 mm, 3 m once with Luer adapter; no. VFA003), and Y-connecting adapter (no. VFA005; all listed equipment was received from Sartorius Lab Instruments, Göttingen, Germany). The filtration was performed as described in the manual (53) with one exception; for the Vivaflow 200 setup, the fluid from the “rubbish” adapter was returned to the sampling bottle until the volume in the sampling bottle was reduced to a volume of 150 mL. Before and after each run, the cassettes were treated as described in the manual (53). The final concentrate consisted of 150 mL of which 50 mL were stabilized with 2% bovine serum albumin (albumin fraction V; no. 8076.4; Carl Roth, Karlsruhe, Germany) for further processing. The remaining 100 mL of the eluate were immediately frozen at −80°C.

**(ii) Surface water filtration using the Rexeed-25-A column.** Rexeed-25-A columns consist of a hollow fiber matrix. It is operated with a peristaltic pump (Hei-Flow Precision 01; no. 224-1354; Heidolph Instruments GmbH & Co. KG, Schwabach, Germany). The filtration followed the principle of dead-end filtration, and the process took place as described in reference 54 with some changes. The sample streamed from the bottom red port through the column to the upper side port. After the complete sample was filtered, some leftovers of water were removed manually by removing the water from the side adapter of the filter with a syringe. The virus was eluted from the membrane by washing the membrane with either 0.2 × PBS (no. 8418-12PCE; CHEMSOLUTE, Th. Geyer GmbH, Renningen, Germany) or 0.2 × PBS supplemented with 0.001% Tween 80 (Tween 80; no. 655207-50; Merck, Darmstadt, Germany). The elution took place from the upper (blue) to the bottom (red), up to a volume of 150 mL. The eluate of 150 mL was then treated as described for the VivaFlow concentrate (see above).

**(iii) Postfiltration measures.** SPE-DOM cartridge RNA extraction: Aliquots of 100 mL of an eluate obtained after Rexeed-25-A purification or a “raw” water sample were adjusted to pH 2 by using 37% smoking concentrated hydrochloric acid (Carl Roth, Karlsruhe, Germany) while stirring. The SPE-DOM column, with a volume of about 3 mL (Bond Elut PPL cartridge; no. 12105005; Agilent Technologies, Santa Clara, CA, USA), was preconditioned by adding a column volume of methanol (Carl Roth) before adding the sample for gravity- and pressure-assisted chromatography. The column then was washed twice with 0.01 M HCl and dried for 5 min at room temperature. The eluate was obtained by rinsing the column using the same 0.5 mL methanol three times. To collect particulate matter, the filter of the column was removed, transferred to a 2-mL reaction tube containing 0.5 mL of cell culture medium, and homogenized (TissueLyser; Qiagen, Hilden, Germany) for 2 min at 300 Hz. After centrifugation, RNA was extracted from both the supernatant of the homogenized particulate matter and the column eluate using the QIAamp Viral RNA kit (no. 52904; Qiagen) as described in the manual.

For ultracentrifugation, aliquots of 100 mL of an eluate obtained after Rexeed-25-A purification or a “raw” water sample were ultracentrifuged at  $175,000 \times g$  for 3 h at 4°C in an SW-32-Ti Beckman rotor using Open-Top Thinwall Ultra-Clear Tubes (no. 344058; Beckman Coulter, Krefeld, Germany). The supernatant was decanted from the buckets, and pellets from three buckets were resuspended in a total volume of 0.5 mL  $0.1 \times TE1 \times TE$  buffer. RNA was extracted from resuspended pellets using the QIAamp Viral RNA minikit (no. 52904; Qiagen, Hilden, Germany) as described below.

The technical setup of the Rexeed filtration and postfiltration approaches is shown in Fig. 2.

**(iv) RNA extraction.** Rexeed-25-A and Vivaflow 200 eluates and other water samples, respectively, were processed using the NucliSens Magnetic Extraction kit (no. 200293; bioMérieux, Marcy-l'Étoile, France) as described previously (55). In brief, 5 mL of the sample was incubated for 10 min in 10 mL of lysis buffer (NUCLISENS easyMAG Lysis Buffer; no. 280134; bioMérieux, Marcy-l'Étoile, France). After removal of floating particles via centrifugation ( $5,889 \times g$  for 5 min), the RNA extraction proceeded essentially as described in the manual.

In addition, the water enrichment Zymo Environ Water RNA kit (no. R2042; Zymo Research Europe GmbH, Freiburg, Germany) was utilized to determine the viral enrichment within the ultracentrifugation post-Rexeed-25-A filtration.

SPE-DOM eluates, ultracentrifugation pellets, feathers, and feces samples were extracted using the QIAamp Viral RNA (no. 52904; Qiagen, Hilden, Germany) system.

The RNA extraction of sediments from water bodies was performed via the RNeasy PowerSoil Total RNA kit (no. 12866-25; Qiagen, Hilden, Germany), according to the protocol provided by references 52.

**(v) Collection of environmental avian fecal samples (active surveillance).** During the winter months (November 2020 until March 2021 and December 2021 until April 2022), 1,620 and 500 avian fecal droppings were collected at locations (Fig. 5) in or adjacent to the German Wadden Sea national park. Samples were collected by ornithologically experienced rangers at sites where they observed large flocks of bamaclae geese (*Branta leucopsis*), Eurasian wigeons (*Mareca penelope*), and brent geese (*Branta bernicla*) immediately before sampling fresh droppings. Several of the sampling sites were situated adjacent to surface water sampling spots (Fig. 5). For RNA extraction, approximately 100 mg of fecal matter was resuspended in 1 mL cell culture medium supplemented with penicillin/streptomycin (10,000 U/mL/10,000 µg/mL; no. A2213; Biochrom, Berlin, Germany) and shaken at room temperature at 230 rpm for 30 min (Varioshake VS 15 O; no. 9837945; LAUDA, Lauda-Königshofen, Germany). The medium was transferred to a 1.5-mL reaction tube and centrifuged for 5 min at  $2,655 \times g$  (Eppendorf centrifuge 5430R; no. 5428000205; Eppendorf SE, Hamburg, Germany) to remove larger floating particles. RNA extraction from the supernatant was performed using the NucleoMag VET kit (no. 744200.1; MACHERY-NAGEL GmbH & Co. KG, Düren, Germany) on a KingFisher 96 BioSprint platform (Qiagen, Hilden, Germany).

**(vi) Metagenome sequencing of a field water sample.** A generic sequencing workflow as previously described in reference 56 was employed with some modifications. These included the use of the

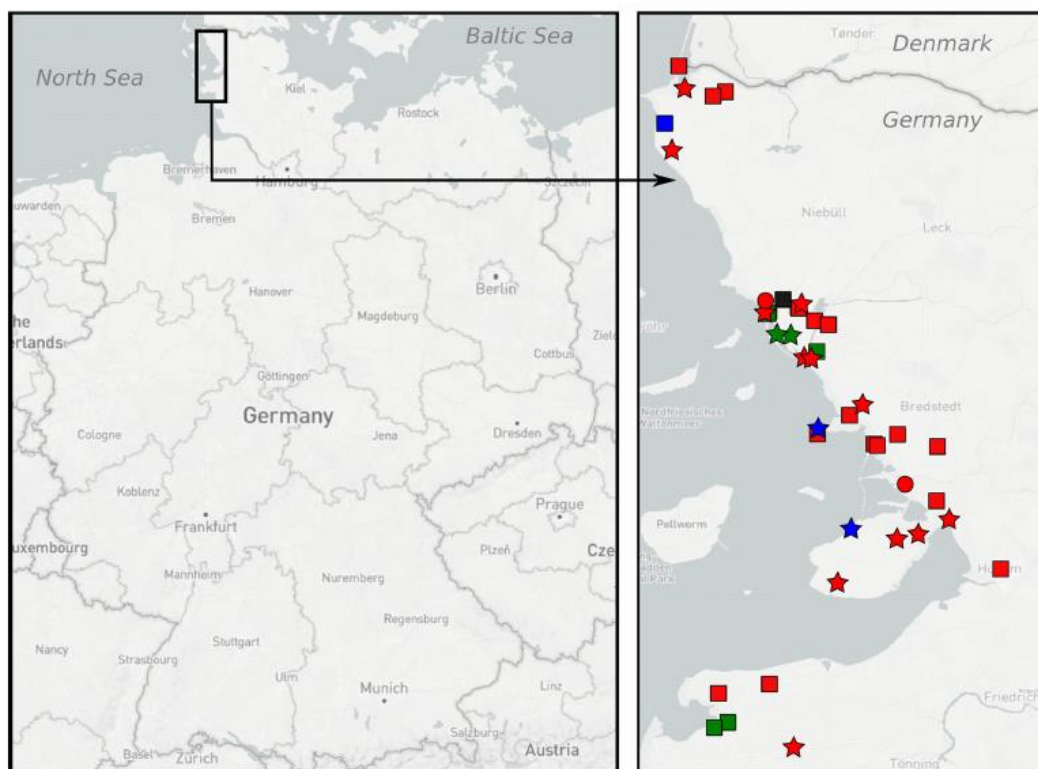


**FIG 5** Geographic locations in the Wadden Sea national park in the German Federal State of Schleswig-Holstein depicting sampling sites of environmental fresh avian fecal samples of three anatid species (*Branta leucopsis*, red markings; *Branta bennicla*, blue markings; *Mareca penelope*, green markings) in 2020 (circles), 2021 (squares), and 2022 (stars). (Maps © Mapbox [www.mapbox.com/about/maps] and © OpenStreetMap [www.openstreetmap.org/about].)

SuperScript<sup>IV</sup> First-Strand cDNA Synthesis System (Invitrogen, Germany) as well as the NEBNext Ultra II Non-Directional RNA Second Strand Synthesis Module (New England Biolabs, Germany) to generate cDNA. Furthermore, the QIAseq Library Quant assay kit (Qiagen, Germany) was used for library quantification. A small part (5  $\mu$ L) of the original sequencing library was sequenced using an Ion 530 chip in combination with the chemistry for 400-bp reads on an Ion Torrent S5XL instrument (Thermo Fisher Scientific, Germany). The remaining sequencing library (24.6  $\mu$ L) was treated with a myBaits panel for avian viruses (including baits for Influenza) to specifically enrich virus nucleic acids as described (57) employing a hybridization time of 25 h at 64°C and sequenced as described.

The data sets were analyzed using the software RIEMS version 4 (58). For an in-depth analysis of AIV sequences, the Genome Sequencer software suite (version 2.6; Roche) was used to perform mapping analysis using *A/Anas\_crecca/Hubei/Chenhu1623\_5/2014* (H5N6) and *A/environment sample/China/TZ001/2021* (H5N8) as reference sequences. Obtained contigs were checked via blastn analysis (<https://blast.ncbi.nlm.nih.gov/Blast.cgi>).

**Data availability.** All data pertinent to this study are presented in tables and figures in the main text or in the supplemental materials.

#### SUPPLEMENTAL MATERIAL

Supplemental material is available online only.

**SUPPLEMENTAL FILE 1**, PDF file, 0.3 MB.

#### ACKNOWLEDGMENTS

We thank Aline Maksimov, Patrick Zitzow, and Diana Parlow for technical support and Gabriele Adam for providing the  $\phi$ 6-runoff transcripts. We are indebted to colleagues collecting water samples in the field. We are grateful to the Landesbetrieb

für Küstenschutz, Nationalpark und Meeresschutz Schleswig-Holstein (LKN.SH)-Nationalparkverwaltung Schleswig-Holsteinisches Wattenmeer, location Tönning for the collection of avian fecal samples from the field. This study also used samples provided by the Alfred Wegener Institute Helmholtz-Centre for Polar and Marine Research in Bremerhaven (grant no. AWI-PS124\_03). We thank the members of AWI's Logistic Department and the captain and the entire crew of the vessel "Polarstern" for their dedicated and enthusiastic support prior and during the COSMUS expedition.

This research was funded by German Environment Agency (Umweltbundesamt) grant no. FKZ 3718 62 236 0 (to A.K.A.).

We declare no conflict of interest.

Figure 2 was created with [BioRender.com](https://BioRender.com). We received permission for publication of this figure under license no. F124TTTQMG from BioRender. We received a permission for water sampling in the Antarctic Ocean from the German Environment Agency, under no. II 2.2-94033/176 and no. II 2.8-94033/168. Graphs were created with GraphPad Software version 7-9 (San Diego, CA, USA). The maps were created with [microreact](https://microreact.org) (<https://microreact.org> [59]).

Conceptualization, M.B. and T.C.H.; Methodology, Validation A.K.A. and T.C.H.; Formal Analysis, A.K.A.; Investigation, A.K.A., C.W., H.W., F.P., D.H., and O.S.; Resources, H.-C.S., H.H.H., T.C.M., M.B.; Data Curation, T.C.H.; Writing – Original Draft Preparation, A.K.A. and T.C.H.; Writing – Review and Editing, A.K.A., H.-C.S., C.W., H.W., O.S., H.H.H., F.P., D.H., T.C.M., M.B., and T.C.H.; Visualization, A.K.A.; Supervision, T.C.M., M.B., and T.C.H.; Project Administration, H.C.S.; Funding Acquisition, T.C.M. All authors have read and agreed to the published version of the manuscript.

## REFERENCES

1. Swayne DE, Suarez DL. 2000. Highly pathogenic avian influenza. *Rev Sci Tech* 19:463–482. <https://doi.org/10.20506/rst.19.2.1230>.
2. Nuñez IA, Ross TM. 2019. A review of H5Nx avian influenza viruses. *Ther Adv Vaccines Immunother* 7:2515135518821625. <https://doi.org/10.1177/2515135518821625>.
3. Krammer F, Smith GJD, Fouchier RAM, Peiris M, Kedzierska K, Doherty PC, Palenze P, Shaw ML, Treanor J, Webster RG, García-Sastre A. 2018. Influenza. *Nat Rev Dis Primers* 4:3. <https://doi.org/10.1038/s41572-018-0002-y>.
4. Chatzprodromidou IP, Arvanitidou M, Guitian J, Apostolou T, Vantarakis G, Vantarakis A. 2018. Global avian influenza outbreaks 2010–2016: a systematic review of their distribution, avian species and virus subtype. *Syst Rev* 7:17. <https://doi.org/10.1186/s13643-018-0691-z>.
5. Li Y-T, Linster M, Mendenhall IH, Su YCF, Smith GJD. 2019. Avian influenza viruses in humans: lessons from past outbreaks. *Br Med Bull* 132:81–95. <https://doi.org/10.1093/bmb/ldz036>.
6. Webster RG, Guan Y, Peiris M, Walker D, Krauss S, Zhou NN, Govorkova EA, Ellis TM, Dyrting KC, Sit T, Perez DR, Shortridge KF. 2002. Characterization of H5N1 influenza viruses that continue to circulate in geese in southeastern China. *J Virol* 76:118–126. <https://doi.org/10.1128/JVI.76.1.118-126.2002>.
7. Alexander DJ. 2007. An overview of the epidemiology of avian influenza. *Vaccine* 25:5637–5644. <https://doi.org/10.1016/j.vaccine.2006.10.051>.
8. Verhagen JH, Fouchier RAM, Lewis N. 2021. Highly pathogenic avian influenza viruses at the wild-domestic bird interface in Europe: future directions for research and surveillance. *Viruses* 13:212. <https://doi.org/10.3390/v13020212>.
9. Killingley B, Nguyen-Van-Tam J. 2013. Routes of influenza transmission. *Influenza Other Respir Viruses* 7(suppl 2):42–51. <https://doi.org/10.1111/irv.12080>.
10. Ahrens AK, Selinka H-C, Mettenleiter TC, Beer M, Harder TC. 2022. Exploring surface water as a transmission medium of avian influenza viruses—systematic infection studies in mallards. *Emerg Microbes Infect* 11:1250–1261. <https://doi.org/10.1080/22221751.2022.2065937>.
11. Stallknecht DE, Brown JD. 2009. Tenacity of avian influenza viruses. *Rev Sci Tech* 28:59–67. <https://doi.org/10.20506/rst.28.1.1880>.
12. Nazir J, Haumacher R, Ike A, Stumpf P, Böhm R, Marschang RE. 2010. Long-term study on tenacity of avian influenza viruses in water (distilled water, normal saline, and surface water) at different temperatures. *Avian Diseases* 54:720–724. <https://doi.org/10.1637/8754-033109-ResNote.1>.
13. Keeler SP, Dalton MS, Cressler AM, Berghaus RD, Stallknecht DE. 2014. Abiotic factors affecting the persistence of avian influenza virus in surface waters of waterfowl habitats. *Appl Environ Microbiol* 80:2910–2917. <https://doi.org/10.1128/AEM.03790-13>.
14. Stumpf P, Failing K, Papp T, Nazir J, Böhm R, Marschang RE. 2010. Accumulation of a low pathogenic avian influenza virus in zebra mussels (*Dreissena polymorpha*). *Avian Dis* 54:1183–1190. <https://doi.org/10.1637/9162-111709-Reg.1>.
15. Nazir J, Haumacher R, Ike AC, Marschang RE. 2011. Persistence of avian influenza viruses in lake sediment, duck feces, and duck meat. *Appl Environ Microbiol* 77:4981–4985. <https://doi.org/10.1128/AEM.00415-11>.
16. Gobbo F, Fomasiero D, de Marco MA, Zecchin B, Mulatti P, Delogu M, Terregino C. 2021. Active surveillance for highly pathogenic avian influenza viruses in wintering waterbirds in Northeast Italy, 2020–2021. *Microorganisms* 9:2188. <https://doi.org/10.3390/microorganisms9121888>.
17. Hoyer BJ, Munster VJ, Nishiura H, Klaassen M, Fouchier RAM. 2010. Surveillance of wild birds for avian influenza virus. *Emerg Infect Dis* 16:1827–1834. <https://doi.org/10.3201/eid1612.100589>.
18. Feare CJ. 2010. Role of wild birds in the spread of highly pathogenic avian influenza virus H5N1 and implications for global surveillance. *Avian Dis* 54:201–212. <https://doi.org/10.1637/8766-033109-ResNote.1>.
19. Coombe M, Iwasawa S, Byers KA, Prystajek N, Hsiao W, Patrick DM, Himswoth CG. 2021. A systematic review and narrative synthesis of the use of environmental samples for the surveillance of avian influenza viruses in wild waterbirds. *J Wildl Dis* 57:1–18. <https://doi.org/10.7589/jwd-d-20-00082>.
20. Leung YHC, Zhang L-J, Chow C-K, Tsang C-L, Ng C-F, Wong C-K, Guan Y, Peiris JSM. 2007. Poultry drinking water used for avian influenza surveillance. *Emerg Infect Dis* 13:1380–1382. <https://doi.org/10.3201/eid1309.070517>.
21. Mehle N, Gutiérrez-Aguirre I, Kutnjak D, Ravnikar M. 2018. Water-mediated transmission of plant, animal, and human viruses. *Adv Virus Res* 101:85–128. <https://doi.org/10.1016/bs.aivir.2018.02.004>.
22. Rönqvist M, Ziegler T, von Bonsdorff C-H, Maunula L. 2012. Detection method for avian influenza viruses in water. *Food Environ Virol* 4:26–33. <https://doi.org/10.1007/s12560-011-9075-4>.
23. Pawar SD, Keng SS, Tare DS, Thormothe AL, Sapkal GN, Anukumar B, Lole KS, Mullick J, Mourya DT. 2019. A virus precipitation method for concentration & detection of avian influenza viruses from environmental water resources & its possible application in outbreak investigations. *The Indian J Medical Res* 150:612–619. [https://doi.org/10.4103/ijmr.IJMR\\_1697\\_18](https://doi.org/10.4103/ijmr.IJMR_1697_18).

24. Minh AD, Kamen AA. 2021. Critical assessment of purification and analytical technologies for enveloped viral vector and vaccine processing and their current limitations in resolving co-expressed extracellular vesicles. *Vaccines* 9:823. <https://doi.org/10.3390/vaccines9080823>.
25. Polson A. 1993. Purification and aggregation of influenza virus by precipitation with polyethylene glycol. *Prep Biochem* 23:207–225. <https://doi.org/10.1080/10826069308544551>.
26. Kramerberger P, Urbas L, Štrancar A. 2015. Downstream processing and chromatography based analytical methods for production of vaccines, gene therapy vectors, and bacteriophages. *Hum Vaccin Immunother* 11:1010–1021. <https://doi.org/10.1080/21645515.2015.1009817>.
27. Mulholland C, McMenemy MJ, Hoffmann B, Earley B, Markey B, Cassidy J, Allan G, Welsh MD, McKillen J. 2017. The development of a real-time reverse transcription-polymerase chain reaction (RT-PCR) assay using TaqMan technology for the pan detection of bluetongue virus (BTV). *J Virological Methods* 245:35–39. <https://doi.org/10.1016/j.jviromet.2017.03.009>.
28. Dittmar T, Koch B, Hertkom N, Kattner G. 2008. A simple and efficient method for the solid-phase extraction of dissolved organic matter (SPE-DOM) from seawater. *Limnol Oceanogr Methods* 6:230–235. <https://doi.org/10.4319/lom.2008.6.230>.
29. European Food Safety Authority; European Centre for Disease Prevention and Control; European Union Reference Laboratory for Avian Influenza; Adlhoch C, Fusaro A, Gonzales JL, Kuiken T, Marangon S, Niqueux E, Staubach C, Terregino C, Guajardo IM, Chuzhakina K, Baldinelli F. 2022. Avian influenza overview June–September 2022. *EFSA J* 20:e07597. <https://doi.org/10.2903/j.efsa.2022.7597>.
30. King J, Harder T, Conraths FJ, Beer M, Pohlmann A. 2021. The genetics of highly pathogenic avian influenza viruses of subtype H5 in Germany, 2006–2020. *Transbound Emerg Dis* 68:1136–1150. <https://doi.org/10.1111/tbed.13843>.
31. Adlhoch C, Fusaro A, Gonzales JL, Kuiken T, Marangon S, Niqueux E, Staubach C, Terregino C, Azar I, Muñoz Guajardo I, Baldinelli F. European Centre for Disease Prevention, Control, European Union Reference Laboratory for Avian Influenza. 2022. Avian influenza overview May–September 2021. *EFSA J* 20:e07122. <https://doi.org/10.2903/j.efsa.2022.7122>.
32. MacLachlan J, Dubovi EJ (ed). 2017. The nature of viruses. *Fenner's veterinary virology*, p 3–16. Elsevier, Amsterdam, The Netherlands.
33. Germeeraad EA, Elbers ARW, de Bruijn ND, Heutink R, van Voorst W, Hakzevan der Honing R, Bergervoet SA, Engelsma MY, van der Poel WHM, Beerens N. 2020. Detection of low pathogenic avian influenza virus subtype h10n7 in poultry and environmental water samples during a clinical outbreak in commercial free-range layers, Netherlands 2017. *Front Vet Sci* 7:237. <https://doi.org/10.3389/fvets.2020.00237>.
34. Das A, Spackman E, Pantin-Jackwood MJ, Suarez DL. 2009. Removal of real-time reverse transcription polymerase chain reaction (RT-PCR) inhibitors associated with cloacal swab samples and tissues for improved diagnosis of Avian influenza virus by RT-PCR. *J Vet Diagn Invest* 21:771–778. <https://doi.org/10.1177/104063870902100603>.
35. Tindale LC, Baticados W, Duan J, Coombe M, Jassem A, Tang P, Uyaguari-Diaz M, Moore R, Himswoorth C, Hsiao W, Prystajeky N. 2020. Extraction and detection of avian influenza virus from wetland sediment using enrichment-based targeted resequencing. *Front Vet Sci* 7:301. <https://doi.org/10.3389/fvets.2020.00301>.
36. Pannwitz G, Wolf C, Harder T. 2009. Active surveillance for avian influenza virus infection in wild birds by analysis of avian fecal samples from the environment. *J Wildl Dis* 45:512–518. <https://doi.org/10.7589/0090-3558-45.2.512>.
37. Bárbara A, Torontegi O, Camacho M-C, Barral M, Hernández J-M, Höfle U. 2017. Avian influenza virus surveillance in south-central Spain using fecal samples of aquatic birds foraging at landfills. *Front Vet Sci* 4:178. <https://doi.org/10.3389/fvets.2017.00178>.
38. Khalil AM, Kojima I, Fukunaga W, Okajima M, Mitral S, Fujimoto Y, Matsui T, Kuwahara M, Masatani T, Okuya K, Ozawa M. 2022. Improved method for avian influenza virus isolation from environmental water samples. *Transbound Emerg Dis* 69:e2889–e2897. <https://doi.org/10.1111/tbed.14639>.
39. Aquino de Carvalho N, Stachler EN, Cimabue N, Bibby K. 2017. Evaluation of Phi6 persistence and suitability as an enveloped virus surrogate. *Environ Sci Technol* 51:8692–8700. <https://doi.org/10.1021/acs.est.7b01296>.
40. Leibniz-Institut DSMZ-Deutsche Sammlung von Mikroorganismen und Zellkulturen GmbH. 2011. Tryptone soya broth (TSB). [https://www.dsmz.de/microorganisms/medium/pdf/DSMZ\\_Medium545.pdf](https://www.dsmz.de/microorganisms/medium/pdf/DSMZ_Medium545.pdf). Accessed 15 May 2020.
41. Leibniz-Institut DSMZ-Deutsche Sammlung von Mikroorganismen und Zellkulturen GmbH. 2008. Supply, storage and propagation of supply, storage and propagation of phages. special instructions. <https://www.dsmz.de/fileadmin/Bereiche/Microbiology/Dateien/Kultivierungshinweise/Phages-neu.pdf>. Accessed 15 May 2020.
42. ENMEMO DNA/RNA copy number calculator. <http://endmemo.com/bio/dnacopynum.php#:~:text=1%20%2010%2D9%20%206.02,each%20base%20was%20325%20dalton>. Accessed 23 October 2021.
43. World Organisation for Animal Health. 2009. Chapter 2.3.4. Avian influenza. *OIE terrestrial manual* 2009. [https://www.oie.int/fileadmin/Home/eng/Animal\\_Health\\_in\\_the\\_World/docs/pdf/2.03.04\\_AI.pdf](https://www.oie.int/fileadmin/Home/eng/Animal_Health_in_the_World/docs/pdf/2.03.04_AI.pdf). Accessed 19 April 2022.
44. Kärber G. 1931. Beitrag zur kollektiven Behandlung pharmakologischer Reihenversuche. *Archiv f experiment Pathol u Pharmakol* 162:480–483. <https://doi.org/10.1007/BF01863914>.
45. Elnagar A, Harder TC, Blome S, Beer M, Hoffmann B. 2021. Optimizing release of nucleic acids of African swine fever virus and influenza A virus from FTA cards. *Int J Mol* 22:12915. <https://doi.org/10.3390/ijms222312915>.
46. Hoffmann B, Harder T, Lange E, Kalthoff D, Reimann I, Grund C, Oehme R, Vahlenkamp TW, Beer M. 2010. New real-time reverse transcriptase polymerase chain reactions facilitate detection and differentiation of novel A/H1N1 influenza virus in porcine and human samples. *Berl Munch Tierarztl Wochenschr* 123:286–292.
47. Hoffmann B, Depner K, Schirmeier H, Beer M. 2006. A universal heterologous internal control system for duplex real-time RT-PCR assays used in a detection system for pestiviruses. *J Virological Methods* 136:200–209. <https://doi.org/10.1016/j.jviromet.2006.05.020>.
48. Graaf A, Beer M, Harder T. 2017. Real-time reverse transcription PCR-based sequencing-independent pathotyping of Eurasian avian influenza A viruses of subtype H7. *Virology* 14:137. <https://doi.org/10.1186/s12985-017-0808-3>.
49. Naguib MM, Graaf A, Fortin A, Luttermann C, Wernery U, Amarin N, Hussein HA, Sultan H, Al Adhadh B, Hassan MK, Beer M, Monne I, Harder TC. 2017. Novel real-time PCR-based patho- and phylotyping of potentially zoonotic avian influenza A subtype H5 viruses at risk of incursion into Europe in 2017. *Euro Surveill* 22:30435. <https://doi.org/10.2807/1560-7917.es.2017.22.1.30435>.
50. Hassan KE, Ahrens AK, Ali A, El-Kady MF, Hafez HM, Mettenleiter TC, Beer M, Harder T. 2022. Improved subtyping of avian influenza viruses using an RT-qPCR-based low density array: “Riems Influenza A Typing Array,” version 2 (RITA-2). *Viruses* 14:415. <https://doi.org/10.3390/v14020415>.
51. Hoffmann B, Hoffmann D, Henritzi D, Beer M, Harder TC. 2016. Riems influenza a typing array (RITA): an RT-qPCR-based low density array for subtyping avian and mammalian influenza A viruses. *Sci Rep* 6:27211. <https://doi.org/10.1038/srep27211>.
52. Chaparro J, Vivanco J. 2013. Isolating RNA from the soil. *Bio-Protocol* 3:e903. <https://doi.org/10.21769/BioProtoc.903>.
53. Sartorius Lab Instruments. 2016. Vivaflow 50|50R|200 (SLU6097-e160609). <https://www.sartorius.hr/media/elma0gg4/usemanual-en-manual-vivaflow50-200-slu6097-e.pdf>. Accessed 15 March 2020.
54. Smith CM, Hill VR. 2009. Dead-end hollow-fiber ultrafiltration for recovery of diverse microbes from water. *Appl Environ Microbiol* 75:5284–5289. <https://doi.org/10.1128/AEM.00456-09>.
55. Hartmann NM, Dartscht M, Szewzyk R, Selinka H-C. 2013. Monitoring of adenovirus serotypes in environmental samples by combined PCR and melting point analyses. *Virology* 10:190. <https://doi.org/10.1186/1743-422X-10-190>.
56. Wyleżich C, Papa A, Beer M, Höper D. 2018. A versatile sample processing workflow for metagenomic pathogen detection. *Sci Rep* 8:13108. <https://doi.org/10.1038/s41598-018-31496-1>.
57. Wyleżich C, Calvelage S, Schlottau K, Ziegler U, Pohlmann A, Höper D, Beer M. 2021. Next-generation diagnostics: virus capture facilitates a sensitive viral diagnosis for epizootic and zoonotic pathogens including SARS-CoV-2. *Microbiome* 9:51. <https://doi.org/10.1186/s40168-020-00973-z>.
58. Scheuch M, Höper D, Beer M. 2015. RIEMS: a software pipeline for sensitive and comprehensive taxonomic classification of reads from metagenomics datasets. *BMC Bioinformatics* 16:69. <https://doi.org/10.1186/s12859-015-0503-6>.
59. Argimón S, Abudahab K, Goater RJE, Fedosejev A, Bhai J, Glasner C, Feil EJ, Holden MTG, Yeats CA, Grundmann H, Spratt BG, Aanensen DM. 2016. Microreact: visualizing and sharing data for genomic epidemiology and phylogeography. *Microb Genom* 2:e000093. <https://doi.org/10.1099/mgen.0.000093>.
60. Dreyer S, Globig A, Bachmann L, Schütz AK, Schauler K, Homeier-Bachmann T. 2022. Longitudinal study on extended-spectrum beta-lactamase-E. coli in sentinel mallard ducks in an important Baltic stop-over site for migratory ducks in Germany. *Microorganisms* 10:1968. <https://doi.org/10.3390/microorganisms10101968>.



**3.3 Exploring surface water as a transmission medium of avian influenza viruses –  
systematic infection studies in mallards.**

Ann Kathrin Ahrens, Hans-Christoph Selinka, Thomas C. Mettenleiter,  
Martin Beer, Timm C. Harder

Emerging Microbes & Infections

11(1), 2022

doi: 10.1080/22221751.2022.206593



## Exploring surface water as a transmission medium of avian influenza viruses – systematic infection studies in mallards

Ann Kathrin Ahrens, Hans-Christoph Selinka, Thomas C. Mettenleiter, Martin Beer & Timm C. Harder

To cite this article: Ann Kathrin Ahrens, Hans-Christoph Selinka, Thomas C. Mettenleiter, Martin Beer & Timm C. Harder (2022) Exploring surface water as a transmission medium of avian influenza viruses – systematic infection studies in mallards, *Emerging Microbes & Infections*, 11:1, 1250-1261, DOI: [10.1080/22221751.2022.2065937](https://doi.org/10.1080/22221751.2022.2065937)

To link to this article: <https://doi.org/10.1080/22221751.2022.2065937>



© 2022 The Author(s). Published by Informa UK Limited, trading as Taylor & Francis Group, on behalf of Shanghai Shangyixun Cultural Communication Co., Ltd



[View supplementary material](#)



Published online: 03 May 2022.



[Submit your article to this journal](#)



Article views: 902





[View related articles](#)



[View Crossmark data](#)

## Exploring surface water as a transmission medium of avian influenza viruses – systematic infection studies in mallards

Ann Kathrin Ahrens<sup>a</sup>, Hans-Christoph Selinka<sup>b</sup>, Thomas C. Mettenleiter<sup>c</sup>, Martin Beer <sup>a</sup> and Timm C. Harder <sup>a</sup>

<sup>a</sup>Institute of Diagnostic Virology, Friedrich-Loeffler-Institute, Isle of Riems, Germany; <sup>b</sup>Section II 1.4 Microbiological Risks, German Environment Agency (UBA), Berlin, Germany; <sup>c</sup>Friedrich-Loeffler-Institute, Isle of Riems, Germany

### ABSTRACT

Mallards (*Anas platyrhynchos*) are an abundant anseriform migratory wild bird species worldwide and an important reservoir for the maintenance of low pathogenicity (LP) avian influenza viruses (AIV). They have also been implicated in the spread of high pathogenicity (HP) AIV after spill-over events from HPAIV-infected poultry. The spread of HPAIV within wild water bird populations may lead to viral contamination of natural habitats. The role of small shallow water bodies as a transmission medium of AIV among mallards is investigated here in three experimental settings. (i) Delayed onset but rapid progression of infection seeded by two mallards inoculated with either LP or HP AIV to each eight sentinel mallards was observed in groups with access to a small 100 L water pool. In contrast, groups with a bell drinker as the sole source of drinking water showed a rapid onset but lengthened course of infection. (ii) HPAIV infection also set off when virus was dispersed in the water pool; titres as low as  $10^2$  TCID<sub>50</sub> L<sup>-1</sup> (translating to 0.1 TCID<sub>50</sub> mL<sup>-1</sup>) proved to be sufficient. (iii) Substantial loads of viral RNA (and infectivity) were also found on the surface of the birds' breast plumage. "Unloading" of virus infectivity from contaminated plumage into water bodies may be an efficient mechanism of virus spread by infected mallards. However, transposure of HPAIV via the plumage of an uninfected mallard failed. We conclude, surface water in small shallow water bodies may play an important role as a mediator of AIV infection of aquatic wild birds.

**ARTICLE HISTORY** Received 7 March 2022; Revised 5 April 2022; Accepted 10 April 2022

**KEYWORDS** Avian influenza; transmission; high pathogenicity; surface water; spread; mallard


### Introduction


Avian influenza A viruses (AIV) are classified in the *Orthomyxoviridae* family. Their octo-segmented single-stranded RNA genome of negative polarity encodes at least 10 structural viral proteins, including the membrane glycoproteins hemagglutinin (HA) and neuraminidase (NA) [1–4]. Based on their antigenicity 16 different HA and 9 NA subtypes can be distinguished [1]. According to their virulence in experimentally infected chickens AIV reveals an either low (LP) or high (HP) pathogenicity phenotype [1,5]. Until today, naturally occurring HP phenotypes are restricted to the subtypes H5 and H7 [5].

In 1996, a flock of domestic geese in the Chinese Guangdong province was identified to be infected with HPAIV termed A/goose/Guangdong/1/1996 (H5N1) [6,7]. Descendants of this virus later became known as the Goose/Guangdong (gs/GD)-lineage [8]. While wild aquatic birds are a long-established natural reservoir for all different LP AIV subtypes [2], they became first infected with gs/GD HPAIV due to spill-back events from poultry in 2003 [9].

Domestic ducks fattened in harvested rice paddies in Southeast Asia probably played a prominent "seeding" role [9,10]. Gs/GD HPAIV remained endemic in poultry populations in several countries in the region and elsewhere [10–13]; continued circulation with frequent host species switches stimulated viral diversification into several phylogenetically distinguishable clades and numerous genotypes. Transmission events at wild bird-poultry-interfaces have continued [14–17]. HPAIV-infected migrating waterbird populations, in addition to (prohibited) transboundary trading, are an important vector of long-distance transmission resulting in several "out-of-Asia" waves of viral escape from endemic regions in the last 15 years hitting Europe [10,18–20] North America [21], and Africa [10,15,22] with unprecedented impact.

Before 2002, only very few sporadic HPAIV infections of restricted geographic expansion were known to have occurred in wild birds [14,23]. Almost all of these cases were traced back to spill-over infections from likewise rarely occurring HPAI outbreaks in poultry, all unrelated to the gs/GD lineage. The

**CONTACT** Timm C. Harder  [tim.harder@fli.de](mailto:tim.harder@fli.de)

 Supplemental data for this article can be accessed online at <https://doi.org/10.1080/22221751.2022.2065937>.

© 2022 The Author(s). Published by Informa UK Limited, trading as Taylor & Francis Group, on behalf of Shanghai Shangyixun Cultural Communication Co., Ltd  
This is an Open Access article distributed under the terms of the Creative Commons Attribution License (<http://creativecommons.org/licenses/by/4.0/>), which permits unrestricted use, distribution, and reproduction in any medium, provided the original work is properly cited.

emergence of the gs/GD lineage of HPAI viruses has caused a paradigm shift: promoted by the grossly expanded poultry production in Southeast Asia and elsewhere and fostered by the ability of many of the gs/GD lineage viruses to infect Pekin ducks, and other dabbling duck species, asymptotically or only causing mild clinical signs, these viruses quickly established an endemic status in poultry. For the first time in the history of HPAIV migratory wild birds were assigned a pivotal role as vectors in the transboundary and transcontinental spread of HPAIV. Due to the possible widespread presence of HPAIV in wild bird habitats and spill back by direct or indirect contacts from infected wild birds into poultry the vicious cycle of mutual virus transmission at the wild bird bird-poultry interface had been closed.

It has been estimated that a single HPAIV infected duck can shed  $10^{10}$  EID<sub>50</sub> doses into the environment within a range of 24 h [24,25]. As fecal-oral transmission chains are highly effective this would be theoretically sufficient to infect another  $10^6$  ducks assuming, conservatively, the minimal infectious dose per animal would amount to  $10^3$ – $10^4$  EID<sub>50</sub> [24]. Dispersion of virus-contaminated fecal matter and oropharyngeal excretions in surface waters is expected to potentiate transmission efficacy: (1) Depending on the AI virus strain but also on various physico-chemical properties of the water body such as temperature, pH, salinity, sedimentation rates, presence of biologic compounds and so on, the infectivity of virus particles shed into such water is retained for astonishingly long periods of up to several months [26]. Conversely, higher water temperatures (22°C), alkaline or acid pH and high salinity inactivate viral infectivity within hours to days [26–30,31]. Furthermore, the presence of invertebrate animals (clams, snails, shrimps, insects) may modulate the retention time of infectious AIV in surface water and sediments [26,32–34]. (2) Several studies succeeded to detect AIV infectivity in free-floating natural water bodies as well as in their sediments [35–38]. (3) Dabbling ducks and swans feed on or closely below the surface of shallow water bodies and may come into contact with dispersed viral infectivity. Viruses deposited in sediments of freshwater bodies over winter have been reported to close a gap in the avian influenza infection cycle of aquatic wild birds in North America [39,40].

So far, most reports on the natural biology of AIV in metapopulations of wild birds concentrated on the birds themselves. Few studies have actively examined the putative role of the environment acting as a source for virus spread and persistence [41,42] and even less targeted water as a transmission medium [43,44]. Here we focussed on experimental infections using surface water as a medium of virus transmission among small flocks of mallards. We show that minute amounts of viral infectivity suspended in surface water

are sufficient to start infections in mallard groups and that the presence of a pool versus a bell drinker as a water source has a synchronizing effect on the course of both LP and HPAIV infections.

## Materials and methods

### Virus origin and propagation

Avian influenza virus isolates A/mallard/Germany/AR511/2018 (H4N6) and A/barnacle goose/Germany-SH/2020AI02167/2020 (HP H5N8) were selected from the virus repository at Friedrich-Loeffler-Institute, Germany. Both viruses were cultivated in embryonated chicken eggs in a BSL-3 environment as previously described [45]. Infectivity (TCID<sub>50</sub>) was titrated in MDCK-II cells. Cells (suspension of 100 µL) were either seeded a day before or simultaneously (i.e. together with virus) into 96 well plates. Cell counts were adjusted to  $10^5$  cells/ml. Growth medium consisted of MEM supplemented with 2% FKS, Penicillin/Streptomycin (100 U/mL, final) and TPCK-Trypsin (2 µg/mL, final). In case pre-seeded cells were used, the growth medium was discarded before adding 100 µL of virus dilution per well. Virus was diluted in log<sub>10</sub> steps in a growth medium without FCS supplementation. Cytopathic effects were scored by light microscopy, and, in addition, cells were stained by an immune peroxidase assay as previously described [46]. Briefly, infected cell cultures after 3–5 days of incubation at 37°C were heat fixated at 80 °C for four hours. For primary staining, the cells were incubated with 50 µl of a 1:50 dilution PBS with 0.005% Tween 20 (PBST) overnight at 4°C of the nucleocapsid protein-specific monoclonal antibody 890 (H16-L20-5R5, FLI Biobank). After discarding the supernatant and washing the cells three times, the secondary antibody (50 µL of a 1:500 dilution in PBST of goat anti-mouse IgG (H/L):HRP, Bio-Rad Laboratories GmbH, Feldkirchen, Germany, Lot#151517), was added for 1 hour at 37°C. 3-Amino-9-Ethylcarbazol was used as a chromogene. Between incubation steps, plates were washed three times using 150 µL of PBST. The TCID<sub>50</sub> was calculated using the Kärber formula as cited in [47].

Virus isolation from selected clinical or environmental samples was carried out in embryonated chicken eggs as detailed elsewhere [48].

## Animal experiments

### Ethical statement, animal rearing

All animal experimental work has been licensed by the animal ethics committee of the Federal State of Mecklenburg-Vorpommern (LALLF 7221.3-1-023/21, TV „FLI 08/21: Aviäre Influenza in Oberflächenwasser). A total of 80 subadult male and female mallards (10–13 weeks of age) were purchased from a

commercial breeder in Germany. At FLI, birds were housed on the floor in BSL-3 stables for acclimatization for 2 weeks together in two large groups of 40 birds each. Blood (0.5 mL) was collected from 20 randomly selected animals on arrival. When separating into smaller groups of up to 10 birds in stable units of about 11 m<sup>2</sup>, a balanced gender ratio was observed. No bedding material was used. Instead, elevated foot-protecting rubber slabs were laid out in parts of the unit to provide a dry area; floors were cleaned on a regular daily base using water. Depending on the experiment, drinking water was provided to the animals either only via bell drinkers or with an additional freshwater pool of 80 cm in diameter into which tap water was added to a fill height of 20 cm representing 100 L. Water in bell drinkers was replenished daily, pool water was fully replaced every 4 days but topped up with fresh water daily. Tap water is tested regularly in accordance with legal requirements. Chlorination or other disinfectant treatment of tap water is not regularly practiced in Germany. Pelleted commercial duck feed to which wheat corns were added was provided ad libitum. A 12-h day–night light cycle was provided.

#### Statistical analysis

Differences in clinical scores between the groups were assessed by an unpaired *t*-test with Welch's correction employing the statistical analysis tool of the GraphPad Prism software version 7 (GraphPad Software, San Diego, CA, USA).

#### Sampling schemes

**Swabs:** Each animal was sampled on a daily base. Swab samples were obtained orally, cloacally and from the plumage by rubbing the swab repeatedly over the feather-covered breast of the birds. The swabs were stored until further processing – in cell culture growth medium supplemented with penicillin and streptomycin but lacking FCS at –80°C.

**Feathers:** A secondary flight feather was collected from the animals at days 4 and 9 in the first round of experiments and at days 0, 4, 9, and 13 for part 2.

**Sera:** Blood samples for serum analysis were collected from 20 randomly chosen animals at arrival at the FLI. Additional blood samples were collected from each bird when the experiments commenced and ended. The sera were heat inactivated at 56°C for 2 h and stored at 4 °C.

**Water:** Water amount of roughly 15 mL was collected daily either from bell drinkers or pools depending on the group.

**Organs:** Animals that died spontaneously during the infection or had to be euthanized when defined humane endpoints were reached were necropsied

and tissue samples from lung and brain were taken for virological analyses.

#### RNA extraction

RNA was extracted from swabs by the Macherey-Nagel NucleoMag® VET-Kit (#744200.4) according to the instructions of the manufacturer by using the Biosprint 96 extraction robot (Qiagen, Hilden, Germany). Elution was achieved in 100 µL of the supplied elution buffer. Cones from feather samples were cut longitudinally and then across into cell culture medium and then shred in a tissue-lyzer for 2 minutes at 300 Hz; supernatant was then extracted as described above. Similarly, up to 20 mg of an organ sample was processed uncut in a cell culture medium in a tissue lyzer. Clarified supernatant was used to extract RNA manually via the QIAamp Viral RNA kit (Qiagen, Hilden, Germany). Water samples were extracted using the Zymo Environ Water RNA Kit (Cat# R2042, Zymo Research Europe GmbH, Freiburg, Germany) including also the viral enrichment step as described in the kit's manual. After the viral enrichment step, the samples were stored at –80°C until further processing. In some cases, samples were also extracted via the Macherey-Nagel NucleoMag® VET-Kit (#744200.4).

#### Real-time RT-PCRs

All samples were analysed by real-time RT–PCR (RT–qPCR). The samples were examined using a generic RT–qPCR targeting a fragment of the NP gene [49] supplemented with internal control (IC-2 [50]) to control for PCR inhibitory reactions. Samples with a Cq-value <40 were considered positive. Samples >40 were considered negative, if the Cq-value of the IC-2 target was 30 (± 2). All RT–qPCRs were carried out using the AgPath-ID™ One-Step RT–PCR Kit (Applied Biosystems™, AM1005) in a CFX96™ Real-Time-System C1000™ Thermal Cycler or the C1000Touch™ Thermal Cycler (BioRad, Munich, Germany). Cycling conditions were as follows: Reverse transcription 45°C, 10 min; Taq pol activation 95°C, 10 min, and 45 cycles of denaturation (95°C, 15 sec), annealing (56°C, 20 s), elongation (72°C, 30 s).

#### Serology

All serum samples were tested by ELISA for influenza-A-specific antibodies. Generic, influenza-A-nucleocapsid protein-specific antibodies were detected by the ID Screen® Influenza A Antibody Competition assay (ID-Vet, Grabels, France). Samples testing positive in the generic NP-ELISA were further tested in an influenza-A-H5-specific ELISA (ID Screen® Influenza H5 Antibody Competition, ID-Vet).

## Results

### *Virus spread in stabled mallard groups with or without a surface water pool (experimental infection setting 1)*

Four groups each of 10 mallards were assigned to inoculation experiments using an LPAIV of subtype H4N6 and an HPAIV of subtype H5N8, clade 2.3.4.4b, respectively. In contrast to standard inoculation experiments, only two mallards per group were inoculated oro-oculonasally with  $10^6$  TCID<sub>50</sub> in 1 mL of the respective viruses. These birds were kept separate for 1 day and provided as virus seeder a source of infection for the eight naïve mallards of each group. While groups were housed in identical stable units, one group each of the respective viruses was offered a small swimming pool of 100 L of water adjusted with solid NaCl to a salinity of 0.15% (w/v), i.e. 1500 ppm, which equalizes the salinity of the Baltic Sea at its southern coast line. The other stable unit was equipped with bell drinkers as the sole drinking water source (Figure 1a). Ducks in the pool groups made extensive use of the pool with often up to five birds simultaneously dabbling and diving in the pool. Birds that were offered bell drinkers drank frequently and made surrogate movements to imitate dabbling and washing on surface water. The spread of infection

in each group was followed by daily swabbing and by selected serum sampling before infection and at the end of the experiment.

Clinical scoring during the observation period of 11 days inconsistently revealed minor clinical signs of disease in very few individual mallards in the H4N6 groups (supplemental Figure 1a and b). The same mild progression of the infection was evident in the HPAIV exposed bell drinker group (supplemental Figure 1d). In contrast, in the HPAIV pool group two contact mallards developed a slowly progressing neurological disease consisting of disorientation, head tilting, ataxia and, finally, somnolence. Statistical analysis showed a significant difference between the two HP groups (bell drinker vs pool;  $p = 0.0019$ ). One bird died overnight from 6 to 7 dpi while the other was removed from the experiment at 7 dpi when humane endpoints were reached (supplemental Figure 1c). Postmortal brain tissue samples of each mallard were obtained and harboured high HPAIV H5N8 viral loads ranging at Cq 15–23 (not shown). Four further mallards in this group showed very mild and transient (often only for a single day) clinical signs (supplemental Figure 1c). While an asymptomatic to mild course of the infection has been expected for the LPAIV virus groups, the low frequency and mild nature of

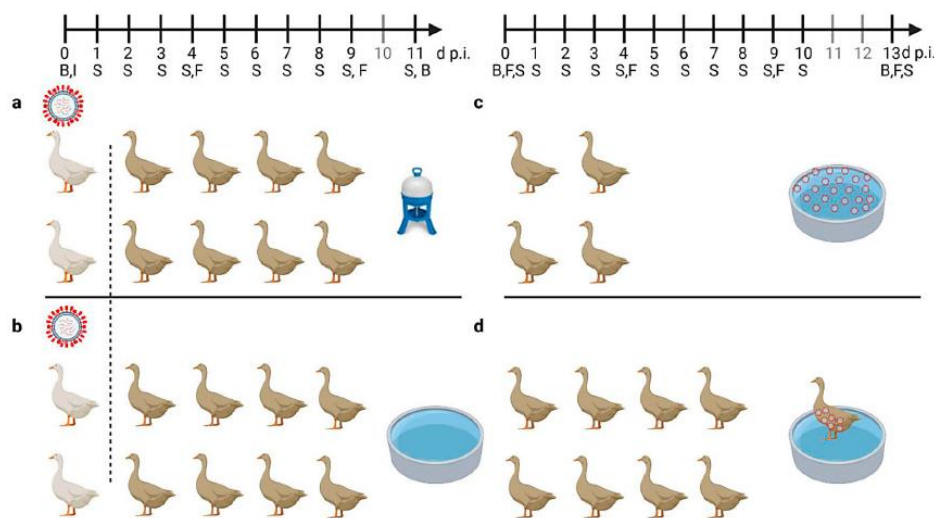


**Figure 1.** General settings of infection experiments in mallards using two infected “seeder” ducks (light colour), eight contact mallards (dark colour) and two different sources of water (a) bell drinker versus and (b) pool. Seeder ducks of (a) received LP H4N6 while those of (b) were inoculated with HP H5N8. Setting (c) provides artificially contaminated pool water to four ducks as a source of infection and (d) uses a non-infected “seeder” duck with virus-contaminated plumage as contact to eight contact mallards. Created with BioRender.com. An observation time line is indicated at the top; I – Inoculation of two seeder ducks (a, b) B – blood sample, S – Swab sample (oropharyngeal, cloacal, plumage), F – Feather sample (secondary flight feather); red circled dots indicate presence of virus in water (c) or adhering to plumage (d).

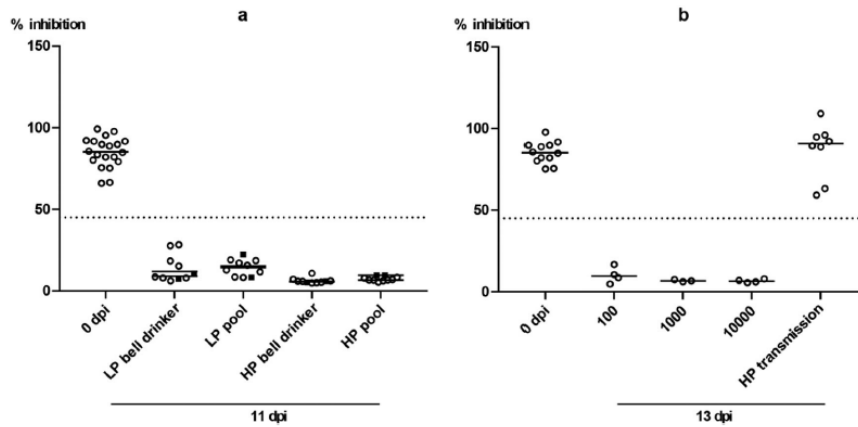


**Figure 2.** Seroconversion at the beginning and at the end of the observation period (11 or 13 dpi, respectively) against AIV nucleoprotein as measured by blocking ELISA in inoculated (black squares) and naïve (open circles) mallards exposed to LPAIV H4N6 (LP) or HPAIV H5N8 (HP) via inoculated “seeder” ducks (a) or via pool water (b) artificially loaded with HPAIV H5N8 at 100, 1000 or 10,000 TCID<sub>50</sub> L<sup>-1</sup>. The dotted line represents the ELISA threshold. % inhibition indicates the blocking efficacy of mallard sera.

clinical affection of 18 of 20 HPAIV-exposed mallards were surprising. Seroconversion in all mallards finally surviving until day 11 of the experiments indicated that all naïve mallards had been infected with the respective LP and HP viruses (Figure 2a).

Evidence for productive infection in the inoculated and contact mallards was also obtained from analysing viral RNA loads in swab samples (Figure 3). The four LP- and HP-inoculated mallards started oropharyngeal virus excretion at day 1 post-infection (dpi). Cloacal

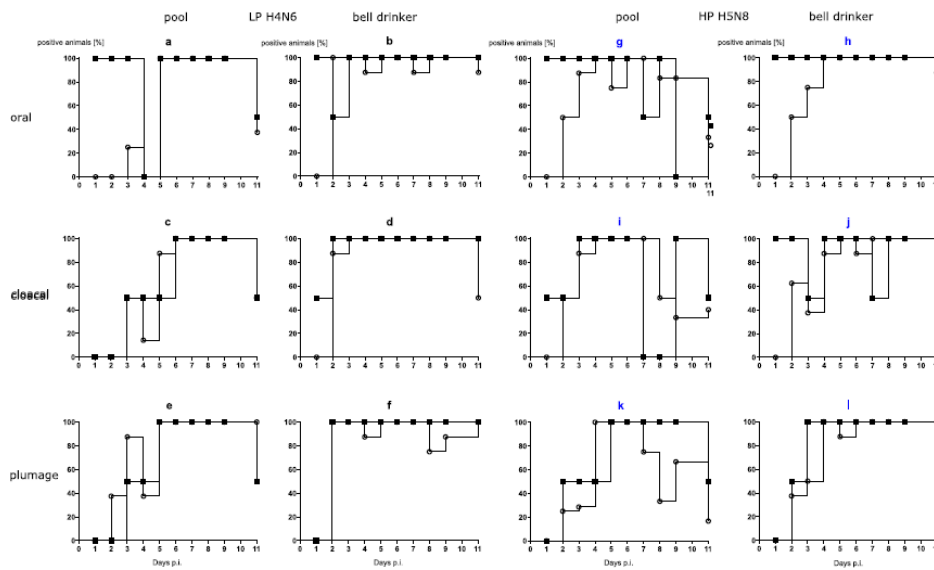


**Figure 3.** (1) Dynamics of influenza A virus infection of eight naïve mallards exposed to two “seeder” ducks inoculated with LPAIV H4N6 (figure subsets a-f) or HPAIV H5N8 (g-l, blue) and housed in the presence of a small swimming pool or a bell drinker only. Qualitative results of viral RNA excreted orally, cloacally, and adhering to the breast plumage (percentage RT-qPCRs-positive mallards per sampled animal in each group) are shown. Black squares indicate inoculated mallards, open circles represent contact ducks. (2) Influenza A virus RNA loads excreted orally (a and b), cloacally (c and d), and adhering to the breast plumage (e and f), by each ten LPAIV H4N6 infected mallards exposed to pool or bell drinker water. A similar experimental set up was run with ten mallards each infected by HPAIV H5N8 (right panels, blue label).

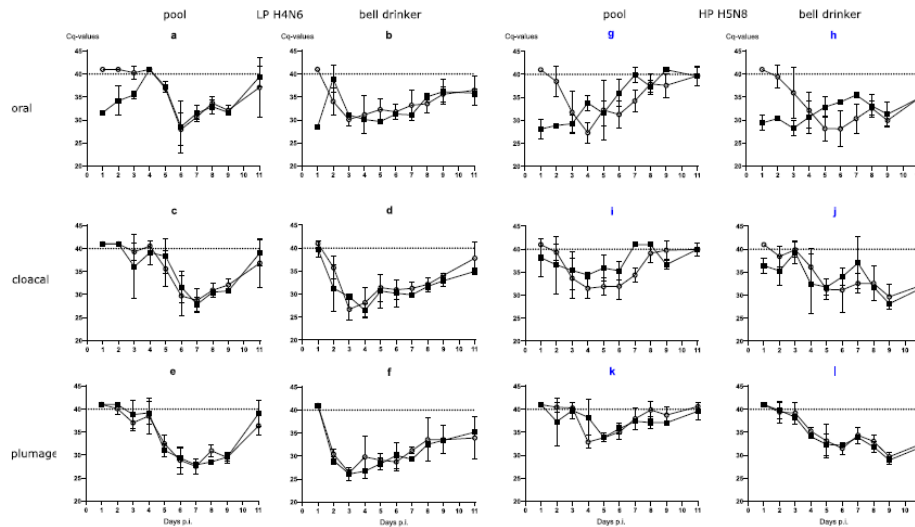


Figure 3 Continued

virus excretion commenced with 1–6 days of delay (Figure 3(1)). Swabs of some but not all of the inoculated mallards stayed virus-positive until the end of the observation period (11 dpi) although with receding viral loads (Figure 3(2)). In the bell drinker group of the H4N6 exposed mallards, infection transmitted immediately to contact ducks and peak excretion of viral RNA was reached around days 3–5 (Figure 3(2 a,b)) for oral swabs; similar patterns evolved in plumage and cloacal swabs, although higher RNA loads peaked one day earlier in cloacal swabs. The presence of a pool apparently delayed transmission of H4N6 infection for almost two to four days but then the infection progressed rapidly and viral RNA loads peaked at days 6 and 7. Similar patterns were also measured for HPAIV exposed mallards although here hardly a delayed transmission of virus to sentinels in the pool group was visible (Figure 3(2)). Viral excretion adjourned earlier (at around day 8) in the pool group. No significant difference regarding oral versus cloacal excretion was observed in these groups.

#### Approximation of a minimal infectious dose of HPAIV suspended in surface water (experimental infection setting 2)

Concluding from the previous experiment, the water source made available in the stable units might have some influence on the course of an AIV infection in mallards. The transmission of both LP and HPAIV from inoculated seeder ducks to naïve sentinels was possible also in the presence of a small pool resembling a source of brackish surface water. However, direct contact between seeder and sentinel ducks or other indirect contacts (e.g. via contaminated food)

could have played a more important role compared to water as a medium of virus transmission. Therefore, we next investigated the contagiousness of brackish surface water artificially seeded with HPAIV virus and in the absence of infected seeder ducks (Figure 1c). Three different virus concentrations were used where each litre of a 100-L pool contained  $10^2$ ,  $10^3$  or  $10^4$  TCID<sub>50</sub> of HPAIV H5N8. This translates to 0.1, 1 and 10 TCID<sub>50</sub> per mL. Four ducks were associated with each of the pools and observed for 13 consecutive days.

With the exception of a single mallard that succumbed to a neurological disease (humanely killed on 10 dpi) in the group exposed to the lowest concentration of HPAIV in the water, no clear clinical signs were observed in other ducks (supplemental Figure 2a–c). Mallard #33 in the  $10^3$  group had to be removed at 2 dpi after it contracted a severe leg injury (supplemental Figure 2b). Viral RNA loads in swabs showed a delayed onset of infection (Figure 4). In the  $10^2$  group it took until 6 dpi until all mallards tested positive (Figure 4(1 a, d)) for oral and cloacal and 7 dpi for plumage swabs (Figure 4(1g)). However, a similar pattern (3–6 days for cloacal and oral swabs [Figure 4(1 e and f)], and 6–7 days for plumage swabs [Figure 4(1h and i)]) of delayed infection was also evident for the groups which were exposed to higher virus titres (Figure 4(1)). Quantitative assessment of virus excretion showed a very similar course of infection independent of the exposure dose in water (Figure 4(2)); from 9 dpi on only marginal RNA loads were detected. Seroconversion against AIV nucleoprotein in all mallards surviving until 13 dpi confirmed RT-qPCR results in that all mallards in all groups became infected.



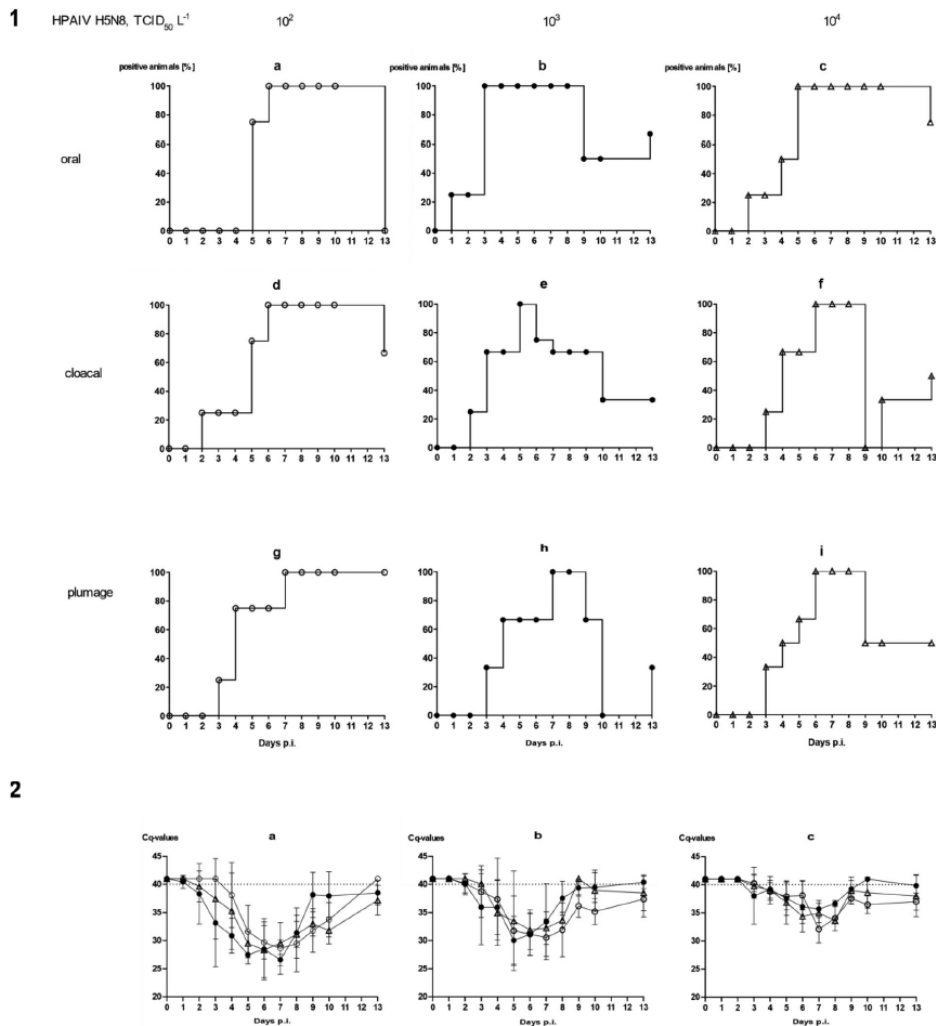


**Figure 4.** Dynamics of influenza A virus infection of four naïve mallards each exposed to artificially pool water containing  $10^2$ ,  $10^3$  or  $10^4$  TCID<sub>50</sub> L<sup>-1</sup> of HPAIV H5N8. (1) Qualitative results; percentage of mallards excreting viral RNA orally, cloacally, and of RNA adhering to the breast plumage (percentage RT-qPCRs-positive mallards per group) are shown. (2) Quantitative results of viral RNA excretion compared between exposure groups  $10^2$  (open circle),  $10^3$  (filled circle), and  $10^4$  (open triangle) in (a) oral, (b) cloacal and (c) plumage swabs.

#### **A possible role of plumage for transmission of AIV (experimental infection setting 3)**

In experimental settings 1 and 2, swabs were also sampled to detect viral RNA adhering to the breast plumage of the mallards. For the collection of material, the swab was rubbed several times carefully down the surface of the breast plumage before being transferred to a transport medium. RT-qPCR revealed identical patterns of viral RNA with slightly lower loads as obtained for oropharyngeal and cloacal swabs (Figures 3(2 e-l) and 4(2 a-c)). The viral RNA detected at the

plumage surface could represent contamination from accessing virus-loaded surface water. However, since the plumage was likewise positive for viral RNA in the bell drinker groups, it is more likely to originate from virus-containing oropharyngeal fluids deposited by the individual birds during plumage care and preening. Alternatively, viral RNA on plumage might have been a result of infection of the feather cone epithelia. To test this hypothesis, a small secondary flight feather was plucked in regular intervals (0, 4 and 9 dpi, setting 1; 0, 4, 9 and 13 dpi, setting 2) from a

**Table 1.** Detection of viral infectivity in selected RT-qPCR-positive plumage swab samples obtained from mallards in experiments 1 and 2.

Animal/ experiment	Group	Day (p.i.)	Cq value <sup>a</sup>	Virus replication
57/1	LP-Pool	7	29.64	+++ <sup>b</sup>
57/1	LP-Pool	8	32.40	++
74/1	LP bell drinker	3	26.12	---
16/1	HP bell drinker	9	29.11	---
17/1	HP bell drinker	11	31.24	---
23*/1	HP bell drinker	11	31.30	---
496/2	HP 10,000	4	35.94	++
496/2	HP 10,000	6	33.62	++
382/2	HP 10,000	6	33.91	---
363/2	HP 10,000	13	33.48	---

\*indicates an inoculated animal.

<sup>a</sup>Cq value of the original sample as measured by generic RT-qPCR targeting the NP gene.

<sup>b</sup>+ indicates virus-positive embryonated chicken egg (three eggs per sample used).

wing, its shaft removed and its conus cut and shredded in a tissue lyzer before RNA extraction. While all feather cones were negative at 0 dpi, the majority of them tested positive at 4 dpi. However, only very low virus loads between Cq 35 and 39 were measured; no differences were seen between LP and HP infected birds (not shown). By 9 and 13 dpi, the majority of feather cones tested negative again. Thus, efficient infection of feather epithelium does not seem to be the source of the viral RNA detected on the plumage.

We selected 10 plumage swabs from a range of high (Cq = 26) to low (Cq = 36) viral RNA loads and subjected them to virus isolation in 11 days old embryonated hen eggs. Isolation was difficult because of the high bacterial burden of the samples. Four swabs yielded infectious virus on days 4–8 (Table 1). This indicates that breast plumage of infected mallards not only harboured viral RNA but, at least in some birds, also carried virus particles that were infection-competent.

In a third experimental setting, we investigated whether infectious virus can also be carried in the plumage of uninfected ducks. A single mallard (“carrier duck”) was placed for 2 hours in the surface water pool of experimental setting 2 (Figure 1c) spiked with 10,000 TCID<sub>50</sub> of HPAIV H5N8 per litre. Thereafter the animal was transferred immediately (while “dripping wet”) to another stable unit with a pool of the same size which had not been spiked with virus (Figure 1d). Eight naïve mallard ducks stayed in contact for four hours with this “carrier duck”. Finally, the carrier was removed (after 6 hours of its initial contact with contaminated water) and the remaining eight ducks were observed for 13 days. Within this period none of the contact ducks became infected as judged by consistently negative RT-qPCRs in swabs, lack of clinical signs and failure to seroconvert (Figure 2b)

while the carrier duck developed infection and seroconverted as one of the animals used in experimental setting 2. Daily water samples obtained from the pool of experimental setting 3 never tested positive for viral RNA (not shown).

#### Presence of moderate to high viral RNA loads in water accessed by infected mallards

Daily samples of water obtained from bell drinkers and pools were tested for NP-specific RNA by RT-qPCR. In contrast to animal swabs, these environmental samples were extracted using the Zymo Environ™ Water RNA Kit. As shown in Table 2 moderate to high RNA loads, represented by low Cq values, were observed in both water sources. In experimental setting 1, particularly high loads were detected in the bell drinker samples; the comparatively small surface of water accessible to ducks via the bell drinker may have produced a concentrating effect (Table 2a). In experimental setting 2, the period and amplitude of viral RNA presence correlated with the initial loading dose of the water (Table 2b). However, RNA was detectable immediately after loading of the pool water only in the group with the highest dose (10<sup>4</sup> TCID<sub>50</sub> L<sup>-1</sup>). For lower inoculation doses virus amplification by infected mallards was required. Overall, the kinetics of viral RNA in pool water followed the patterns described for the mallard swab samples.

#### Discussion

Mallards (*Anas platyrhynchos*) are the most abundant anseriform migratory wild bird species in many regions of Europe. They are occupying an important role as reservoir species in the maintenance and spread of LPAI viruses [2,51]. They have been implicated also at least in regional, but possibly also long distance, spread of HPAI viruses following spill-over events from infected poultry [52,53]. The importance of abiotic factors in the spread and perseverance of AIV in the environment has been pointed out repeatedly [27,54–56]. Here we combined abiotic and biotic factors in controlled infection experiments aiming to study the role of water bodies in the epidemiology of AIV.

Figure 5 (nos. 1–4) provides a mechanistic synthesis of some of the possible drivers of AIV infection in this respect: AIV-infected mallards land on surface waters and excrete virus into the water which disperses and might float in the water column or eventually sediment. This situation is mimicked by our experiment 1, in which two inoculated seeder ducks were used as a source of infection of eight contact mallards. Using detecting excretion of AIV RNA and seroconversion, we showed that LP as well as HP virus transmitted successfully and initiated productive infection in naïve contact mallards both in the presence and

**Table 2.** Detection of viral RNA by generic RT-qPCR in water samples of infection experiments 1 (a) and 2 (b) and (c) detection of viral infectivity in selected RT-qPCR-positive water samples obtained from experiments 1 and 2.

(a)													
Days p.i.													
	0	1	2	3	4	5	6	7	8	9	11		
LP bell drinker	neg	neg	22.10	20.15	18.55	18.16	19.93	23.25	25.11	25.17	26.25		
LP pool	neg	neg	34.44	neg	neg	27.59	20	24	19.48	23.72	25.36		
HP bell drinker	neg	neg	29.18	34.25	neg#	29.37	26.65	27.11	neg	neg	n.e.		
HP pool	neg	25.54	29.08	25.04	25.28	23.43	24.77	26.17	30.85	32.36	36.01		
(b)													
Days p.i.													
	0	1	2	3	4	5	6	7	8	9	11	12	13
HP 100	neg	neg	neg	36.06	neg	neg	37.75	28.17	27.41	34.44	neg	neg	neg
HP 1,000	neg	neg	neg	30.87	28.09	30.90#	34.72#	34.03#	34.13#	30.599	neg	neg	neg
HP 10,000	neg	30.84	30.98	31.03	28.17	25.78	27.06	29.14	30.09	29.23	32.98	31.71	38.15
(c)													
Group/ experiment	Day p.i.	Cq value <sup>a</sup>	Virus replication <sup>b</sup>										
LP bell drinker/1	5	18.16	++										
LP pool/1	6	20	++										
HP bell drinker/1	6	26.65	--										
HP pool/1	6	24.77	+-										
HP 100/2	7	28.17	--										
HP 10,000/2	5	25.78	++										

<sup>a</sup>Cq value of the original sample as measured by generic RT-qPCR targeting the NP gene.

<sup>b</sup>+ indicates virus-positive embryonated chicken egg (two eggs per sample used).

Neg – Cq value  $\geq 40$ ; n.e. – not examined; # RNA extraction by Macherey-Nagel NucleoMag® VET-Kit. All other samples were extracted by the Zymo Environ Water RNA Kit.

absence of a small pool resembling shallow surface water bodies. In this respect, the seeder duck concept proved successful; virus transmissions in such an experimental setting more closely resemble natural infections of ducks as compared to the standard oculo-oronasal inoculation. As the infection started to transmit and progressed in the contact ducks, slight differences in the dynamics of virus excretion became detectable between the pool and the bell drinker groups. The LP pool group in particular was slow to start the infection but eradicated the virus faster as shown by receding virus excretion. Causes for delayed onset of infection in the wet housing surrounding were not due to slowed progression of infection of the seeder ducks of the different groups. Instead, the larger volume of water available in the pool group might have had a diluting effect on virus available for infection of sentinel ducks. In contrast, the very

limited volume of water accessible at a time in the bell drinker might have provided higher-titred virus inocula. This is at least suggested by the high virus loads detected over a long period in the LP bell drinker group. Yet, a long period of moderate to high viral RNA loads was also recorded for the HP pool group of experiment 1 (Table 2). In addition, using selected water samples from both bell drinker and pool groups we demonstrated the presence of AIV infectivity.

As shown in Figure 5, no. 5, other AIV-negative, naïve mallards may access surface water that had been virus-contaminated before. Experiment 2 establishes this situation in a stable unit where pool water was artificially loaded with infectious HPAIV. Surprisingly low titres of infective HP virus of  $10^2$  TCID<sub>50</sub> per litre water were sufficient to set off an infection in all of the exposed mallards within four to five days of observation. Infection progressed rapidly through the

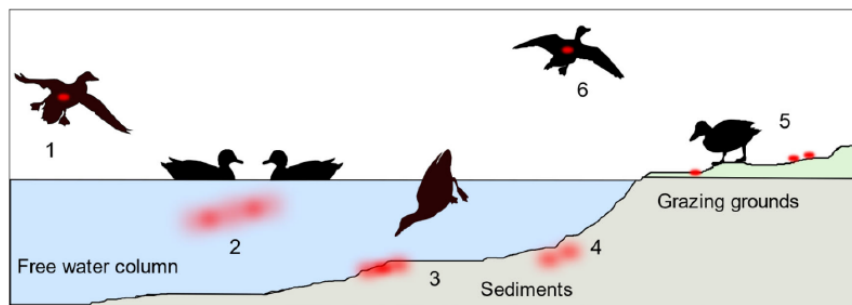


**Figure 5.** Schematic view of entry (1), dispersal (2–5) and exit (6) of avian influenza viruses within a waterbird habitat by infected aquatic wild birds. Red dots/clouds symbolize infectious virus.

groups of four mallards once the first bird had caught the infection and served itself as a virus seeder. Progression of infection in the group may well have been achieved through other contacts than surface water.

Transposure of AI viruses from contaminated surface waters over wider geographic regions is most easily conceivable via infected migrating birds (Figure 5, no. 6). This requires that mobility is retained in the infected birds. In our experiments 1 and 2, very few clinical signs could be verified and only three out of 32 mallards succumbed to a neurological manifestation of the HPAIV infection. There are field investigation data suggesting that aquatic birds, in particular dabbling ducks, may also carry AIV infectivity in their plumage while accessing contaminated water bodies [57]. “Charging” the plumage in one water body and unloading it into another one would help spreading virus effectively. We showed that considerable amounts of viral RNA are present on surface plumage swabs of infected mallards and that at least some of them harbour viral infectivity. Our findings seem to indicate that the presence of virus at the breast plumage is likely due to plumage care/preening as hardly any differences in the viral RNA loads in the plumage of the pool versus bell drinker groups was evident. In our experimental setting 3, however, we were unsuccessful to demonstrate virus transmission via putatively “charged” plumage of uninfected mallards. Failure may be due to a limited amount of virus to effectively load the plumage or due to insufficient contact times to the sentinel due which hindered proper unloading of substantial virus amounts.

In conclusion, considering the environment, and water bodies in particular, as a potential source of infection of aquatic wild birds is important. Quantifying the risks that emanate from such sources, however, will remain challenging since many factors influence amount, stability, and availability of viruses to susceptible hosts. We showed that astonishingly low titres of HPAI virus that even escaped RT-qPCR detection, when dispersed in surface water, started an infection in mallards. Virus exposure and infection in such settings may be rare stochastic events but once a single bird enters productive infection, the likelihood of spread increases exponentially.

### Acknowledgments

AKA has been funded by a grant from the German Environment Agency (FKZ 3718 62 236 0). We are grateful to animal keepers at FLI (Doreen Fiedler, Frank Klipp, Harald Manthei, Steffen Kiepert and Christian Lipinski) and thank Aline Maksimov and Diana Parlow for technical support. We would like to thank Annika Graaf and Jana Schulz for her help in preparing the animal experiment application.

### Disclosure statement

No potential conflict of interest was reported by the author(s).

### Funding

This research was funded by a grant to A.K.A. from the German Environment Agency (Umweltbundesamt), grant number FKZ 3718 62 236 0.

### Author contributions

Conceptualization, T.C.H., M.B.; methodology, validation A.K.A., T.C.H.; formal analysis, A.K.A.; investigation, A.K.A.; resources, H.C.S., T.C.M., M.B.; data curation, T.C.H.; writing—original draft preparation, A.K.A. and T.C.H.; writing—review and editing, A.K.A., H.C.S., T.C.M., M.B. and T.C.H.; visualization, A.K.A.; supervision, T.C.M., M.B., and T.C.H.; project administration, H.C.S.; funding acquisition, T.C.M. All authors have read and agreed to the published version of the manuscript.

### Data availability statement

All data pertinent to this study are presented in tables and figures in the main text or in the supplementary materials.


### Institutional Review board statement


The animals for the infection experiments were licensed by the animal ethics committee of the Federal State of Mecklenburg-Vorpommern (LALLF 7221.3-1-023/21, TV „FLI 08/21: Aviäre Influenza in Oberflächenwasser“).

### Software

Figure 1 was created with BioRender.com and licensed by the company under agreement number VP23LU0PN1. Other figures were created with GraphPad Prism software version 7 (GraphPad Software, San Diego, CA, USA) or with Inkscape version 1.01.

### ORCID

Martin Beer  <http://orcid.org/0000-0002-0598-5254>

Timm C. Harder  <http://orcid.org/0000-0003-2387-378X>

### References

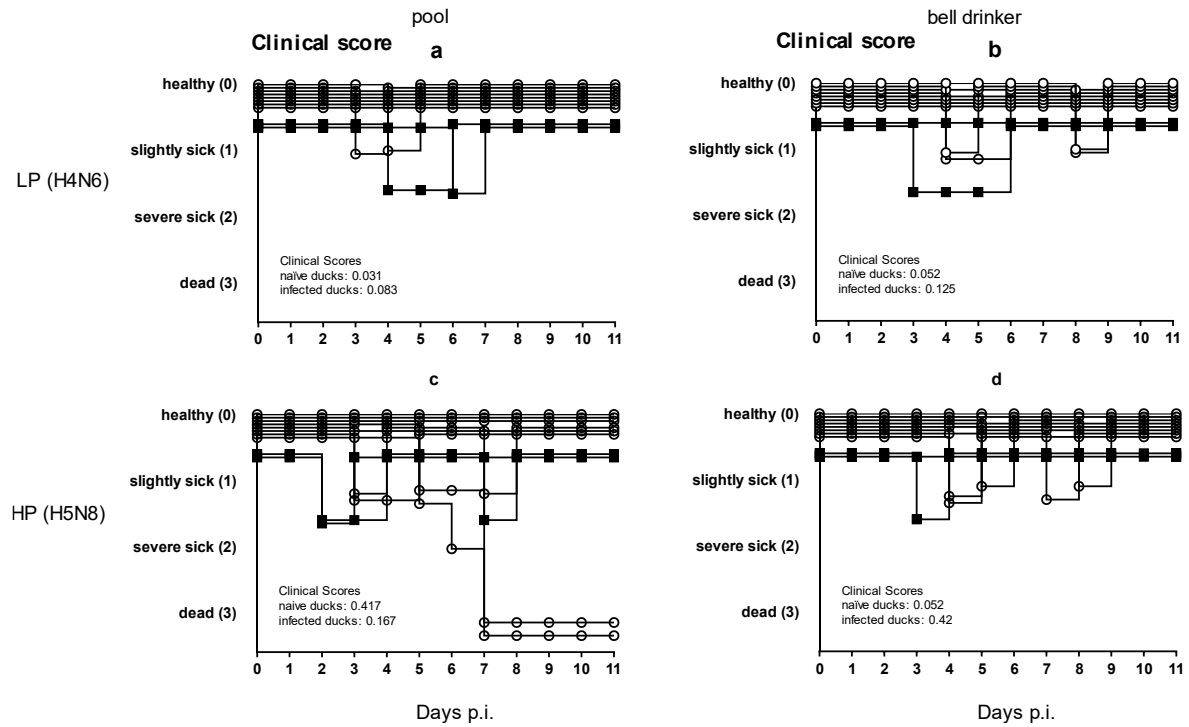
- [1] Li Y-T, Linster M, Mendenhall IH, et al. Avian influenza viruses in humans: lessons from past outbreaks. *Br Med Bull.* 2019;132(1):81–95. Available from: <https://pubmed.ncbi.nlm.nih.gov/31848585>.
- [2] Long JS, Mistry B, Haslam SM, et al. Host and viral determinants of influenza A virus species specificity. *Nat Rev Microbiol.* 2019;17(2):67–81.

- [3] Rosário-Ferreira N, Preto AJ, Melo R, et al. (2020). The Central Role of Non-Structural Protein 1 (NS1) in Influenza Biology and Infection.
- [4] Devi AB, Sarala R. Substantial effect of phytochemical constituents against the pandemic disease influenza—a review. *Futur J Pharm Sci.* 2021;7(1):120. Available from: <https://pubmed.ncbi.nlm.nih.gov/34150912>.
- [5] Luczo JM, Stambas J, Durr PA, et al. Molecular pathogenesis of H5 highly pathogenic avian influenza: the role of the haemagglutinin cleavage site motif. *Rev Med Virol.* 2015;25(6):406–430.
- [6] Zhao Z-M, Shortridge KF, Garcia M, et al. Genotypic diversity of H5N1 highly pathogenic avian influenza viruses. *J Gen Virol.* 2008;89(Pt 9):2182–2193.
- [7] Ramey AM, Hill NJ, DeLiberto TJ, et al. Highly pathogenic avian influenza is an emerging disease threat to wild birds in North America. *J Wildl Manag.* 2022.
- [8] Mine J, Uchida Y, Nakayama M, et al. Genetics and pathogenicity of H5N6 highly pathogenic avian influenza viruses isolated from wild birds and a chicken in Japan during winter 2017–2018. *Virology.* 2019;533:1–11. Available from: <https://www.sciencedirect.com/science/article/pii/S0042682219301114>.
- [9] Prosser DJ, Cui P, Takekawa JY, et al. Wild bird migration across the Qinghai-Tibetan plateau: a transmission route for highly pathogenic H5N1. *PLoS One.* 2011;6(3):e17622–e17622. Available from: <https://pubmed.ncbi.nlm.nih.gov/21408010>.
- [10] Gilbert M, Slingenbergh J, Xiao X. Climate change and avian influenza. *Rev Sci Tech OIE.* 2008;27(2):459–466. Available from: <https://pubmed.ncbi.nlm.nih.gov/18819672>.
- [11] Sutton TC. The pandemic threat of emerging H5 and H7 avian influenza viruses. *Viruses.* 2018;10(9):461.
- [12] Naguib MM, Verhagen JH, Samy A, et al. Avian influenza viruses at the wild-domestic bird interface in Egypt. *Infect Ecol Epidemiol.* 2019;9(1):1575687.
- [13] EFSA Panel on Animal Health and Welfare (AHAW), More S, Bicot D, Bötner A, et al. Avian influenza. *EFSA Journal European Food Safety Authority.* 2017;15(10):e04991–e04991. Available from: <https://pubmed.ncbi.nlm.nih.gov/32625288>.
- [14] Pantin-Jackwood MJ, Swayne DE. Pathogenesis and pathobiology of avian influenza virus infection in birds. *Rev Sci Tech OIE.* 2009;28(1):113–136.
- [15] Prosser DJ, Hungerford LL, Erwin MR, et al. Spatial modeling of wild bird risk factors for highly pathogenic A(H5N1) avian influenza virus transmission. *Avian Dis.* 2015;60(1s):329–336.
- [16] Shin D-L, Siebert U, Lakemeyer J, et al. Highly pathogenic avian influenza A(H5N8) virus in gray seals, Baltic Sea. *Emerg Infect Dis.* 2019;25(12):2295–2298.
- [17] Pulit-Penalzo JA, Brock N, Pappas C, et al. Characterization of highly pathogenic avian influenza H5Nx viruses in the ferret model. *Sci Rep.* 2020;10(1):12700.
- [18] Bragstad K, Jørgensen PH, Handberg K, et al. First introduction of highly pathogenic H5N1 avian influenza A viruses in wild and domestic birds in Denmark, Northern Europe. *Virology.* 2007;4:43. Available from: <https://pubmed.ncbi.nlm.nih.gov/17498292>.
- [19] King J, Harder T, Conraths FJ, et al. The genetics of highly pathogenic avian influenza viruses of subtype H5 in Germany, 2006–2020. *Transbound Emerg Dis.* 2021;68(3):1136–1150.
- [20] Verhagen JH, Fouchier RAM, Lewis N. Highly pathogenic avian influenza viruses at the wild-domestic bird interface in Europe: future directions for research and surveillance. *Viruses.* 2021;13(2):212.
- [21] Lee D-H, Bertran K, Kwon J-H, et al. Evolution, global spread, and pathogenicity of highly pathogenic avian influenza H5Nx clade 2.3.4.4. *J Vet Sci.* 2017;18(S1):269–280. Available from: <https://pubmed.ncbi.nlm.nih.gov/28859267>.
- [22] La Sala LF, Burgos JM, Blanco DE, et al. Spatial modelling for low pathogenicity avian influenza virus at the interface of wild birds and backyard poultry. *Transbound Emerg Dis.* 2019;66(4):1493–1505.
- [23] Spickler AR. (2016). Highly Pathogenic Avian. Available from: [https://www.cfsph.iastate.edu/Factsheets/pdfs/highly\\_pathogenic\\_avian\\_influenza.pdf](https://www.cfsph.iastate.edu/Factsheets/pdfs/highly_pathogenic_avian_influenza.pdf). Accessed 17 January 2022.
- [24] Koch G, Elbers A. Outdoor ranging of poultry: a major risk factor for the introduction and development of high-pathogenicity avian influenza. *NJAS Wageningen J Life Sci.* 2006;54(2):179–194. Available from: <https://www.sciencedirect.com/science/article/pii/S1573521406800217>.
- [25] Stallknecht DE, Brown JD. Tenacity of avian influenza viruses. *Rev Sci Tech OIE.* 2009;28(1):59–67.
- [26] Blagodatski A, Trutneva K, Glazova O, et al. Avian influenza in wild birds and poultry: dissemination pathways, monitoring methods, and virus ecology. *Pathogens.* 2021;10(5):630. Available from: <https://pubmed.ncbi.nlm.nih.gov/34065291>.
- [27] Webster RG, Yakhno M, Hinshaw VS, et al. Intestinal influenza: replication and characterization of influenza viruses in ducks. *Virology.* 1978;84(2):268–278. Available from: <https://www.sciencedirect.com/science/article/pii/0042682278902477>.
- [28] Alexander DJ. An overview of the epidemiology of avian influenza. *Vaccine.* 2007;25(30):5637–5644. Available from: <https://www.sciencedirect.com/science/article/pii/S0264410X0601187X>.
- [29] Vandegrift KJ, Sokolow SH, Daszak P, et al. Ecology of avian influenza viruses in a changing world. *Ann N Y Acad Sci.* 2010;1195:113–128.
- [30] Sooryanarain H, Elankumaran S. Environmental role in influenza virus outbreaks. *Annu Rev Anim Biosci.* 2015;3(1):347–373.
- [31] McCuen MM, Pitesky ME, Buler JJ, et al. A comparison of amplification methods to detect avian influenza viruses in California wetlands targeted via remote sensing of waterfowl. *Transbound Emerg Dis.* 2021;68(1):98–109. Available from: <https://pubmed.ncbi.nlm.nih.gov/32592444>.
- [32] Stumpf P, Failing K, Papp T, et al. Accumulation of a low pathogenic avian influenza virus in zebra mussels (*Dreissena polymorpha*). *Avian Dis.* 2010;54(4):1183–1190.
- [33] Abbas MD, Nazir J, Stumpf P, et al. Role of water fleas (*Daphniamagna*) in the accumulation of avian influenza viruses from the surrounding water. *Intervirology.* 2012;55(5):365–371. Available from: <https://www.karger.com/DOI/10.1159/000334691>.
- [34] Huyvaert KP, Carlson JS, Bentler KT, et al. Freshwater clams as bioconcentrators of avian influenza virus in water. *Vector Borne and Zoonotic Diseases (Larchmont, N.Y.).* 2012;12(10):904–906.
- [35] Horm SV, Gutiérrez RA, Sorn S, et al. Environment: a potential source of animal and human infection with influenza A (H5N1) virus. *Influenza Other Respir Viruses.* 2012;6(6):442–448.

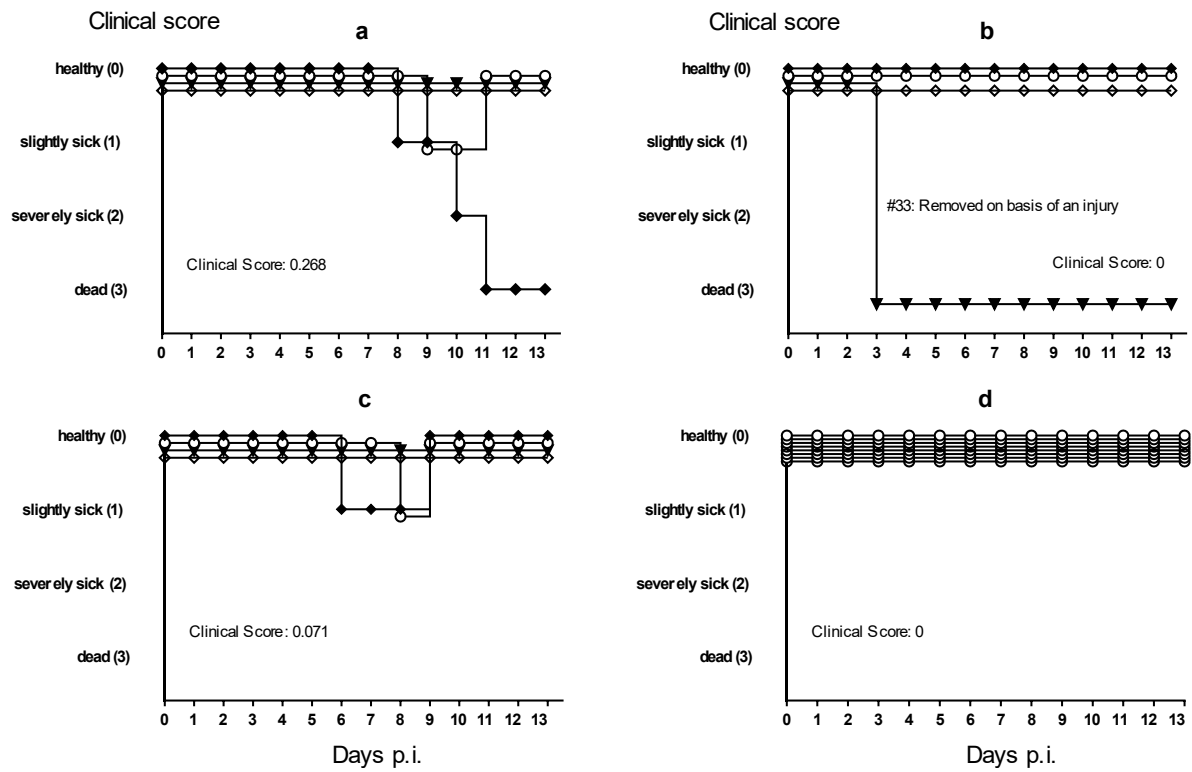
- [36] Rönnqvist M, Ziegler T, von Bonsdorff C-H, et al. Detection method for Avian Influenza viruses in water. *Food Environ Virol.* 2012;4(1):26–33.
- [37] Densmore CL, Iwanowicz DD, Ottinger CA, et al. Molecular detection of Avian Influenza virus from sediment samples in waterfowl habitats on the Delmarva Peninsula, United States. *Avian Dis.* 2017;61(4):520–525.
- [38] Tindale LC, Baticados W, Duan J, et al. Extraction and detection of Avian Influenza virus from wetland sediment using enrichment-based targeted resequencing. *Front Vet Sci.* 2020;7:301. Available from: <https://pubmed.ncbi.nlm.nih.gov/32548133>.
- [39] Rohani P, Breban R, Stallknecht DE, et al. Environmental transmission of low pathogenicity avian influenza viruses and its implications for pathogen invasion. *Proc Natl Acad Sci USA.* 2009;106(25):10365–10369.
- [40] Ramey AM, Reeves AB, Drexler JZ, et al. Influenza A viruses remain infectious for more than seven months in northern wetlands of North America. *Proc Roy Soc B Biol Sci.* 2020;287(1934):20201680.
- [41] Ito T, Okazaki K, Kawaoka Y, et al. Perpetuation of influenza A viruses in Alaskan waterfowl reservoirs. *Arch Virol.* 1995;140(7):1163–1172.
- [42] Zhang H, Li Y, Chen J, et al. Perpetuation of H5N1 and H9N2 avian influenza viruses in natural water bodies. *J Gen Virol.* 2014;95(7):1430–1435. Available from: <https://www.microbiologyresearch.org/content/journal/jgv/10.1099/vir.0.063438-0>.
- [43] Nazir J, Haumacher R, Ike A, et al. Long-term study on tenacity of avian influenza viruses in water (distilled water, normal saline, and surface water) at different temperatures. *Avian Dis.* 2010;54(1 Suppl):720–724.
- [44] Krammer F, Smith GJD, Fouchier RAM, et al. Influenza. *Nature Reviews. Disease Primers.* 2018;4(1):3.
- [45] World Organisation for Animal Health Avian Influenza (Including infection with high pathogenicity avian influenza viruses). Available from: [https://www.oie.int/fileadmin/Home/fr/Health\\_standards/tahm/3.03.04\\_AI.pdf](https://www.oie.int/fileadmin/Home/fr/Health_standards/tahm/3.03.04_AI.pdf).
- [46] Postel A, Letzel T, Müller F, et al. In vivo biotinylated recombinant influenza A virus hemagglutinin for use in subtype-specific serodiagnostic assays. *Anal Biochem.* 2011;411(1):22–31. Available from: <https://www.sciencedirect.com/science/article/pii/S0003269710008080>.
- [47] Hierholzer JC, Killington RA, Mahy BWJ, et al. Virus isolation and quantitation. *Virology Methods Manual.* 1996: 25–46. Available from: <https://www.ncbi.nlm.nih.gov/pmc/articles/PMC7173433/>.
- [48] World Organisation for Animal Health Chapter 3.3.4. - Avian influenza (including infection with high pathogenicity avian influenza viruses). Available from: [https://www.oie.int/fileadmin/Home/fr/Health\\_standards/tahm/3.03.04\\_AI.pdf](https://www.oie.int/fileadmin/Home/fr/Health_standards/tahm/3.03.04_AI.pdf).
- [49] Elnagar A, Harder TC, Blome S, et al. Optimizing release of nucleic acids of African swine fever virus and influenza A virus from FTA cards. *Int J Mol Sci.* 2021;22(23):12915.
- [50] Hoffmann B, Depner K, Schirmeier H, et al. A universal heterologous internal control system for duplex real-time RT-PCR assays used in a detection system for pestiviruses. *J Virol Methods.* 2006;136(1-2):200–209.
- [51] van Dijk JGB, Verhagen JH, Wille M, et al. Host and virus ecology as determinants of influenza A virus transmission in wild birds. *Curr Opin Virol.* 2018;28:26–36. Available from: <https://www.sciencedirect.com/science/article/pii/S1879625717300780>.
- [52] Gilbert M, Newman SH, Takekawa JY, et al. Flying over an infected landscape: distribution of highly pathogenic avian influenza H5N1 risk in South Asia and satellite tracking of wild waterfowl. *Ecohealth.* 2010;7(4):448–458. Available from: <https://pubmed.ncbi.nlm.nih.gov/21267626>.
- [53] Shriner SA, Root JJ. A Review of avian influenza A virus associations in synanthropic birds. *Viruses.* 2020;12(11):1209. Available from: <https://pubmed.ncbi.nlm.nih.gov/33114239>.
- [54] Keeler SP, Dalton MS, Cressler AM, et al. Abiotic factors affecting the persistence of avian influenza virus in surface waters of waterfowl habitats. *Appl Environ Microbiol.* 2014;80(9):2910–2917. Available from: <https://pubmed.ncbi.nlm.nih.gov/24584247>.
- [55] Dalziel AE, Delean S, Heinrich S, et al. Persistence of low pathogenic influenza A virus in water: A systematic review and quantitative meta-analysis. *PLOS ONE.* 2016;11(10):e0161929–e0161929. Available from: <https://pubmed.ncbi.nlm.nih.gov/27736884>.
- [56] Labadie T, Batéjat C, Manuguerra J-C, et al. Influenza virus segment composition influences viral stability in the environment. *Front Microbiol.* 2018;9:1496. Available from: <https://pubmed.ncbi.nlm.nih.gov/30038604>.
- [57] Delogu M, de Marco MA, Di Trani L, et al. Can preening contribute to influenza A virus infection in wild waterbirds. *PLOS ONE.* 2010;5(6):e11315.

## Supplemental Material

**Supplemental figure 1.** Clinical scores of “seeder” ducks (black squares) inoculated with LPAIV H4N6 (a, b) or HPAIV H5N8 (c, d) and of exposed contact mallards (open circles) housed in the presence of a small swimming pool (a, c) or of a bell drinker only (b, d).



**Supplemental figure 2.** Clinical scores of mallard ducks exposed to pool water artificially loaded with HPAIV H5N8 at (a)  $10^2$ , (b)  $10^3$  or (c)  $10^4$  TCID<sub>50</sub> L<sup>-1</sup> or to a “carrier duck” with virus-contaminated plumage (d).





### 3.4 Own contributions to publications

#### Paper I

#### Improved Subtyping of Avian Influenza Viruses Using an RT-qPCR-Based Low Density Array: ‘Riems Influenza a Typing Array’, Version 2 (RITA-2).

Kareem E Hassan, Ann Kathrin Ahrens, Ahmed Ali, Magdy F El-Kady, Hafez M Hafez, Thomas C Mettenleiter, Martin Beer, Timm Harder

Viruses, 14 (2), 2022  
doi: 10.3390/v14020415

**Kareem E Hassan:** methodology, validation, formal analysis, investigation, writing—original draft preparation, visualization, funding acquisition

**Ann Kathrin Ahrens:** methodology, validation, formal analysis, investigation, writing—original draft preparation

**Ahmed Ali:** software, investigation

**Magdy F El-Kady:** writing—review and editing, supervision, funding acquisition

**Hafez M Hafez:** supervision

**Thomas C Mettenleiter:** resources, funding acquisition for AKA

**Martin Beer:** Conceptualization, resources, supervision

**Timm Harder:** Conceptualization, data curation, writing—original draft preparation, writing—review and editing, supervision, project administration

## Paper II

### Investigating environmental matrices for use in avian influenza virus surveillance – surface water, sediments and avian fecal samples

Ann Kathrin Ahrens, Hans-Christoph Selinka, Claudia Wylezich,  
Hubert Wonnemann, Ole Sindt, Hartmut H. Hellmer, Florian Pfaff, Dirk Höper,  
Thomas C. Mettenleiter, Martin Beer and Timm C. Harder

Microbiology Spectrum, 11 (2), March/April 2023

doi: 10.1128/spectrum.02664-22

**Ann Kathrin Ahrens:** methodology, validation, formal analysis, investigation, writing – original draft preparation, writing – review and editing, visualization

**Hans-Christoph Selinka:** resources, writing – review and editing, project administration

**Claudia Wylezich:** investigation, writing – review and editing

**Hubert Wonnemann:** investigation, writing – review and editing

**Ole Sindt:** investigation, writing – review and editing

**Hartmut H. Hellmer:** resources, writing – review and editing

**Florian Pfaff:** investigation, writing – review and editing

**Dirk Höper:** investigation, writing – review and editing

**Thomas C. Mettenleiter:** resources, writing – review and editing, supervision, funding acquisition

**Martin Beer:** resources, conceptualization, writing – review and editing, supervision

**Timm C. Harder:** methodology, validation, conceptualization, data curation, writing – original draft preparation, writing – review and editing, supervision

### Paper III

#### Exploring surface water as a transmission medium of avian influenza viruses – systematic infection studies in mallards

Ann Kathrin Ahrens, Hans-Christoph Selinka, Thomas C. Mettenleiter,  
Martin Beer, Timm C. Harder

Emerging Microbes & Infections, 11(1), 2022

doi: 10.1080/22221751.2022.2065937

**Ann Kathrin Ahrens**: methodology, validation, formal analysis, investigation, writing—  
original draft preparation, writing—review and editing, visualization

**Hans-Christoph Selinka**: resources, writing—review and editing, project administration

**Thomas C. Mettenleiter**: resources, writing—review and editing, supervision, funding  
acquisition

**Martin Beer**: Conceptualization, resources, writing—review and editing, supervision

**Timm C. Harder**: Conceptualization, methodology, validation, data curation, writing—  
original draft preparation, writing—review and editing, supervision

## **In agreement Paper (I – III)**

.....

Place, Date

.....

Prof. Dr. Dr. h.c. Thomas C. Mettenleiter

.....

Ann Kathrin Ahrens

## 4 Summarizing discussion

Until today, and with an increasing impact, high pathogenicity avian influenza represents one of the most feared infectious diseases of poultry with a huge economic impact and a potential zoonotic risk for humans. HPAI viruses are recruited from subtypes H5 and H7 and initially are generated, most oftenly in galliform poultry, by spontaneous mutation from low pathogenicity precursor viruses. Once emerged, they can be spread horizontally like any LPAIV among poultry and by spill-over infections into wild bird populations.

Most avian species are known to be susceptible to AIV infection. Aquatic bird species compared to Galliformes are less likely to develop severe signs of disease upon infection. This is the reason why aquatic wild birds are acting as a natural LPAIV reservoir. On basis of this situation the question arose, if or which role does water play in the infection cycle of AIV? Is the water the main transmission reservoir that is fed by infected aquatic wild birds and where naïve birds pick up the virus again? In extrapolation from there: Can surface water be used a matrix for active AIV surveillance delivering useful data in terms of outbreak predictions or spread? In order to tackle some of these questions, the presented project was divided into three parts:

- (i) To improve the diagnostic RT-qPCRs for detection of AIV,
- (ii) To design and validate a filtering system to enrich AIV from natural water sources as a means of active surveillance in order to assess the role of surface and drinking water for virus transmission in infection experiments and in the field,
- (iii) To explore the minimum AI virus concentration in surface water required to initiate infection of aquatic wild birds.

Objective (i) is dealt within **paper I** where an up-dated version of the previously introduced Riems Influenza A Typing Array, version 1 (RITA1)-approach [87] , an array of RT-qPCRs, was designed and validated. Due to the high error rate of IAV genome replication, detection of RNA of different AIV strains can be compromised if primer and probe binding sites are affected by random mutations. Loss of sensitivity will be inevitable in these cases. Therefore, the RITA1-primer and probes have been updated to provide an array with improved specificity and sensitivity. Additionally, the system has been modified to occupy a lower number of wells in the array by compacting reactions into duplex assays. For use with poultry samples, targets for important viral differential diagnoses such as Newcastle virus and Avian infectious bronchitis virus have been included as well. As a response to the increasing numbers of wild bird cases

and poultry outbreaks, a reduced version of RITA-2 has been established. Only eight parallel PCR reactions are required to test for H5 or H7 AIV and their corresponding pathotypes. All samples run at the same temperature profile which saves material, time and RT-qPCR-cycler resources. Within the next years, the system should be updated regularly to maintain the performance levels for diagnosis of then circulating AIV. Compared to the classical assays including virus isolation in ECE, serological and biological virus characterization, PCR in general and the RITA method in particular can provide a much more sensitive result in significantly shorter time. Compared to nucleotide sequencing methods, including next and third generation methods, that analyse the exact viral sequence of a sample, the RITA method can only differentiate between subtypes and high and low pathogenicity using the previously known HA cleavage site motifs as a probe target sequence. Furthermore, the RITA method does not give any indication of possible mutations of the currently circulating subtypes. However, RITA is much faster, cheaper and suitable for investigation of a larger sample size. New methods for detection include biosensors providing a very high sensitivity, and analyses are possible in 5 minutes [165]. The RITA method is not as sensitive and is also much slower. Nevertheless, the RITA method allows a much more comprehensive analysis than the biosensor-based analyses introduced so far [165]. The costs of such methods also play a considerable role with a large number of samples. In summary, the PCR method, and especially the RITA method, is currently regarded as the most suitable technology for rapid and accurate AIV analyses.

Obtaining and analysing individual wild bird samples for AIV surveillance is a cumbersome and laborious process. Sampling, in particular, may be difficult and limited, if highly protected wild birds are encountered [166]. Therefore, surrogate samples, i.e. environmental matrices, are an enticing subject to improve active surveillance of AIV.

In an approach to objective (ii) we tackled surface water and sediments as such surrogate matrices (**paper II**). Two different ultrafiltration approaches were validated to enrich virus particles from large water volumes (10 L). As an internal validation marker, the bacteriophage  $\Phi 6$ , an enveloped virion with a segmented double stranded RNA genome, was used. Appropriate detection systems for  $\Phi 6$  infectivity and RNA were established. The analyses show that AIV RNA can be detected, at least at low loads, in water as well as in other environmental matrices such as sediments or environmentally deposited avian feces. For water and sludge, only few samples contained high enough virus loads that subtyping was possible. Interestingly, the AIV subtypes detected in the water column and in the corresponding sediments of the same

site did not fully match each other or the presently circulating AIV subtypes according to passive surveillance in the same region. This could indicate that the sediments act as a kind of long-term AIV store. However, it is questionable whether and if so how long AI viruses deposited in sediments remain stable and infectious. In this study, no infectious AIV could be isolated from any of the environmental samples. This could be caused by the low viral load considering that virus isolation is less sensitive compared to RT-qPCR [167,122]. Additional post-filtration methods aiming to increase the RNA yield did not lead to higher RNA-levels. In contrast, some of these methods such as SPE-DOM filtration led to a loss of RNA. Nevertheless, compared to other studies, like [103,104], we were able to detect AIV in a substantial number of samples from shallow water bodies and corresponding sediments obtained in areas with a large population of aquatic wild birds. However, the effort, costs and the AIV RNA yield are disproportionate to the result. When compared to passive surveillance in the same area, investigations of environmental samples did not succeed as an alternative surveillance or early warning system.

While in **paper II** the more technical features of virus detection in surface water were explored, **paper III** focussed on functional aspects of water as a transmission medium of AIV.

In fact, data in **paper III** show, for the first time according to our knowledge, that a very low level of viral infectivity suspended in water were sufficient to initiate an HPAIV infection in mallards. Productively infected mallards generally did not develop clinical symptoms showing that this species likely acts as a useful vehicle for widely spreading HPAIV of clade 2.3.4.4b. The data further indicated that the type of drinking water source, e.g. in poultry holdings, does play an important role during infection and for the inter-animal-infection spread. In the run of the infection experiments we also showed that AIV-RNA can be extracted from the breast plumage of infected mallards [168]. However, RNA levels on the bird's breast plumage always were lower compared to oropharyngeal or cloacal swab. YAMAMOTO and colleagues previously showed presence of infectious AIV keeps in feathers [169]. In addition, results from [170] indicated that higher RNA levels are detectable in the quills than in the classical oral or cloacal swabs, speculating that infectious AIV may also be transferred between water bodies in the plumage of waterbirds. [171] as they were able to isolate AIV from wild bird plumage swabs.

Our data (**paper II** and **III**), in contrast, indicated that feathers and plumage swabs are not best suited for monitoring approaches due to virus loads lower than in other sampling sites of the bird (oral, cloacal swabs). By using feathers alone as sampling targets, the false-negative rate is probably quite high.

Taken together, this study provided a deeper insight into the AIV ecology in surface waters and sediments. Data were partly obtained in highly artificial experimental setting (**paper III**) where interfering effects (biotic or abiotic) have largely be excluded and, thus, results and interpretation can be compromised [55,121,122,132,133].

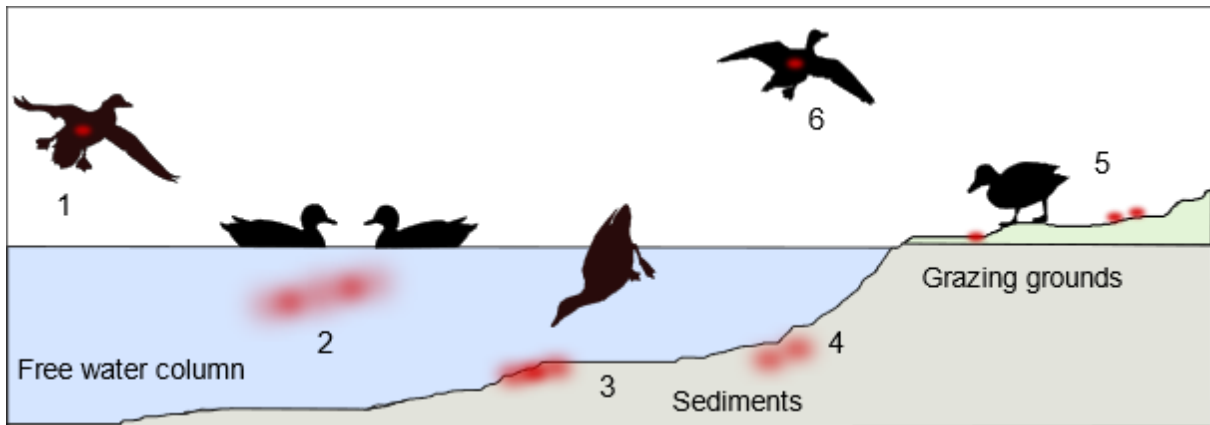


**Figure 6: Schematic overview of the putative role of water and sediments for AIV epidemiology**

Experimental and surveillance data obtained in this study provide evidence for the important role of surface waters as an efficient transmission medium. The effects of AIV deposition in the water column (Figure 6, No. 2), in sediments (Figure 6, No. 3, 4) and on grazing grounds close to such water bodies (Figure 6, No. 5) has been demonstrated in **papers II** and **III**. However, there are several questions unsolved yet, which should be investigated in further experiments to deepen the insights: such as the influence of various abiotic but also full biotic factors, some of which can accumulate AIV in themselves. Or the maximum detection period of genomic material in the different matrices. It also needs to be determined whether climate change has already interfered with AIV epidemiology due to influencing the annually bird migration patterns; birds may migrate earlier and stay longer in areas with endemic exposure of HPAIV [172]. The current wave of HPAIV infections in colony-breeding seabirds in the German Wadden Sea may be an indication of such mechanisms.



## 5 Summary

Until today, more than 100 years after its first description in Italy, the highly pathogenic avian influenza virus (HPAIV) has not lost its fearsome character for wild birds, poultry and humans. On the contrary, the number of outbreaks with high casualty rates in wild birds and poultry has multiplied in recent years and cases of zoonotic infections are also increasingly reported from HPAI endemic areas. The epidemiology of these infections is complex and also involves surface water and possibly sediments of shallow standing waters, which could play a role as a vector medium and/or virus reservoir. The goal of this project was to expand current knowledge of the influence of water on the spread of AIV. As part of this project, we were able to ...

1. ...improve AIV detection methods using real time RT-PCR in terms of sensitivity and breadth of viruses detected. In addition, we succeeded in economizing the procedure so that fewer resources are required and results are obtained faster (publication I: [173]).

2. ...develop an ultrafiltration-based enrichment method for AIV from surface water and evaluate it with field samples from HPAI outbreak areas in wild bird habitats (Wadden Sea coast of Schleswig-Holstein) and previously unaffected regions (Antarctic Weddell Sea) (publication II: [174]). Furthermore, protocols for testing different environmental sample matrices for AIV screening were tested and compared to results of passive monitoring by dabbling diseased or dead wild birds. AIV was detected in more than half (61%) of 44 water samples. We received additional sediment samples from 36 of the 44 water samples. In 18 of 36 of the sediments tested, as well as in 4.16% of 1705 fecal samples tested AIV was detected. However, the studies of the environmental samples mostly yielded only generic AIV detections, with viral loads in the range of the detection limit. This massively hampered further investigations for sub- and pathotyping. In contrast, 79.41% of 68 samples from passive monitoring showed high to very high HPAIV viral loads which also allowed sub- and pathotyping.

3. ...demonstrate in animal experiments that even very low titers ( $0.1 \text{ TCID}_{50} \text{ ml}^{-1}$ ) of HPAI viral infectivity in water can induce productive infection in susceptible but clinically largely resistant mallard ducks (publication III: [175]). Furthermore, we were able to develop evidence that there is a difference in virus spread that depends on the type of (contaminated) water source. This means that infections on poultry farms with inverted or nipple drinkers may follow a different course than infections in the wild, which are mediated via larger surface waters.

Overall, the results of this project highlight the important role of surface and drinking water, as well as aquatic sediments, in the spread of AIV. The methods developed here for AIV detection extend the possibilities for surveillance of AIV infections; however, passive remains superior to active surveillance of HPAIV infections in several aspects. Examination of various environmental samples did not yield a significant advantage in terms of an early warning system that would indicate the presence or spread of HPAIV in wild bird habitats prior to the occurrence of lethal infections in wild birds.

## 6 Zusammenfassung

Bis heute, mehr als 100 Jahre nach seiner Erstbeschreibung in Italien, hat das hoch pathogene aviäre Influenzavirus (HPAIV) seinen furchterregenden Charakter für Wildvögel, Geflügel und Menschen nicht verloren. Im Gegenteil, die Zahl der Ausbrüche mit hohen Opferzahlen bei Wildvögeln und Geflügel hat sich in den letzten Jahren vervielfacht, und auch Fälle von zoonotischen Infektionen werden zunehmend aus HPAI-Endemiegebieten gemeldet. Die Epidemiologie dieser Infektionen ist komplex und bezieht auch Oberflächenwasser und möglicherweise Sedimente flacher stehender Gewässer mit ein, die als Überträger und/oder Virusreservoir eine Rolle spielen könnten. Ziel dieses Projekts war es, das derzeitige Wissen über den Einfluss von Wasser auf die Verbreitung von AIV zu erweitern. Im Rahmen dieses Projekts konnten wir...

1. ...AIV-Nachweisverfahren mittels Echtzeit-RT-PCR in Bezug auf Empfindlichkeit und Breite der nachgewiesenen Viren verbessern. Darüber hinaus ist es uns gelungen, das Verfahren zu rationalisieren, so dass weniger Ressourcen benötigt werden und schneller Ergebnisse erzielt werden (Publikation I: [173]).

2. ...eine auf Ultrafiltration basierende Anreicherungsmethode für AIV aus Oberflächenwasser zu entwickeln und mit Feldproben aus HPAI-Ausbruchsgebieten in Wildvogellebensräumen (schleswig-holsteinische Wattenmeerküste) und bisher nicht betroffenen Regionen (antarktisches Weddellmeer) zu evaluieren (Publikation II: [174]). Darüber hinaus wurden Protokolle für die Untersuchung verschiedener Umweltprobenmatrices für das AIV-Screening getestet und mit den Ergebnissen der passiven Überwachung durch Abtupfen erkrankter oder toter Wildvögel verglichen. AIV wurde in mehr als der Hälfte (61 %) der 44 Wasserproben nachgewiesen. Von 36 der 44 Wasserproben erhielten wir zusätzliche Sedimentproben. In 18 von 36 der untersuchten Sedimente sowie in 4,16 % der 1705 untersuchten Kotproben wurde AIV nachgewiesen. Die Untersuchungen der Umweltproben ergaben jedoch meist nur generische AIV-Nachweise mit Viruslasten im Bereich der Nachweisgrenze. Dadurch wurden weitere Untersuchungen zur Sub- und Pathotypisierung massiv behindert. Im Gegensatz dazu wiesen 79,41% der 68 Proben aus dem passiven Monitoring hohe bis sehr hohe HPAIV-Viruslasten auf, die auch eine Sub- und Pathotypisierung ermöglichten.

3. ...im Tierversuch zeigen, dass bereits sehr niedrige Titer ( $0,1 \text{ TCID}_{50} \text{ ml}^{-1}$ ) der HPAI-Virusinfektiosität im Wasser eine produktive Infektion bei empfänglichen, aber klinisch weitgehend resistenten Stockenten auslösen können (Publikation III: [175]). Darüber hinaus

konnten wir nachweisen, dass es einen Unterschied in der Virusausbreitung gibt, der von der Art der (kontaminierten) Wasserquelle abhängt. Das bedeutet, dass Infektionen auf Geflügelfarmen mit Stülp- oder Nippeltränken möglicherweise einen anderen Verlauf nehmen als Infektionen in freier Wildbahn, die über größere Oberflächengewässer vermittelt werden.

Insgesamt unterstreichen die Ergebnisse dieses Projekts die wichtige Rolle von Oberflächen- und Trinkwasser sowie von Gewässersedimenten bei der Verbreitung von AIV. Die hier entwickelten Methoden zum AIV-Nachweis erweitern die Möglichkeiten zur Überwachung von AIV-Infektionen; die passive Überwachung ist jedoch der aktiven Überwachung von HPAIV-Infektionen in mehreren Aspekten überlegen. Die Untersuchung verschiedener Umweltproben erbrachte keinen signifikanten Vorteil im Hinblick auf ein Frühwarnsystem, das das Vorhandensein oder die Ausbreitung von HPAIV in den Lebensräumen von Wildvögeln anzeigen würde, bevor es zu tödlichen Infektionen bei Wildvögeln kommt.

## 7 References

1. (2001) Glossary of biotechnology for food and agriculture. A revised and augmented edition of the glossary of biotechnology and genetic engineering. Rome: Food and Agriculture Organization. 305 p.
2. Woźniak-Kosek A, Kempieńska-Mirosławska B, Hoser G (2014) Detection of the influenza virus yesterday and now. *Acta biochimica Polonica* 61 (3): 465–470.
3. Alexander DJ, Brown IH (2009) History of highly pathogenic avian influenza.
4. Perroncito E Epizoozia tifoide nei gallinacei. *Annali Accad Agri Torino* 1878 (21): 87–126.
5. Lupiani B, Reddy SM (2009) The history of avian influenza. *Comparative Immunology, Microbiology and Infectious Diseases* 32 (4): 311–323. Available: <https://www.sciencedirect.com/science/article/pii/S0147957108000088>.
6. Schäfer W (1955) Vergleichende sero-immunologische Untersuchungen über die Viren der Influenza und klassischen Geflügelpest.
7. Lycett SJ, Duchatel F, Digard P (2019) A brief history of bird flu. *Philosophical Transactions of the Royal Society B: Biological Sciences* 374 (1775): 20180257.
8. Samuel MD, Hall JS, Brown JD, Goldberg DR, Ip H et al. (2015) The dynamics of avian influenza in Lesser Snow Geese: implications for annual and migratory infection patterns. *Ecological applications* : a publication of the Ecological Society of America 25 (7): 1851–1859.
9. Simms L, Jeggo M (2014) Avian Influenza from an Ecohealth Perspective. *EcoHealth* 11 (1): 4–14.
10. Alexander DJ (2008) Avian influenza - diagnosis. *Zoonoses and public health* 55 (1): 16–23.
11. Brown I, Mulatti P, Smietanka K, Staubach C, Willeberg P et al. Avian influenza overview October 2016-August 2017. *EFSA journal*. European Food Safety Authority 15 (10): e05018.
12. Li Y-T, Linster M, Mendenhall IH, Su YCF, Smith GJD (2019) Avian influenza viruses in humans: lessons from past outbreaks. *British medical bulletin* 132 (1): 81–95.
13. Ge E, Zhang R, Li D, Wei X, Wang X et al. (2017) Estimating Risks of Inapparent Avian Exposure for Human Infection: Avian Influenza Virus A (H7N9) in Zhejiang Province, China. *Scientific reports* 7: 40016.
14. European Centre for Disease Prevention and Control (2021) First identification of human cases of avian influenza A (H5N8) infection. ECDC 2021.

15. International Committee on Taxonomy of Viruses (ICTV) Influenza taxonomy. Available: <https://talk.ictvonline.org/taxonomy>. Accessed 2 July 2021.
16. Hause Ben M., Collin Emily A., Liu Runxia, Huang Bing, Sheng Zizhang et al. Characterization of a Novel Influenza Virus in Cattle and Swine: Proposal for a New Genus in the Orthomyxoviridae Family. *mBio* 5 (2): e00031-14.
17. Mostafa A, Abdelwhab EM, Mettenleiter TC, Pleschka S (2018) Zoonotic Potential of Influenza A Viruses: A Comprehensive Overview.
18. Krammer F, Smith GJD, Fouchier RAM, Peiris M, Kedzierska K et al. (2018) Influenza. *Nature reviews. Disease primers* 4 (1): 3.
19. Long JS, Mistry B, Haslam SM, Barclay WS (2019) Host and viral determinants of influenza A virus species specificity. *Nature reviews. Microbiology* 17 (2): 67–81.
20. Verhagen JH, Fouchier RAM, Lewis N (2021) Highly Pathogenic Avian Influenza Viruses at the Wild-Domestic Bird Interface in Europe: Future Directions for Research and Surveillance. *Viruses* 13 (2): 212. Available: <https://pubmed.ncbi.nlm.nih.gov/33573231>.
21. Lamb RA, Choppin PW (1983) The gene structure and replication of influenza virus. *Annual review of biochemistry* 52: 467–506.
22. Badham MD, Rossman JS (2016) Filamentous Influenza Viruses. *Current clinical microbiology reports* 3 (3): 155–161.
23. Rossman Jeremy S., Leser George P., Lamb Robert A. (2012) Filamentous Influenza Virus Enters Cells via Macropinocytosis. *Journal of Virology* 86 (20): 10950–10960.
24. Szewczyk B, Bieńkowska-Szewczyk K, Król E (2014) Introduction to molecular biology of influenza a viruses. *Acta biochimica Polonica* 61 (3): 397–401.
25. Dou D, Revol R, Östbye H, Wang H, Daniels R (2018) Influenza A Virus Cell Entry, Replication, Virion Assembly and Movement. *Frontiers in Immunology* 9: 1581. Available: <https://www.frontiersin.org/article/10.3389/fimmu.2018.01581>.
26. Parry R, Wille M, Turnbull OMH, Geoghegan JL, Holmes EC (2020) Divergent Influenza-Like Viruses of Amphibians and Fish Support an Ancient Evolutionary Association. *Viruses* 12 (9).
27. Hao W, Wang L, Li S (2020) Roles of the Non-Structural Proteins of Influenza A Virus. *Pathogens* 9 (10).
28. Hutchinson EC, Charles PD, Hester SS, Thomas B, Trudgian D et al. (2014) Conserved and host-specific features of influenza virion architecture. *Nature communications* 5: 4816.
29. Blaurock C, Blohm U, Luttermann C, Holzerland J, Scheibner D et al. (2021) The C-terminus of non-structural protein 1 (NS1) in H5N8 clade 2.3.4.4 avian influenza virus

- affects virus fitness in human cells and virulence in mice. *Emerging microbes & infections* 10 (1): 1760–1776.
30. Pinto RM, Lycett S, Gaunt E, Digard P (2021) Accessory Gene Products of Influenza A Virus. *Cold Spring Harbor perspectives in medicine* 11 (12).
  31. Schrauwen EJA, Bestebroer TM, Munster VJ, Wit E de, Herfst S et al. (2011) Insertion of a multibasic cleavage site in the haemagglutinin of human influenza H3N2 virus does not increase pathogenicity in ferrets. *J Gen Virol* 92 (Pt 6): 1410–1415. Available: <https://pubmed.ncbi.nlm.nih.gov/21346026>.
  32. Brown EG (2000) Influenza virus genetics. *Biomedicine & Pharmacotherapy* 54 (4): 196–209. Available: <https://www.sciencedirect.com/science/article/pii/S0753332200890265>.
  33. McAuley JL, Gilbertson BP, Trifkovic S, Brown LE, McKimm-Breschkin JL (2019) Influenza Virus Neuraminidase Structure and Functions. *Front Microbiol* 10: 39.
  34. Zhang X, Cunningham FL, Li L, Hanson-Dorr K, Liu L et al. (2020) Tissue Tropisms of Avian Influenza A Viruses Affect Their Spillovers from Wild Birds to Pigs. *Journal of Virology* 94 (24).
  35. Webster RG, Bean WJ, Gorman OT, Chambers TM, Kawaoka Y (1992) Evolution and ecology of influenza A viruses. *Microbiological Reviews* 56 (1): 152.
  36. Schneider EK, Li J, Velkov T (2017) A Portrait of the Sialyl Glycan Receptor Specificity of the H10 Influenza Virus Hemagglutinin—A Picture of an Avian Virus on the Verge of Becoming a Pandemic?
  37. Shao W, Li X, Goraya MU, Wang S, Chen J-L (2017) Evolution of Influenza A Virus by Mutation and Re-Assortment. *International journal of molecular sciences* 18 (8).
  38. Ciminski K, Ran W, Gorka M, Lee J, Malmlov A et al. (2019) Bat influenza viruses transmit among bats but are poorly adapted to non-bat species. *Nat Microbiol* 4 (12): 2298–2309. Available: <https://pubmed.ncbi.nlm.nih.gov/31527796>.
  39. Świątoń E, Tarasiuk K, Śmietanka K (2020) Low pathogenic avian influenza virus isolates with different levels of defective genome segments vary in pathogenicity and transmission efficiency. *Veterinary Research* 51 (1): 108.
  40. Stubbs TM, Te Velthuis AJ (2014) The RNA-dependent RNA polymerase of the influenza A virus. *Future virology* 9 (9): 863–876.
  41. Samji T (2009) Influenza A: understanding the viral life cycle. *The Yale journal of biology and medicine* 82 (4): 153–159.
  42. Burnham AJ, Miller JR, Singh I, Billings EA, Rush MA et al. (2021) Novel isoforms of influenza virus PA-X and PB1-F2 indicated by automatic annotation. *Virus Research* 304:

198545. Available:  
<https://www.sciencedirect.com/science/article/pii/S0168170221002525>.
43. Vreede FT, Jung TE, Brownlee GG (2004) Model suggesting that replication of influenza virus is regulated by stabilization of replicative intermediates. *Journal of Virology* 78 (17): 9568–9572.
  44. Sriwilaijaroen N, Suzuki Y (2012) Molecular basis of the structure and function of H1 hemagglutinin of influenza virus. *Proc Jpn Acad Ser B Phys Biol Sci* 88 (6): 226–249. Available: <https://pubmed.ncbi.nlm.nih.gov/22728439>.
  45. Chutiwitoonchai N, Mano T, Kakisaka M, Sato H, Kondoh Y et al. (2017) Inhibition of CRM1-mediated nuclear export of influenza A nucleoprotein and nuclear export protein as a novel target for antiviral drug development. *Virology* 507: 32–39. Available: <https://www.sciencedirect.com/science/article/pii/S0042682217301022>.
  46. Nayak DP, Balogun RA, Yamada H, Zhou ZH, Barman S (2009) Influenza virus morphogenesis and budding. *Virus Research* 143 (2): 147–161. Available: <https://www.sciencedirect.com/science/article/pii/S0168170209002093>.
  47. Petrova VN, Russell CA (2018) The evolution of seasonal influenza viruses. *Nature reviews. Microbiology* 16 (1): 47–60.
  48. Johnson KEE, Ghedin E (2020) Quantifying between-Host Transmission in Influenza Virus Infections. *Cold Spring Harbor perspectives in medicine* 10 (8).
  49. Balkhy H, Al-Hajjar S (2006) Avian influenza: are our feathers ruffled. *Annals of Saudi medicine* 26 (3): 175–182.
  50. ANDREWES CH (1965) The troubles of a virus. The seventh Marjory Stephenson Memorial Lecture. *Journal of general microbiology* 40 (2): 149–156.
  51. Treanor J (2004) Influenza Vaccine — Outmaneuvering Antigenic Shift and Drift. *New England Journal of Medicine* 350 (3): 218–220.
  52. Altman MO, Angeletti D, Yewdell JW (2018) Antibody Immunodominance: The Key to Understanding Influenza Virus Antigenic Drift. *Viral Immunol* 31 (2): 142–149. Available: <https://pubmed.ncbi.nlm.nih.gov/29356618>.
  53. Webster RG, Govorkova EA (2014) Continuing challenges in influenza. *Annals of the New York Academy of Sciences* 1323 (1): 115–139.
  54. Ziegler T, Mamahit A, Cox NJ (2018) 65 years of influenza surveillance by a World Health Organization-coordinated global network. *Influenza and other respiratory viruses* 12 (5): 558–565.



55. Blagodatski A, Trutneva K, Glazova O, Mityaeva O, Shevkova L et al. (2021) Avian Influenza in Wild Birds and Poultry: Dissemination Pathways, Monitoring Methods, and Virus Ecology. *Pathogens* 10 (5): 630. Available: <https://pubmed.ncbi.nlm.nih.gov/34065291>.
56. Mary J. Pantin-Jackwood, Diane M. Smith, Jamie L. Wasilenko, Erica Spackman (2012) Low Pathogenicity Avian Influenza Viruses Infect Chicken Layers by Different Routes of Inoculation. *Avian Diseases* 56 (2): 276–281.
57. Avian Influenza. General disease information sheets. Accessed <https://www.oie.int/doc/ged/D13947.PDF>.
58. Pantin-Jackwood MJ, SWAYNE DE (2009) Pathogenesis and pathobiology of avian influenza virus infection in birds. *Revue scientifique et technique (International Office of Epizootics)* 28 (1): 113–136.
59. World Organisation for Animal Health (OIE), editor (2009) OIE Terrestrial Animal Health Code. CHAPTER 2.3.4. Avian Influenza.
60. Yoon S-W, Kayali G, Ali MA, Webster RG, Webby RJ et al. (2013) A single amino acid at the hemagglutinin cleavage site contributes to the pathogenicity but not the transmission of Egyptian highly pathogenic H5N1 influenza virus in chickens. *Journal of Virology* 87 (8): 4786–4788. Available: <https://pubmed.ncbi.nlm.nih.gov/23408622>.
61. Jang Y, Seo SH (2020) Age-Dependent Lethality in Ducks Caused by Highly Pathogenic H5N6 Avian Influenza Virus. *Viruses* 12 (6): 591. Available: <https://pubmed.ncbi.nlm.nih.gov/32485904>.
62. Reperant LA, Kuiken T, Osterhaus, Albert D M E (2012) Influenza viruses: from birds to humans. *Human vaccines & immunotherapeutics* 8 (1): 7–16.
63. Alexander DJ (2008) Avian Influenza – Diagnosis. *Zoonoses and public health* 55 (1): 16–23.
64. Straus MR, Whittaker GR (2017) A peptide-based approach to evaluate the adaptability of influenza A virus to humans based on its hemagglutinin proteolytic cleavage site. *PLOS ONE* 12 (3): e0174827.
65. Olsen B, Munster VJ, Wallensten A, Waldenström J, Osterhaus, Albert D. M. E. et al. (2006) Global Patterns of Influenza A Virus in Wild Birds. *Science* 312 (5772): 384.
66. World Organisation for Animal Health (OIE), editor (2021) OIE Terrestrial Animal Health Code. CHAPTER 3.3.4. Avian Influenza (Including Infection with High Pathogenicity Avian Influenza Viruses).

67. (2018) Verordnung zum Schutz gegen die Geflügelpest (Geflügelpest-Verordnung). Bekanntmachung der Neufassung der Geflügelpest-Verordnung vom 15.10.2018.
68. OFFLU - OIE/FAO Network of Expertise on Animal Influenza Influenza A Cleavage Sites. Available: <https://www.oie.int/doc/ged/D13484.PDF>. Accessed 14 July 2021.
69. Centanni E (1902) Die vogelpest. Beitrag zu dem durch Kerzen filtrierbaren Virus. Centralblatt für Bakteriologie, Parasitenkunde und Infektionskrankheiten 1: 145–152.
70. Burnet FM, Ferry JD (1934) The Differentiation of the Viruses of Fowl Plague and Newcastle Disease: Experiments Using the Technique of Chorio-Allantoic Membrane Inoculation of the Developing Egg. British Journal of Experimental Pathology 15 (1): 56.
71. Lush D (1943) The chick red cell agglutination test with the viruses of Newcastle disease and fowl plague. Journal of Comparative Pathology and Therapeutics 53: 157–160.
72. Hirst GK (1942) The Quantitative Determination of Influenza Virus and Antibodies by Means of Red Cell Agglutination. J Exp Med 75 (1): 49–64.
73. Storch GA (2000) Diagnostic Virology. Clin Infect Dis 31 (3): 739–751.
74. Louten J (2016) Detection and Diagnosis of Viral Infections. Essential Human Virology: 111–132. Available: <https://www.ncbi.nlm.nih.gov/pmc/articles/PMC7150318/>.
75. Brauer R, Chen P (2015) Influenza virus propagation in embryonated chicken eggs. Journal of visualized experiments : JoVE (97).
76. Weller T, ENDERS JF (1948) Production of hemagglutinin by mumps and influenza A viruses in suspended cell tissue cultures. Proceedings of the Society for Experimental Biology and Medicine. Society for Experimental Biology and Medicine (New York, N.Y.) 69 (1): 124–128.
77. Enders JF, Weller TH, Robbins FC (1949) Cultivation of the Lansing Strain of Poliomyelitis Virus in Cultures of Various Human Embryonic Tissues. Science 109 (2822): 85.
78. R R, Dalal A, Mohan H, Prasad M, Pundir CS (2020) Detection methods for influenza A H1N1 virus with special reference to biosensors: a review. Bioscience reports 40 (2).
79. Comin A, Toft N, Stegeman A, Klinkenberg D, Marangon S (2013) Serological diagnosis of avian influenza in poultry: is the haemagglutination inhibition test really the 'gold standard'. Influenza and other respiratory viruses 7 (3): 257–264.
80. Li Y, Ye H, Liu M, Song S, Chen J et al. (2021) Development and evaluation of a monoclonal antibody-based competitive ELISA for the detection of antibodies against H7 avian influenza virus. BMC Veterinary Research 17 (1): 64.

81. Trombetta CM, Ulivieri C, Cox RJ, Remarque EJ, Centi C et al. (2018) Impact of erythrocyte species on assays for influenza serology. *Journal of preventive medicine and hygiene* 59 (1): E1-E7.
82. Munster VJ, Baas C, Lexmond P, Waldenström J, Wallensten A et al. (2007) Spatial, temporal, and species variation in prevalence of influenza A viruses in wild migratory birds. *PLOS Pathogens* 3 (5): e61.
83. Ellis JS, Zambon MC (2002) Molecular diagnosis of influenza. *Reviews in medical virology* 12 (6): 375–389.
84. Artika IM, Wiyatno A, Ma'roef CN (2020) Pathogenic viruses: Molecular detection and characterization. *Infect Genet Evol* 81: 104215. Available: <https://pubmed.ncbi.nlm.nih.gov/32006706>.
85. Denomme GA, Rios M, Reid ME, editors (2000) *Molecular Protocols in Transfusion Medicine*. London: Academic Press.
86. Denomme GA, Rios M, Reid ME (2000) Part 2 - General Considerations. In: Denomme GA, Rios M, Reid ME, editors. *Molecular Protocols in Transfusion Medicine*. London: Academic Press. pp. 9–18.
87. Hoffmann B, Hoffmann D, Henritzi D, Beer M, Harder TC (2016) Riems influenza a typing array (RITA): An RT-qPCR-based low density array for subtyping avian and mammalian influenza a viruses. *Scientific reports* 6: 27211.
88. Goyal SM, Gerba CP (1983) Viradel method for detection of rota virus from seawater. *Journal of Virological Methods* 7 (5-6): 279–285.
89. Park YC, Song JM (2017) Preparation and immunogenicity of influenza virus-like particles using nitrocellulose membrane filtration. *Clinical and experimental vaccine research* 6 (1): 61–66.
90. Haramoto E, Kitajima M, Hata A, Torrey JR, Masago Y et al. (2018) A review on recent progress in the detection methods and prevalence of human enteric viruses in water. *Water research* 135: 168–186.
91. Stallknecht DE, Brown JD (2009) Tenacity of avian influenza viruses. *Revue scientifique et technique (International Office of Epizootics)* 28 (1): 59–67.
92. Calvert JG (1990) Glossary of atmospheric chemistry terms (Recommendations 1990). *Pure and Applied Chemistry* 62 (11): 2167–2219.
93. Del Espuny Garcia Real G, Davies J, Bracewell DG (2014) Scale-down characterization of post-centrifuge flocculation processes for high-throughput process development. *Biotechnology and bioengineering* 111 (12): 2486–2498.

94. CHANG SL, STEVENSON RE, BRYANT AR, WOODWARD RL, KABLER PW (1958) Removal of Coxsackie and bacterial viruses in water by flocculation. II. Removal of Coxsackie and bacterial viruses and the native bacteria in raw Ohio River water by flocculation with aluminum sulfate and ferric chloride. *American journal of public health and the nation's health* 48 (2): 159–169.
95. John SG, Mendez CB, Deng L, Poulos B, Kauffman AKM et al. (2011) A simple and efficient method for concentration of ocean viruses by chemical flocculation. *Environmental microbiology reports* 3 (2): 195–202.
96. Melgaço FG, Victoria M, Corrêa AA, Ganime AC, Malta FC et al. (2016) Virus recovering from strawberries: Evaluation of a skimmed milk organic flocculation method for assessment of microbiological contamination. *International journal of food microbiology* 217: 14–19.
97. Yeh Y-T, Tang Y, Sebastian A, Dasgupta A, Perea-Lopez N et al. (2016) Tunable and label-free virus enrichment for ultrasensitive virus detection using carbon nanotube arrays. *Science advances* 2 (10): e1601026.
98. Calabrò V, Basile A (2011) 1 - Fundamental membrane processes, science and engineering. In: Basile A, Nunes SP, editors. *Advanced Membrane Science and Technology for Sustainable Energy and Environmental Applications* : Woodhead Publishing Series in Energy: Woodhead Publishing. pp. 3–21.
99. Calabrò V, Basile A (2011) Fundamental membrane processes, science and engineering. *Advanced Membrane Science and Technology for Sustainable Energy and Environmental Applications*: Elsevier. pp. 3–21.
100. Berk Z (2009) Chapter 8 - Filtration. In: Berk Z, editor. *Food Process Engineering and Technology* : Food Science and Technology. San Diego: Academic Press. pp. 195–216.
101. Berk Z, editor (2009) *Food Process Engineering and Technology* : Food Science and Technology. San Diego: Academic Press.
102. Lickfett TM, Clark E, Gehring TM, Alm EW (2018) Detection of Influenza A viruses at migratory bird stopover sites in Michigan, USA. *Infection ecology & epidemiology* 8 (1): 1474709.
103. Pérez-Ramírez E, Acevedo P, Allepuz A, Gerrickagoitia X, Alba A et al. (2012) Ecological factors driving avian influenza virus dynamics in Spanish wetland ecosystems. *PLOS ONE* 7 (11): e46418.

104. Okuya K, Kawabata T, Nagano K, Tsukiyama-Kohara K, Kusumoto I et al. (2015) Isolation and characterization of influenza A viruses from environmental water at an overwintering site of migratory birds in Japan. *Archives of Virology* 160 (12): 3037–3052.
105. Michelle Coombe, Stefan Iwasawa, Kaylee A. Byers, Natalie Prystajecy, William Hsiao et al. (2021) A Systematic Review And Narrative Synthesis Of The Use Of Environmental Samples For The Surveillance Of Avian Influenza Viruses In Wild Waterbirds. *Journal of Wildlife Diseases* 57 (1): 1–18.
106. Guinat C, Comin A, Kratzer G, Durand B, Delesalle L et al. (2020) Biosecurity risk factors for highly pathogenic avian influenza (H5N8) virus infection in duck farms, France. *Transbound Emerg Dis* 67 (6): 2961–2970.
107. Ladman BS, Gelb J, Sauble LA, Murphy MV, Spackman E (2019) Protection afforded by avian influenza vaccination programmes consisting of a novel RNA particle and an inactivated avian influenza vaccine against a highly pathogenic avian influenza virus challenge in layer chickens up to 18 weeks post-vaccination. *Avian Pathology* 48 (4): 371–381.
108. Nobilis Influenza H5N2 - annex i. summary of product characteristics.
109. Jeong S, Lee D-H, Kim Y-J, Lee S-H, Cho AY et al. Introduction of Avian Influenza A(H6N5) Virus into Asia from North America by Wild Birds. *Emerg Infect Dis* 25 (11): 2138–2140.
110. Dugan VG (2012) A robust tool highlights the influence of bird migration on influenza A virus evolution. *Molecular ecology* 21 (24): 5905–5907.
111. Lee D-H, Torchetti MK, Winker K, Ip HS, Song C-S et al. (2015) Intercontinental Spread of Asian-Origin H5N8 to North America through Beringia by Migratory Birds. *Journal of Virology* 89 (12): 6521–6524.
112. Gear DA, Hall JS, Dusek RJ, Ip HS (2018) Inferring epidemiologic dynamics from viral evolution: 2014-2015 Eurasian/North American highly pathogenic avian influenza viruses exceed transmission threshold,  $R_0 = 1$ , in wild birds and poultry in North America. *Evolutionary applications* 11 (4): 547–557.
113. Caliendo V, Lewis NS, Pohlmann A, Baillie SR, Banyard AC et al. (2022) Transatlantic spread of highly pathogenic avian influenza H5N1 by wild birds from Europe to North America in 2021. *bioRxiv*: 2022.01.13.476155.
114. Reed KD, Meece JK, Henkel JS, Shukla SK (2003) Birds, migration and emerging zoonoses: west nile virus, lyme disease, influenza A and enteropathogens. *Clinical medicine & research* 1 (1): 5–12.

115. Lee MM, Jaspers VLB, Gabrielsen GW, Jenssen BM, Ciesielski TM et al. (2020) Evidence of avian influenza virus in seabirds breeding on a Norwegian high-Arctic archipelago. *BMC Veterinary Research* 16 (1): 48.
116. Zhang Y, Dong J, Bo H, Dong L, Zou S et al. (2019) Genetic and biological characteristics of avian influenza virus subtype H1N8 in environments related to live poultry markets in China. *BMC infectious diseases* 19 (1): 458.
117. Shahid MA, Abubakar M, Hameed S, Hassan S (2009) Avian influenza virus (H5N1); effects of physico-chemical factors on its survival. *Virology Journal* 6: 38.
118. Welch D, Buonanno M, Grilj V, Shuryak I, Crickmore C et al. (2018) Far-UVC light: A new tool to control the spread of airborne-mediated microbial diseases. *Scientific reports* 8 (1): 2752.
119. McDevitt JJ, Rudnick SN, Radonovich LJ (2012) Aerosol susceptibility of influenza virus to UV-C light. *Applied and Environmental Microbiology* 78 (6): 1666–1669.
120. Terrier O, Essere B, Yver M, Barthélémy M, Bouscambert-Duchamp M et al. (2009) Cold oxygen plasma technology efficiency against different airborne respiratory viruses. *Journal of clinical virology : the official publication of the Pan American Society for Clinical Virology* 45 (2): 119–124.
121. Petra Stumpf, Klaus Failing, Tibor Papp, Jawad Nazir, Reinhard Böhm et al. (2010) Accumulation of a Low Pathogenic Avian Influenza Virus in Zebra Mussels (*Dreissena polymorpha*). *Avian Diseases* 54 (4): 1183–1190.
122. Abbas MD, Nazir J, Stumpf P, Marschang RE (2012) Role of Water Fleas (*Daphniamagna*) in the Accumulation of Avian Influenza Viruses from the Surrounding Water. *Intervirology* 55 (5): 365–371. Available: <https://www.karger.com/DOI/10.1159/000334691>.
123. Daniel Gonzalez MS (2015) Potential Role of Fresh Water Apple Snails on H5N1 Influenza Virus Persistence and Concentration in Nature. *Air Water Borne Diseases* 04 (01).
124. Pathak AP, Murugkar HV, Nagarajan S, Sood R, Tosh C et al. (2018) Survivability of low pathogenic (H9N2) avian influenza virus in water in the presence of *Atyopsis moluccensis* (Bamboo shrimp). *Zoonoses and public health* 65 (1): e124-e129.
125. Webster RG, Yakhno M, Hinshaw VS, Bean WJ, Murti KG (1978) Intestinal influenza: replication and characterization of influenza viruses in ducks. *Virology* 84 (2): 268–278. Available: <https://pubmed.ncbi.nlm.nih.gov/23604>.

126. Swayne DE (2006) Microassay for measuring thermal inactivation of H5N1 high pathogenicity avian influenza virus in naturally infected chicken meat. *International journal of food microbiology* 108 (2): 268–271.
127. Zou S, Guo J, Gao R, Dong L, Zhou J et al. (2013) Inactivation of the novel avian influenza A (H7N9) virus under physical conditions or chemical agents treatment. *Virology Journal* 10: 289.
128. Poulson RL, Tompkins SM, Berghaus RD, Brown JD, Stallknecht DE (2016) Environmental Stability of Swine and Human Pandemic Influenza Viruses in Water under Variable Conditions of Temperature, Salinity, and pH. *Applied and Environmental Microbiology* 82 (13): 3721–3726. Available: <https://pubmed.ncbi.nlm.nih.gov/27084011>.
129. Russell CJ, Hu M, Okda FA (2018) Influenza Hemagglutinin Protein Stability, Activation, and Pandemic Risk. *Trends in Microbiology* 26 (10): 841–853. Available: <https://www.sciencedirect.com/science/article/pii/S0966842X18300684>.
130. Reed ML, Bridges OA, Seiler P, Kim J-K, Yen H-L et al. (2010) The pH of activation of the hemagglutinin protein regulates H5N1 influenza virus pathogenicity and transmissibility in ducks. *Journal of Virology* 84 (3): 1527–1535.
131. Russier M, Yang G, Marinova-Petkova A, Vogel P, Kaplan BS et al. (2017) H1N1 influenza viruses varying widely in hemagglutinin stability transmit efficiently from swine to swine and to ferrets. *PLOS Pathogens* 13 (3): e1006276-e1006276. Available: <https://pubmed.ncbi.nlm.nih.gov/28282440>.
132. Brown JD, Goekjian G, Poulson R, Valeika S, Stallknecht DE (2009) Avian influenza virus in water: Infectivity is dependent on pH, salinity and temperature. *Veterinary Microbiology* 136 (1): 20–26. Available: <https://www.sciencedirect.com/science/article/pii/S0378113508004884>.
133. Cole EC, Cook CE (1998) Characterization of infectious aerosols in health care facilities: an aid to effective engineering controls and preventive strategies. *American journal of infection control* 26 (4): 453–464.
134. Anderson BD, Lednicky JA, Torremorell M, Gray GC (2017) The Use of Bioaerosol Sampling for Airborne Virus Surveillance in Swine Production Facilities: A Mini Review. *Frontiers in Veterinary Science* 4: 121. Available: <https://www.frontiersin.org/article/10.3389/fvets.2017.00121>.
135. Augère-Granier M-L (2019) The EU poultry meat and egg sector. Main features, challenges and prospects : in-depth analysis. [Luxembourg]: [Publications Office of the European Union]. 1 online resource p.

136. Jonges M, van Leuken J, Wouters I, Koch G, Meijer A et al. (2015) Wind-Mediated Spread of Low-Pathogenic Avian Influenza Virus into the Environment during Outbreaks at Commercial Poultry Farms. *PLOS ONE* 10 (5): e0125401.
137. Ypma RJF, Jonges M, Bataille A, Stegeman A, Koch G et al. (2013) Genetic data provide evidence for wind-mediated transmission of highly pathogenic avian influenza. *The Journal of infectious diseases* 207 (5): 730–735.
138. Lv J, Gao J, Wu B, Yao M, Yang Y et al. (2021) Aerosol Transmission of Coronavirus and Influenza Virus of Animal Origin. *Frontiers in Veterinary Science* 8: 572012.
139. Anderson BD, Ma M, Xia Y, Wang T, Shu B et al. (2016) Bioaerosol Sampling in Modern Agriculture: A Novel Approach for Emerging Pathogen Surveillance. *The Journal of infectious diseases* 214 (4): 537–545.
140. Hood G, Roche X, Brioude A, Dobschuetz S von, Fasina FO et al. (2021) A literature review of the use of environmental sampling in the surveillance of avian influenza viruses. *Transbound Emerg Dis* 68 (1): 110–126.
141. Bui VN, Nguyen TT, Nguyen-Viet H, Bui AN, McCallion KA et al. (2019) Bioaerosol Sampling to Detect Avian Influenza Virus in Hanoi's Largest Live Poultry Market. *Clin Infect Dis* 68 (6): 972–975.
142. Numberger D, Dreier C, Vullioud C, Gabriel G, Greenwood AD et al. (2019) Correction: Recovery of influenza A viruses from lake water and sediments by experimental inoculation. *PLOS ONE* 14 (6): e0218882.
143. Tindale LC, Baticados W, Duan J, Coombe M, Jassem A et al. (2020) Extraction and Detection of Avian Influenza Virus From Wetland Sediment Using Enrichment-Based Targeted Resequencing. *Frontiers in Veterinary Science* 7: 301. Available: <https://www.frontiersin.org/article/10.3389/fvets.2020.00301>.
144. Schrader C, Schielke A, Ellerbroek L, Johne R (2012) PCR inhibitors – occurrence, properties and removal. *J Appl Microbiol* 113 (5): 1014–1026.
145. Nazir J, Haumacher R, Ike AC, Marschang RE (2011) Persistence of Avian Influenza Viruses in Lake Sediment, Duck Feces, and Duck Meat. *Applied and Environmental Microbiology* 77 (14): 4981.
146. Nelli RK, Kuchipudi SV, White GA, Perez BB, Dunham SP et al. (2010) Comparative distribution of human and avian type sialic acid influenza receptors in the pig. *BMC Veterinary Research* 6 (1): 4.
147. Kim SM, Kim Y-I, Pascua PNQ, Choi YK (2016) Avian Influenza A Viruses: Evolution and Zoonotic Infection. *Semin Respir Crit Care Med* 37 (4): 501–511.



148. Scull MA, Gillim-Ross L, Santos C, Roberts KL, Bordonali E et al. (2009) Avian Influenza Virus Glycoproteins Restrict Virus Replication and Spread through Human Airway Epithelium at Temperatures of the Proximal Airways. *PLOS Pathogens* 5 (5): e1000424.
149. Massin P, Naffakh N, van der Werf S (2001) Cold-sensitivity of polymerase complexes from human or avian influenza A viruses. *International Congress Series* 1219: 471–477. Available: <https://www.sciencedirect.com/science/article/pii/S0531513101003995>.
150. Bradel-Tretheway BG, Kelley Z, Chakraborty-Sett S, Takimoto T, Kim B et al. (2008) The human H5N1 influenza A virus polymerase complex is active in vitro over a broad range of temperatures, in contrast to the WSN complex, and this property can be attributed to the PB2 subunit. *J Gen Virol* 89 (Pt 12): 2923–2932.
151. Gabriel G, Herwig A, Klenk H-D (2008) Interaction of Polymerase Subunit PB2 and NP with Importin  $\alpha$ 1 Is a Determinant of Host Range of Influenza A Virus. *PLOS Pathogens* 4 (2): e11.
152. Neumann G, Kawaoka Y (2015) Transmission of influenza A viruses. *Virology* 479-480: 234–246.
153. Dornfeld D, Petric PP, Hassan E, Zell R, Schwemmler M (2019) Eurasian Avian-Like Swine Influenza A Viruses Escape Human MxA Restriction through Distinct Mutations in Their Nucleoprotein. *Journal of Virology* 93 (2).
154. Seo SH, Hoffmann E, Webster RG (2002) Lethal H5N1 influenza viruses escape host antiviral cytokine responses. *Nature Medicine* 8 (9): 950–954.
155. Monamele CG, Y P, Karlsson EA, Vernet M-A, Wade A et al. (2019) Evidence of exposure and human seroconversion during an outbreak of avian influenza A(H5N1) among poultry in Cameroon. *Emerging microbes & infections* 8 (1): 186–196.
156. Zhou L, Liao Q, Dong L, Huai Y, Bai T et al. (2009) Risk factors for human illness with avian influenza A (H5N1) virus infection in China. *The Journal of infectious diseases* 199 (12): 1726–1734.
157. World Health Organization (2022) Human infection with avian influenza A(H5) viruses. Avian Influenza Weekly Update Number 850. Available: [https://www.who.int/docs/default-source/wpro---documents/emergency/surveillance/avian-influenza/ai\\_20220422.pdf?sfvrsn=5f006f99\\_93#:~:text=Globally%2C%20from%20January%202003%20to,in%20July%202021%20\(source\)](https://www.who.int/docs/default-source/wpro---documents/emergency/surveillance/avian-influenza/ai_20220422.pdf?sfvrsn=5f006f99_93#:~:text=Globally%2C%20from%20January%202003%20to,in%20July%202021%20(source).). Accessed 10 July 2022.

158. Duan L, Campitelli L, Fan XH, Leung YHC, Vijaykrishna D et al. (2007) Characterization of low-pathogenic H5 subtype influenza viruses from Eurasia: implications for the origin of highly pathogenic H5N1 viruses. *Journal of Virology* 81 (14): 7529–7539.
159. Pohlmann Anne, King Jacqueline, Fusaro Alice, Zecchin Bianca, Banyard Ashley C. et al. (2022) Has Epizootic Become Enzootic? Evidence for a Fundamental Change in the Infection Dynamics of Highly Pathogenic Avian Influenza in Europe, 2021. *mBio* 0 (0): e00609-22.
160. Caliendo V, Leijten L, Begeman L, Poen MJ, Fouchier RAM et al. (2020) Enterotropism of highly pathogenic avian influenza virus H5N8 from the 2016/2017 epidemic in some wild bird species. *Veterinary Research* 51 (1): 117.
161. Adlhoch C, Fusaro A, Gonzales JL, Kuiken T, Marangon S et al. (2021) Avian influenza overview September - December 2021. *EFSA journal*. European Food Safety Authority 19 (12): e07108.
162. Engelsma M, Heutink R, Harders F, Germeraad EA, Beerens N (2022) Multiple Introductions of Reassorted Highly Pathogenic Avian Influenza H5Nx Viruses Clade 2.3.4.4b Causing Outbreaks in Wild Birds and Poultry in The Netherlands, 2020-2021. *Microbiology spectrum* 10 (2): e0249921.
163. Lean FZ, Vitores AG, Reid SM, Banyard AC, Brown IH et al. (2022) Gross pathology of high pathogenicity avian influenza virus H5N1 2021–2022 epizootic in naturally infected birds in the United Kingdom. *One Health* 14: 100392. Available: <https://www.sciencedirect.com/science/article/pii/S2352771422000246>.
164. Adlhoch C, Fusaro A, Gonzales JL, Kuiken T, Marangon S et al. (2022) Avian influenza overview December 2021 - March 2022. *EFSA journal*. European Food Safety Authority 20 (4): e07289.
165. Ribeiro BV, Cordeiro TAR, Oliveira e Freitas, Guilherme Ramos, Ferreira LF, Franco DL (2020) Biosensors for the detection of respiratory viruses: A review. *Talanta Open* 2: 100007. Available: <https://www.sciencedirect.com/science/article/pii/S2666831920300072>.
166. Hoye BJ, Munster VJ, Nishiura H, Klaassen M, Fouchier RAM (2010) Surveillance of wild birds for avian influenza virus. *Emerg Infect Dis* 16 (12): 1827–1834.
167. Meixell BW, Borchardt MA, Spencer SK (2013) Accumulation and inactivation of avian influenza virus by the filter-feeding invertebrate *Daphnia magna*. *Applied and Environmental Microbiology* 79 (23): 7249–7255.

168. Delogu M, Marco MA de, Di Trani L, Raffini E, Cotti C et al. (2010) Can Preening Contribute to Influenza A Virus Infection in Wild Waterbirds. *PLOS ONE* 5 (6): e11315.
169. Yamamoto Y, Nakamura K, Yamada M, Mase M (2010) Persistence of avian influenza virus (H5N1) in feathers detached from bodies of infected domestic ducks. *Applied and Environmental Microbiology* 76 (16): 5496–5499.
170. Gaide N, Foret-Lucas C, Figueroa T, Vergne T, Lucas M-N et al. (2021) Viral tropism and detection of clade 2.3.4.4b H5N8 highly pathogenic avian influenza viruses in feathers of ducks and geese. *Scientific reports* 11 (1): 5928.
171. Gobbo F, Fornasiero D, Marco MA de, Zecchin B, Mulatti P et al. (2021) Active Surveillance for Highly Pathogenic Avian Influenza Viruses in Wintering Waterbirds in Northeast Italy, 2020-2021. *Microorganisms* 9 (11).
172. Gilbert M, Slingenbergh J, Xiao X (2008) Climate change and avian influenza. *Revue scientifique et technique (International Office of Epizootics)* 27 (2): 459–466.
173. Hassan KE, Ahrens AK, Ali A, El-Kady MF, Hafez HM et al. (2022) Improved Subtyping of Avian Influenza Viruses Using an RT-qPCR-Based Low Density Array: 'Riems Influenza a Typing Array', Version 2 (RITA-2). *Viruses* 14 (2).
174. Ahrens AK, Selinka H-C, Wylezich C, Wonnemann H, Sindt O et al. (2023) Investigating Environmental Matrices for Use in Avian Influenza Virus Surveillance-Surface Water, Sediments, and Avian Fecal Samples. *Microbiology spectrum* 11 (2): e0266422.
175. Ahrens AK, Selinka H-C, Mettenleiter TC, Beer M, Harder TC (2022) Exploring surface water as a transmission medium of avian influenza viruses – systematic infection studies in mallards. *Emerging microbes & infections*: 1–30.

## 8 Appendix

### 8.1 Eigenständigkeitserklärung

Hiermit erkläre ich, dass diese Arbeit bisher von mir weder an der Mathematisch-Naturwissenschaftlichen Fakultät der Universität Greifswald noch einer anderen wissenschaftlichen Einrichtung zum Zwecke der Promotion eingereicht wurde.

Ferner erkläre ich, dass ich diese Arbeit selbstständig verfasst und keine anderen als die darin angegebenen Hilfsmittel und Hilfen benutzt und keine Textabschnitte eines Dritten ohne Kennzeichnung übernommen habe.

.....

Ann Kathrin Ahrens

## 8.2 Curriculum vitae

### 8.3 Publications

Kareem E. Hassan, **Ann Kathrin Ahrens**, Ahmed Ali, Magdy F. El-Kady, Hafez M. Hafez, Thomas C. Mettenleiter, Martin Beer, and Timm Harder, 2022. Improved Subtyping of Avian Influenza Viruses Using an RT-qPCR-Based Low Density Array: ‘Riems Influenza a Typing Array’, Version 2 (RITA-2), *Viruses* 14, no. 2: 415. <https://doi.org/10.3390/v14020415>.

**Ann Kathrin Ahrens**, Hans-Christoph Selinka, Claudia Wylezich, Hubert Wonnemann, Ole Sindt, Hartmut H. Hellmer, Florian Pfaff, Dirk Höper, Thomas C. Mettenleiter, Martin Beer and Timm C. Harder, 2023. Investigating environmental matrices for use in avian influenza virus surveillance – surface water, sediments and avian fecal samples, *Microbiology Spectrum* March/April 2023, 11 (2), doi: 10.1128/spectrum.02664-22.

**Ann Kathrin Ahrens**, Hans-Christoph Selinka, Thomas C. Mettenleiter, Martin Beer & Timm C. Harder, 2022. Exploring surface water as a transmission medium of avian influenza viruses – systematic infection studies in mallards, *Emerging Microbes & Infections*, 11:1, 1250-1261, DOI: 10.1080/22221751.2022.2065937.

#### 8.4 Oral and poster presentations

- 20.10. – 21.10.2021 Junior Scientist Symposium,  
Animal Welfare – Challenges and solutions for science and  
agriculture, online. oral talk.  
*Detection and relevance of avian influenza viruses in the  
environment*  
Ann Kathrin Ahrens
- 30.03. - 01.04.2022 31<sup>st</sup> Annual Meeting of the Society for Virology, online. Poster  
presentation  
*Impact of surface and drinking water on transmission of avian  
influenza viruses – experimental evidence*  
Ann Kathrin Ahrens, Hans-Christoph Selinka, Martin Beer,  
Thomas C. Mettenleiter, Timm C. Harder

## 8.5 Acknowledgement

First of all, I would like to thank Prof. Dr. Dr. h. c. Thomas C. Mettenleiter, head of the Friedrich-Loeffler-Institute (FLI) - Federal Research Institute for Animal Health and my supervisor as well as Prof. Dr. Martin Beer, head of the Institute of Diagnostic virology at the FLI for giving me the opportunity to write this thesis at the FLI.

A special thank you to Prof. Dr. Timm Harder, PhD, head of OIE, FAO and National Reference Laboratory for Avian Influenza (AI) / Fowl Plague, who trusted me to work on the back-to-the-virology-roots topic and always had approachable and solution-oriented suggestions when an experiment did not work out so well.

A big 'thank you' to all former and present lab members of the OIE, FAO and National Reference Laboratory for Avian Influenza (AI) / Fowl Plague, especially to Aline Maksimov and Dina Parlow the two who are rocking the diagnostic but were always there if help were needed. I would like to thank Dr. Annika Graaf and Christin Hennig for their encouragement and words of encouragement in Building 40.

Many thanks to the animal keepers, without whom the animal experiment could not be carried out in this form, and for their patience when I needed a little more time during sampling.

Moreover, I would like to thank the Umweltbundesamt (UBA) for the financial support of these work but also Dr. Regine Szewzyk, PD. Dr. Hans-Christoph Selinka and Christian Rien for the introduction in the world of Rexeed-water-filtering. As well as all the other cooperation partners who supported my work by providing any kind of samples - whether far or near.

Thanks to my family and friends who always supported and motivated me to carry on!